2016-01-27

# Establishing a Fluorescence in situ Hybridization Approach for Subcellular mRNA Localization in Arabidopsis thaliana

Halbauer, Johanna

UNIVERSITY OF CALGARY

# Establishing a fluorescence *in situ* hybridization approach for subcellular mRNA localization in *Arabidopsis thaliana*

by

Johanna Marie Halbauer

A THESIS

SUBMITTED TO THE FACULTY OF GRADUATE STUDIES

IN PARTIAL FULFILMENT OF THE REQUIREMENTS FOR THE

DEGREE OF MASTER OF SCIENCE

GRADUATE PROGRAM IN BIOLOGICAL SCIENCES

CALGARY, ALBERTA

DECEMBER, 2015

## Abstract

Post-transcriptional regulation of gene expression is an important cellular process that occurs in eukaryotes during development and in response to environmental cues. Subcellular mRNA localization is one type of post-transcriptional regulation that serves to control translation in a spatial and temporal manner. In higher plants, reports on subcellular mRNA localization are limited and the frequency of this mechanism in different cell types is unknown. The aim of this thesis was to optimize a fluorescence whole mount *in situ* hybridization approach in *Arabidopsis thaliana* with the goal of initiating a large scale screen for examples of subcellular mRNA localization in plants. Multiple visualization techniques were employed, including fluorescent tyramide signal amplification and single mRNA fluorescence approaches. The subcellular localization pattern of three mRNAs is reported here in seedling cotyledon and young leaf cells that were visualized using the optimized fluorescence whole mount *in situ* hybridization approach.

**Acknowledgements**

I would like to thank my supervisor Dr. Doug Muench for taking me on as a Master's student and trusting me with this ambitious project. His positive guidance and unwavering optimism made this journey easier for me.

I would also like to thank my committee members, Dr. John Cobb and Dr. Marcus Samuel for their constructive comments and valuable insight into my project. They were a pleasure to work with. I am very grateful for the advice and training I received from Dr. Ed Yeung. The technical training of embedding and sectioning tissue was pivotal to my project and his genuine encouragement pushed me through to finish strong.

I would like to thank all the members of the Muench Lab for making this experience enjoyable. A special thanks to Ellen Widdup for making an extra effort to welcome me into the lab and help me adjust to grad life at a new University. I am very thankful for her friendship. I would also like to thank Chi Zhang for all of his technical advice and Pritha Saha for patiently showing me how to use the confocal microscope.

I would like to thank my sister, Samantha MacLean, for always believing in me and listening to my frustrations. Her friendship and love is something I will always treasure and her support throughout my schooling has been so important to my success. Thank you to my parents, Pat and John Halbauer, for their constant understanding, support and love which also encouraged me through this journey. Thank you to my aunt, Kathy Halbauer, who provided me with affordable housing while I studied. Lastly, thank you to Stephen De Thomasis for standing by my side and loving me through it all.

## Dedication

To my son Liam Haller

**Table of Contents**

## List of Tables

## List of Figures and Illustrations

## List of Symbols, Abbreviations and Nomenclature

| Symbol | Definition |
|---|---|
| ACD | Advance Cell Diagnostics |
| ACT7 | Actin 7 protein |
| AIM-1 | Abnormal inflorescence meristem 1 protein |
| AlaAT1 | Alanine aminotransferase 1 protein |
| ALP | Alkaline phosphatase buffer |
| AP | Alkaline phosphatase |
| ASH1 | Asymmetric Synthesis of HO protein |
| ATP | Adenosine triphosphate |
| BASL | Breaking of asyemmetry in the stomatal lineage protein |
| BCIP | 5-Bromo-4-chloro-3-indolyl phosphate |
| bDNA | Branched DNA |
| bp | Base pair |
| BSA | Bovine serum albumin |
| $CaCl_2$ | Calcium chloride |
| CAF | Chloroplast autofluorescence |
| CaMIIKα | Calcium/calmodulin-dependent protein kinase II α |
| cDNA | Complementary deoxyribonucleic acid |
| CHL H | Magnesium cheletase subunit H |
| $CO_2$ | Carbon dioxide |
| CY3 | Cyanine 3 |
| D1 | Reaction center protein of photosystem II |
| DapB | 4-hydroxy-tetrahydrodipiconlinate reductase protein |
| ddH2O | Double-distilled water |
| DEPC | Diethyl dicarbonate |
| DIG | Digoxigenin |
| DMF | N, N Dimethylformamide |
| DMSO | Dimethyl sulfoxide |
| DNA | Deoxyribonucleic acid |
| dpg | Days post germination |
| ER | Endoplasmic reticulum |
| EtOH | Ethanol |
| FITC | Fluorescein isothiocyanate |
| GA1 | Ent-copalyl disphosphate synthase protein |
| GFP | Green fluorescent protein |
| GUN5 | Magnesium chelatase subunit H/CHLH |
| $H_2O$ | Water |

| | |
|---|---|
| $H_2O_2$ | Hydrogen peroxide |
| HCl | Hydrogen chloride |
| Hoxa11 | Homeobox A11 protein |
| HRP | Horseradish peroxidase |
| KCl | Postassium chloride |
| $KH_2PO_4$ | Potassium phosphate monobasic |
| LHCII | Light harvesting complex II |
| LHCB5 | Light harvesting complex of photosystem II 5 subunit |
| MAP2 | Microtubule-associated protein 2 |
| MES | 2-(*N*-morpholino)ethanesulfonic acid |
| MeOH | Methanol |
| µg | Microgram |
| $MgCl_2$ | Magnesium chloride |
| Min | Minutes |
| µm | Micrometer |
| mMDH-1 | Mitochondrial malate dehydrogenase 1 protein |
| MMG | MES mannitol magnesium chloride buffer |
| mRNA | Messenger ribonucleic acid |
| MS | Murashige and Skoog medium |
| MSLP | Multiple singly labelled probes |
| $NaH_2PO_4$ | Monosodium phosphate |
| $Na_2HPO_4$ | Sodium phosphate dibasic |
| NAA | 1-Naphthaleneacetic acid |
| NaCl | Sodium chloride |
| NADPH | Nicotinamide adenine dinucleotide phosphate (reduced) |
| NBT | Nitro blue tetrazolium |
| ng | Nanogram |
| nm | Nanometer |
| NTP | Nucleoside triphosphate |
| PB | Protein bodies |
| PBS | Phosphate-buffered saline |
| PBST | Phosphate-buffered saline with 0.1% Tween-20 |
| PHIP1 | Phragmoplastin-interaction protein |
| PCR | Polymerase chain reaction |
| pMDH-1 | Peroxisomal NAD-malate dehydrogenase 1 protein |
| PORB | Protochlorphyllide oxidoreductases B protein |
| POD | Peroxidase |
| PSV | Protein storage vacuoles |
| RBCL | Ribulose bisphosphate carboxylase/oxygenase large subunit |
| RBCS | Ribulose bisphosphate carboxylase/oxygenase small subunit |
| RBCS1A | Ribulose bisphosphate carboxylase/oxygenase small subunit 1A |

| | |
|---|---|
| RBP | RNA-binding protein |
| RFP | Red fluorescent protein |
| RNA | Ribonucleic acid |
| RPM | Revolutions per minute |
| RT | Room temperature |
| Rubsico | Ribulose bisphosphate carboxylase/oxygenase protein |
| Sec | Seconds |
| SSC | Saline-Sodium Citrate |
| TBST | Tris-buffered saline with 0.05% Tween-20 |
| TE | Tris and EDTA buffer |
| TNM-50 | Tris sodium chloride magnesium buffer |
| Tris | Tris(hydroxymethyl)aminomethane |
| UTP | Uridine-5'-triphosphate |
| UTR | Untranslated region |
| UV | Ultra violet |
| W5 | Wash buffer 5 |
| WISH | Whole mount *in situ* hybridization |

# CHAPTER 1: INTRODUCTION

Gene expression is a highly regulated process that is essential for proper development and maintenance of an organism. Regulation occurs at all stages of gene expression, from transcription initiation to translation, and includes downstream events such as epigenetic control. Post-transcriptional control is achieved through a variety of mechanisms, including mRNA decay, mRNA localization and translational repression. These mechanisms involve an array of protein factors that interact with mRNA to allow for flexible and rapid control of protein synthesis in response to developmental and environmental ques (Bailey-Serres et al., 2009). RNA-binding proteins (RBPs) interact with mRNAs throughout their lifetime, from mRNA maturation to decay, and are rapidly reassembled in a dynamic fashion to facilitate post-transcriptional control (Moore, 2005). Subcellular mRNA localization has emerged as an important and common mechanism that contributes to post-transcriptional gene regulation in eukaryotic cells (Donnelly et al., 2010). This thesis research was aimed at providing insight into the prevalence of mRNA localization in plant cells through the optimization of a fluorescence *in situ* hybridization approach and identification of new examples of mRNA localization.

## 1.1 Subcellular mRNA Localization in Eukaryotic cells

Subcellular mRNA localization is a mechanism for regulating gene expression at the post-transcription level by controlling translation in a spatial and temporal manner (Shahbabian and Chartrand, 2012). Mature mRNA can be exported from the nucleus and localized to specific cytoplasmic regions of the cell or to the surface of organelles for

localized translation. This serves to compartmentalize proteins within the cell, a feature that is fundamental for eukaryotic cell organization and function. Localized translation is an efficient method for protein localization because it avoids the creation of unfavorable interactions between proteins, and reduces the energy that is expended to localize individual proteins. It also allows for a rapid response to stimuli by rapidly translating proteins at the site of function within the cell.

### *1.1.1 The Role of mRNA Localization in Eukaryotes*

Subcellular mRNA localization has been studied extensively in a variety of eukaryotic organisms such as *Saccharomyces cerevisiae* (yeast), *Drosophila melanogaster* (Drosophila), and vertebrates (Zarnack and Feldbrügge, 2010; Lécuyer et al., 2007). Once thought of as a relatively rare event, it is now accepted as an important and common mechanism for protein compartmentalization during development. For instance, in the developing Drosophila oocyte and embryo, translation of localized mRNA is essential for the polarized distribution of regulatory proteins involved in axis formation. More than two-thirds of the mRNAs in the developing Drosophila embryo are non-randomly localized in the cytosol (Lécuyer et al., 2007). Transcripts that encode proteins involved in cytoskeleton development, cell division, and nuclear processes were shown to localize in unique patterns. These patterns were observed at different times during different stages of development, and both maternal and zygotic mRNAs displayed non-random localization (Lécuyer et al., 2007).

A classic example of subcellular mRNA localization during development is demonstrated in budding yeast (Shepard et al., 2003). There are 30 mRNAs that are

known to localize to the tip of the budding daughter cell (Jansen and Niessing, 2012). *ASH1* mRNA encodes a transcriptional repressor responsible for mating-type switching suppression in the daughter cell. *ASH1* mRNA moves from the mother cell to the newly developing daughter cell bud using actin filaments and myosin motors. This asymmetric distribution to the tip of the bud insures the encoded Ash1 transcription factor reaches the nucleus of the daughter cell (Long et al., 1997; Takizawa et al., 1997). Subcellular mRNA localization is often used in cell types where a rapid response to stimuli is required for proper cell function. Neurons are long, polarized cells that consist of the cell body, dendrites and axons. mRNA localization is an efficient mechanism that synthesizes proteins specifically at dendrites and the axon termini in a temporal and spatial manner upon synaptic stimulation (Donnelly et al., 2010). The localized translation of mRNA that encodes calcium/calmodulin-dependent protein kinase II α (CaMIIKα) in dendrites is one example of the essential role of mRNA localization and translation as a post-synaptic process (Miller et al., 2002).

### *1.1.2 Mechanisms of mRNA Localization*

Three major mechanisms are known to contribute to establishing an asymmetric distribution of mRNAs in the cell. These include cytoplasmic streaming and anchoring, local protection from mRNA degradation, and active transport along the cytoskeleton. All three mechanisms require the assistance of RBPs.

During cytoplasmic streaming and anchoring, mature mRNA will enter the cytoplasm from the nucleus and diffuse randomly in the cytosol in a translationally repressed state. Anchoring proteins that interact directly or indirectly with the mRNA are

present at the site of localization. When the target mRNA contacts the anchor protein it is captured for localized translation. Cytoplasmic streaming and anchoring localizes *nanos* mRNA to the posterior pole in the developing Drosophila oocyte (Forrest and Gavis, 2003).

The turnover rate of cytosolic mRNA varies between organisms and individual transcripts, and ranges from a few minutes to over 24 hours (Meyer et al., 2015). Local protection from mRNA degradation allows for free flowing cytosolic mRNA to accumulate at a location where mRNA decay is absent. This results in an accumulation of specific transcripts at the site of protection that can be locally translated. For example, *Hsp83* mRNA is distributed evenly in the early Drosophila embryo. However, as the embryo ages, *Hsp83* mRNA becomes restricted to the posterior pole where it is protected from degradation (Ding et al., 1993).

The most common method for subcellular mRNA localization is direct transport along the cytoskeleton (Figure 1.1). Both actin filaments and microtubules have been shown to transport RNAs. In animal cells, the former is typically involved in short-distance transport and the latter in long-distance transport (Kloc et al., 2002). For example, in large growing neuron cells, β-actin mRNA is transported over a long distance to the cell tip in a microtubule dependent manner (Zhang et al., 2001). During direct localization, cytosolic RBPs recognize the target mRNA through *cis*- elements. These combine with other associated proteins to create a ribonucleoprotein (RNP) that interacts

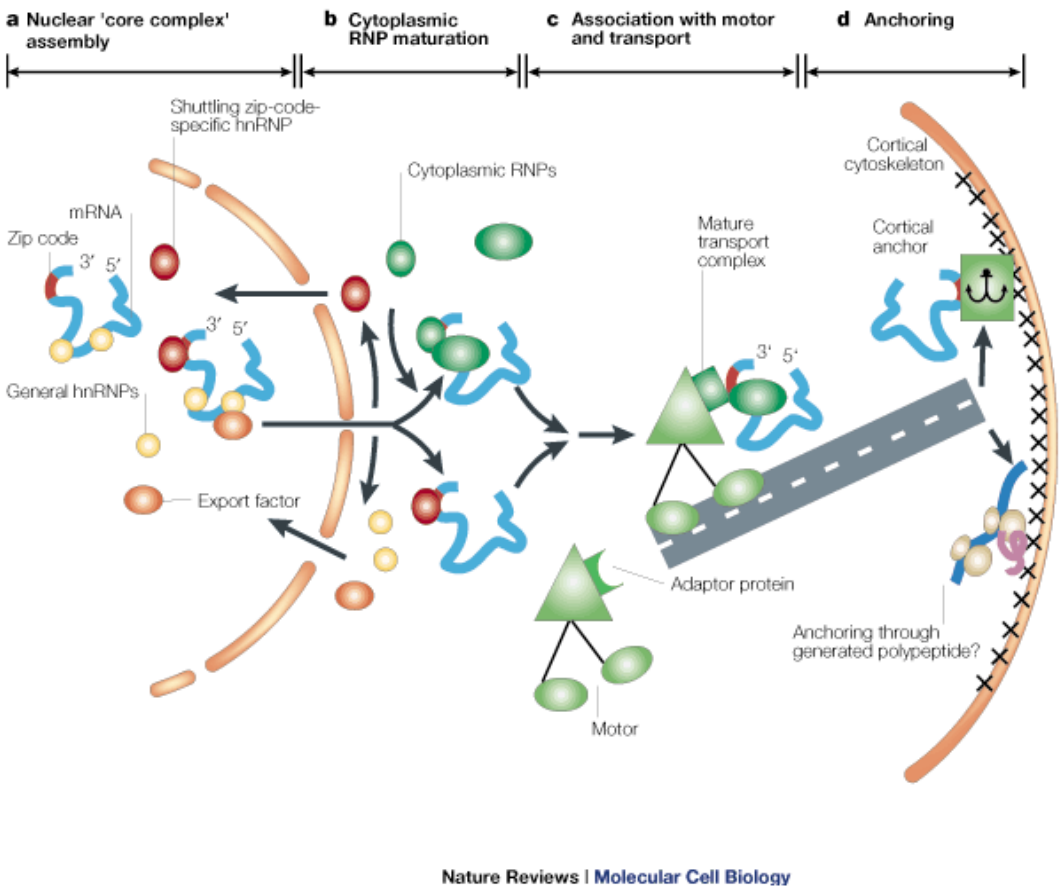


**Figure 1.1 A model for direct transport of mRNA**

A) Mature mRNA interacts with RBPs for export from the nucleus. B) Nuclear RBPs disassociate from the mRNA in the cytoplasm as cytoplasmic RBPs interact with the mRNA to form the cytoplasmic RNP. C) Cytoplasmic RNPs interact with molecular motors and are transported to a subcellular location along the cytoskeleton. D) At the localization site, anchoring proteins interact with the mRNA the nascent polypeptide resulting in localized protein expression. Image from Jansen (2001).

with molecular motors on the cytoskeleton for transport (Figure 1.1). These *cis*-elements are generally found in the 3' UTR of the mRNA, although they can also be located at the 5' UTR and within the coding sequence. Typically one mRNA will have multiple *cis*-elements to achieve efficient transport and can be recognized through the sequence or through RNA secondary and tertiary structures (Van De Bor and Davis, 2004).

Molecular motors are proteins that convert chemical energy into mechanical energy to create movement along microtubules or actin filaments. Dynein motors are a high molecular weight family of ATPases that have minus-end directed movement along microtubules (Sakakibara and Oiwa, 2011). Dynein is responsible for localizing multiple transcripts involved in segment development in the Drosophila syncytial embryo (Wilkie and Davis, 2001). Kinesins are another large family of microtubule motor proteins that generate movement through ATP hydrolysis (Ovechkina and Wordeman, 2003). Kinesins are involved in the movement of *oskar* mRNA along microtubules during Drosophila oocyte development (Zimyanin et al., 2008; Brendza et al., 2000). Myosin is a family of molecular motors that move along actin filaments. *ASH1* mRNA moves along actin filaments in yeast using myosin motors for proper subcellular localization to the bud tip (Takizawa et al., 1997). Myosin motors have also been implemented in the subcellular localization of β-actin to the leading edge in fibroblasts (Latham et al., 2001).

### *1.1.3 RNA-Binding Proteins Involved in mRNA Localization*

RBPs are found in both the nucleus and the cytoplasm. Nuclear RBPs interact with mRNA during maturation and are involved in splicing, capping, polyadenylation and mRNA export from the nucleus (Moore, 2005; Köhler and Hurt, 2007). Cytoplasmic

RBPs can function to repress translation and regulate mRNA stability and decay. For example, the Puf protein family is a group of RBPs found in animal, plant, fungal and protozoan systems that bind to the 3' UTR of target mRNAs and interact with other proteins to inhibit translation or initiate RNA decay (Miller and Olivas 2011) . Other cytoplasmic RBPs interact with certain mRNAs to mediate in subcellular mRNA localization. The nuclear RBP She2p binds to *ASH1* mRNA to facilitate translocation out of the nucleolus where the RBP Loc1p then binds to the complex, along with the RBPs Puf6p and Khd1p (Jansen and Niessing, 2012). This forms an RNP that is competent for proper export from the nucleus. Puf6p and Khd1p remain in the RNP in the cytoplasm to suppress translation while the *ASH1* mRNA and She2p bind with a cytosolic RBP (She3p) to interact with myosin motors for active transport along actin filaments (Jansen and Niessing, 2012). Once the RNP has reached the localization site in the daughter cell, the complex dissociates and translation occurs.

The subcellular localization of *oskar* mRNA in the developing Drosophila oocyte relies on both nuclear and cytosolic RBPs. The formation of the exon junction complex is responsible for splicing mRNA in the nucleus is essential for proper localization of *oskar* mRNA, followed by interactions with multiple RBPs from the heterogeneous nuclear RNP family (hnRNP) that bind to the 3' and 5' UTR of the mRNA (Jansen and Niessing, 2012). Active transport of this RNP is achieved by binding to the RBP Staufen which is thought to facilitate the interactions of the RNP with microtubule motor proteins and assists in anchoring *oskar* mRNA at the localization site (Jansen and Niessing, 2012). Staufen is also involved in the localization of another Drosophila mRNA called *bicoid* which localizes to the anterior pole of the developing embryo in a microtubule-dependent

manner (Ferrandon et al., 1994). Staufen homologs expressed in mammalian neuron cells are involved in the localization of CaMIIKα and poly(A) mRNAs to dendrites through the formation of RNPs (Miki et al., 2005).

Prolamine storage protein in the developing endosperm of *Oryza sativa* (rice) is localized through its targeted mRNA to a specific subdomain of the endoplasmic reticulum (ER). Prolamine mRNAs move on actin filaments to the surface of the protein body ER subdomain to facilitate translation and import of prolamine protein across the membrane at that ER subdomain (Hamada et al., 2003a). Drosophila homologs of hnRNPs were shown to interact with the *cis*-elements identified in the prolamine mRNA *in vitro* (Yang et al., 2014; Crofts et al., 2010). It is suspected that at least five different hnRNPs form three different multiprotein complexes for the proper localization of prolamine mRNA in rice (Yang et al., 2014).

## 1.2 Techniques for Visualizing mRNA Localization

### *1.2.1 In situ Hybridization*

Gene expression can be studied in specific tissues or cells by measuring mRNA levels using techniques such as northern blots, quantitative PCR and microarray analysis. Although these techniques can give valuable quantitative information about transcript levels, they cannot provide information on the localization or mRNAs within the cell. A classic procedure to localize RNA and DNA within tissues and cells is *in situ* hybridization, a procedure that was first used to visualize nucleic acids in sectioned ovaries from *Xenopus* tadpoles (Jacob et al., 1971). This technique preserves the organization of macromolecules and structure of the tissue at a specific time by exposing

the specimen to chemical fixatives. Once properly fixed, various steps can be taken to permeabilize the tissue before hybridization with an antisense probe that targets the mRNA of interest. The final steps in the procedure are performed to allow for visualization of the probe. One of the first studies that successfully localized RNA using *in situ* hybridization was performed on Drosophila tissue sections using radioactive labelled probes (Akam, 1983). Sectioning of the tissue serves to facilitate probe access into cells or tissues that are located deep within the organism. In recent years, an effort has been made to move away from sectioned tissue because it is technically challenging, time consuming, and requires specialized equipment. Focus has shifted to whole mount *in situ* hybridization (WISH) for these reasons and because it is possible to generate a three-dimensional image using confocal microscopy that shows the target mRNA localization throughout the entire cell. Fluorescence WISH was utilized in the global analysis of transcript localization in the developing Drosophila embryo, along with the identification of localized transcripts in *Xenopus* oocytes, yeast, *Chlamydomonas reinhardtii* (Chlamydomonas) and neurons (Vize et al., 2009; Long et al., 1997; Uniacke and Zerges, 2009; Lécuyer et al., 2007; Batish et al., 2012)

Numerous protocols have been developed to optimize tissue preservation and signal resolution using WISH. There are many parameters to consider with *in situ* hybridization that vary between organisms and tissue types. For instance, optimized tissue fixation for RNA preservation, permeabilization of tissue, and probe visualization is required for each step in the procedure. In plants, structures such as the cell wall, the waxy cuticle and endogenous fluorescent pigments create additional challenges to successfully performing WISH analysis.

Researchers were determined to find the optimal fixative solution for histological purposes since as early as the 1920s. Different combinations of chemicals and environmental conditions were used depending on which macromolecule was to be preserved. Paraformaldehyde is a fixative that is dissolved in water to form formaldehyde and has been used commonly for RNA *in situ* hybridization. Formaldehyde reacts with protein side-chains to create reactive complexes that combine to one another creating methylene bridges or crosslinks. The crosslinking of proteins to one another encases the RNA to preserve its location. Formaldehyde will also react with nucleotides and link them to interacting proteins (David et al., 2011). The benefit of using formaldehyde is that it preserves cytoplasmic structure, decreases solubility of lipids and does not shrink tissue as it fixes (Jensen, 1962). The major disadvantage to formaldehyde fixation is some reactive side chains interact to generate fluorescent products. Formaldehyde, acetic acid and alcohol (FAA) is a common fixative mixture used for *in situ* hybridization of plant sections (Marrison et al., 1996; Gibson et al., 1996; Im et al., 2000). The addition of acetic acid helps in the direct preservation of nucleic acids and serves to keep the tissue soft against the hardening effects of formaldehyde (Jensen, 1962). Alcohol penetrates tissue quickly to fix the sample which is beneficial for RNA preservation (Jensen, 1962). Other chemicals and detergents may be added to fixatives to allow for quicker penetration. These include DMSO and Tween-20. Careful consideration must be given into the length of fixation time, particularly when dealing with whole mount samples. Over fixation will inhibit probe access to the target mRNA, whereas under fixation will result in loss of RNA and disruption of tissue and cell morphology (Hejátko et al., 2006).

Adequate permeabilization of the sample is important to ensure that the probe can reach the target mRNA and hybridize to it efficiently. This becomes an important step when performing WISH because of the multiple tissue layers that the probe must penetrate. Permeabilization of the cell membrane is achieved using non-ionic detergents such as Tween-20 and Triton X-100, along with alcohol washes. Proteinase K is commonly used to breakdown some of the protein linkages caused by fixation and to remove proteins that interact with the target mRNA. For plant tissues, xylene is used to remove the cuticle, and cell wall digestion enzymes are often used to breakdown the cell wall to further permeabilize the tissue. Like fixation, permeabilization times for each treatment needs to be optimized to avoid distorting cell morphology while still creating space for probe penetration.

Multiple types of probes have been designed for *in situ* hybridization. These are either DNA oligonucleotides or ribonucleotides and can be directly or indirectly labelled. Initially, probes were directly labelled with radioisotopes. However, they are hazardous to work with, unstable, have low resolution, and require extensively long signal development times (Martone et al., 1998). In the 1980s, radioisotope labelling began to be replaced with non-radioactive labelling using chemically modified nucleotides. Nucleotides can be modified to have a fluorescent molecule attached for direct labelling or contain a hapten label to be recognized by an antibody for indirect labelling. Detection of the hapten label is achieved through hapten specific antibodies that are coupled to a fluorescent molecule or an enzyme. Enzyme detections allow for amplification of the signal and can result in colourmetric or fluorescent visualization, depending on the enzyme used. Alkaline phosphate (AP) is an enzyme that creates a purple precipitate

when incubated with the substrates tetrazolium salt and 5-bromo- 4-chloro-3 idolyl-phosphate. When a hapten-specific antibody coupled to AP is used, a purple precipitate identifies the location of the target mRNA. Horseradish peroxidase (HRP) is an enzyme that, in the presence of $H_2O_2$, will convert a molecule called tyramide into a radical that covalently binds to tyrosine residues found on the nearest protein. Tyramide can be synthesized with a fluorescent tag appended to it so that the area of its precipitation will be fluorescently labelled. Multiple tyramide molecules will be precipitated by the activity of one HRP enzyme. Therefore, when HRP is coupled to the hapten-specific antibody, the probe can be visualized fluorescently with an amplified signal. The benefit of HRP over AP is that the purple precipitate produced by AP can diffuse from the site of origin thereby limiting its detection to the tissue level. In contrast, the tyramide precipitate remains at the site of the probe thereby allowing for high resolution mRNA localization within the cell (Lécuyer et al., 2007).

Recent advances in mRNA visualization have strived to amplify the mRNA at a high enough resolution to successfully visualize single mRNA molecules. The first success was imaging β-actin mRNA molecules in rat kidney cells using multiple tandem oligonucleotide probes that were directly labelled with a fluorophore and designed to anneal to the 3' UTR of the mRNA (Femino et al., 1998). This technique of multiple singly labelled probes (MSLP) has been optimized and used to visualize single mRNAs in *C. elegans*, Drosophila, yeast, neurons and mammalian cells (Batish et al., 2012; Raj et al., 2008; McIsaac et al., 2013; Lyubimova et al., 2013). Another system for single molecule mRNA visualization called the branched DNA (bDNA) technology has been developed. This system uses paired oligonucleotide probes that anneal to the target

mRNAs to form a binding site for scaffold assembly. This scaffold produces a branched structure that contains multiple fluorescence probes and produces a strongly amplified and high resolution signal with low background levels (Wang et al., 2012). This system has been used in a variety of studies in eukaryotic cells and is a cancer diagnostic tool (Vassilakopoulou et al., 2014; Liu et al., 2015; Tomas et al., 2014; Ziskin et al., 2012).

### *1.2.2 Live Cell Imaging*

The majority of analyses of mRNA localization have involved *in situ* hybridization approaches, and these have provided a foundation for understanding the extent of intracellular mRNA localization during development. However, the ability for real-time *in vivo* detection of mRNAs is necessary to fully understand and monitor mRNA localization. This can be achieved through live cell imaging. A classic technique for live cell imaging is directly labelling synthetic target mRNA with a fluorescent moiety and introducing it into the cytoplasm of an organism through microinjection (Figure1.2A). This technique has been used to visualize viral mRNA is live plant cells and *hairy* pair-rule mRNAs in Drosophila (Christensen et al., 2010; Bullock et al., 2003). The advantage of this method is low background noise. However, proper localization of some mRNAs requires nuclear injection to bind the proper *trans* acting factors involved in mRNA trafficking, as seen in *oskar* mRNA localization in Drosophila embryos (Hachet and Ephrussi, 2004). It is technically challenging to microinject the mRNA directly into the nucleus. Therefore, it is not an ideal technique to visualize mRNAs in live cells for which the mechanisms for localization is unknown.

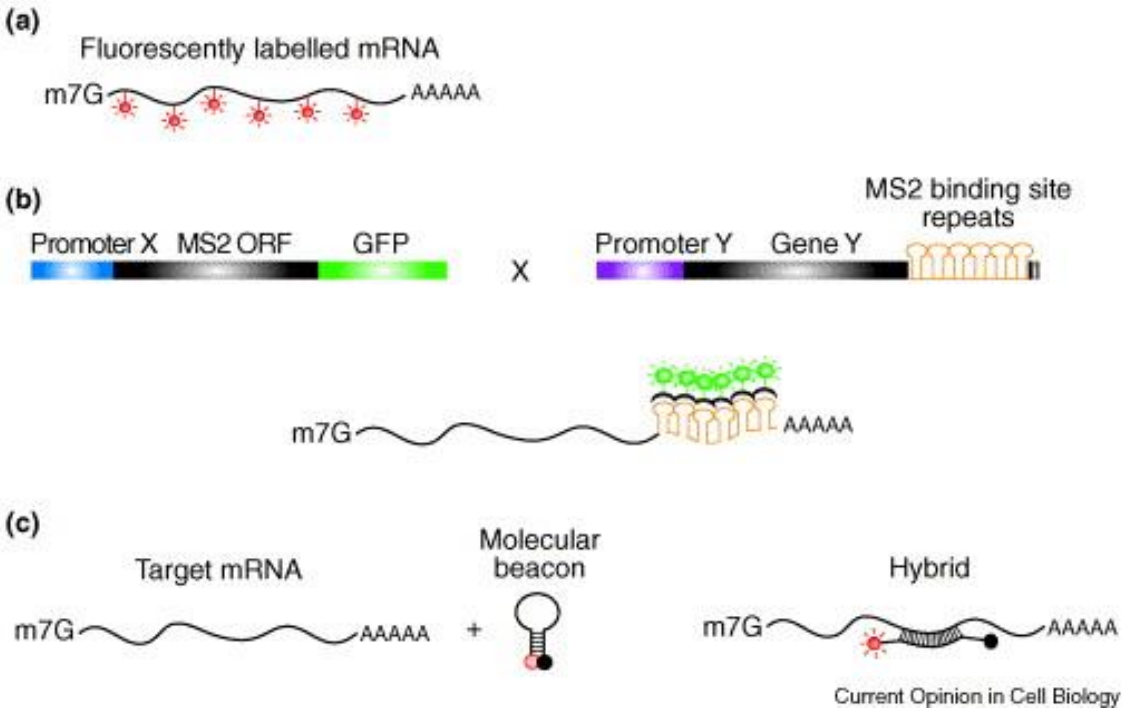


**Figure 1.2 Methods for visualizing mRNA in live cells**

A) Synthetic mRNA that has been directly labelled with fluorescent molecules are injected into living cells to study their movement. B) The MS2 system uses one plasmid under the control of promoter X that contains the bacteriophage RNA-binding protein (MS2) open reading frame fused to the green fluorescent protein gene sequence. The second plasmid contains the cDNA from of the mRNA of interest fused to multiple MS2 binding sites under the control of the genes promoter. When both constructs are expressed in a cell, the MS2-GFP protein will bind to the MS2 binding sites fused to the target mRNA to fluorescently label the transcript. C) A molecular beacon is an oligonucleotide that contains a fluorophore on one end and a fluorescent quencher on the other. The secondary structure of the beacon places the fluorescent quencher close to the fluorophore eliminating the signal. A molecular beacon that has a central sequence that is complementary to the target mRNA is injected into living cells. Upon hybridization the secondary structure is disrupted, and the fluorophore signal is no longer quenched. This results in the fluorescent labeling of the target mRNA. Image from Van De Bor and Davis (2004).

The first live-cell mRNA imaging approach used the MS2 system in budding yeast to determine the dynamics of *ASH1* mRNA movement (Bertrand et al., 1998). This two-plasmid system takes advantage of a bacteriophage RNA-binding protein (MS2) (Figure 1.2B). Expression of both plasmids within a cell will fluorescently label the target transgenic mRNA with multiple fluorescent proteins. This MS2 system has been used in a variety of mRNA localization studies in eukaryotes including Drosophila, *Mus musculus* (mouse), and rice (Belaya and St Johnston, 2011; Forrest and Gavis, 2003; Hamada et al., 2003a; Lange et al., 2008; Park et al., 2014; Tyagi, 2009). Whether the MS2 system provides an accurate representation of the localization dynamics of the mRNA has sometimes been questioned, as the MS2-FP fusion protein can form dimers and large aggregates, and is also subjected to degradation in the cellular environment leading to free fluorescent protein in the cytoplasm (Schönberger et al., 2012). Other systems have been developed using RNA-binding proteins and aptamers which are monomers and arguably more stable in the cellular environment (Schönberger et al., 2012; Chung and Takizawa, 2011). The limitation of these RNA-binding systems is that visualization of endogenous mRNA is not possible and the placement of the aptamer on the target mRNA can interfere with its proper localization.

The molecular beacon is another live-cell imaging technique that aims to visualize endogenously expressed mRNAs (Figure 1.2C). This system has potential as a technique to non-invasively observe endogenous RNAs. However, molecular beacons are limited by background noise caused by degradation of the beacon and also by the potential of secondary mRNA structures interrupting the hybridization of the beacon to the target (Santangelo et al., 2004; Bratu et al., 2011). Nevertheless, molecular beacons have been

employed in multiple studies (Bratu et al., 2003; Tyagi and Alsmadi, 2004; Santangelo et al., 2004, 2005; Bratu et al., 2011)

The most recent advancement in live-cell imaging of mRNAs is the engineering of RNA mimics of fluorescent proteins (Paige et al., 2011; Strack et al., 2013). This technique allows for the direct labelling of fluorescent mRNAs by genetically inserting RNA aptamers into the transcript of interest. These aptamers bind to small fluorescent molecules to activate fluorescence of the molecule. The thermal instability and misfolding of the RNA aptamer in living systems has been a challenge along with the level of fluorescence, as only one fluorophore binding to single RNAs has been achieved. Therefore, an effort to develop a more practical variant is being pursued.

### 1.3 Subcellular mRNA Localization in Plants

In comparison to other eukaryotic systems, the published work related to subcellular mRNA localization in plants is limited, with the majority of studies over ten years old. Localized transcripts have been identified in algae and higher plants. These examples involve the targeting of mRNAs to the surface of organelles, during cell division and embryo development, and in cellular differentiation. However, little is known about the mechanisms involved in the localization of most of these transcripts and the extent that subcellular mRNA localization plays as a role in plant development. Long distant mRNA movement between cells and virus RNA movement within and between cells has been more extensively studied in plant systems and is better understood than intracellular mRNA localization in plants. A comprehensive overview of intercellular

RNA localization in plants can be found in several published reviews (Kehr and Buhtz, 2008; Kragler, 2013; Marín-González and Suárez-López, 2012).

### *1.3.1 Targeting of Nuclear mRNAs to Organelles*

#### 1.3.1.1 Chloroplast

Maintaining a functional chloroplast is dependent upon proper targeting and import of over 2,500 proteins that are encoded by the nucleus (Shi and Theg, 2013). Determining how the nuclear encoded proteins are targeted to the chloroplast is essential in understanding the molecular processes of chloroplast differentiation and maintenance. Evidence has emerged to suggest that protein targeting to the chloroplast can occur through subcellular mRNA localization. The mRNAs that encode a few of the proteins involved in chlorophyll synthesis and photosynthesis have been shown to concentrate to the periphery of the chloroplast in *Arabidopsis thaliana* (Arabidopsis), *Triticum aestivum* (wheat), and Chlamydomonas (Gibson et al., 1996; Marrison et al., 1996; Uniacke and Zerges, 2009). Magnesium protoporphyrin IX chelatase (CHL) is an enzyme complex with three subunits that incorporate a magnesium ion into protoporphyrin IX during chlorophyll synthesis (Papenbrock et al., 2000). It has been demonstrated through colourmetric *in situ* hybridization of leaf tissue sections that one subunit, CHL H, appears to localize to the periphery of chloroplasts in Arabidopsis and wheat leaf cells (Marrison et al., 1996; Gibson et al., 1996).

The light-harvesting complex of photosystem II (LHCII) is imbedded in the thylakoid membrane surrounding photosystem II and functions to bind chlorophyll a and b molecules (Minagawa and Takahashi, 2004). The mRNAs that encode subunits of

LHCII concentrate at the surface of chloroplasts in wheat (using colourometric visualization) and Chlamydomonas (using fluorescence visualization)(Uniacke and Zerges, 2009; Marrison et al., 1996). The mRNA localization pattern observed for the subunits of LHCII in wheat are similar to CHL H. In Chlamydomonas, LHCII mRNAs concentrate in the cytoplasm to the basal lobe of the chloroplast and co-localize with cytoplasmic ribosomes for localized translation (Uniacke and Zerges, 2009). In Chlamydomonas, this localization pattern is depended upon translation and suggests that the subunits of LHCII are localized through the nascent polypeptide in a cotranslational mechanism. Light-dependent NADPH protochlorphyllide oxidoreductase (POR) is a group of enzymes involved in plastid differentiation in chloroplasts. POR catalyzes the reduction of protochlorophyllide to chlorophyllide, which is the first light-dependent step in chlorophyll synthesis (Apel et al., 1980). Colourmetric *in situ* hybridization studies in wheat leaf sections revealed that the mRNA of *POR-A* and *POR-B* is concentrated around the chloroplast in the cytosol in the same manner to that of CHL-H and LHCII (Marrison et al., 1996).

Ribulose bisphosphate carboxylase/oxygenase (Rubisco) is an enzyme involved in carbon fixation during photosynthesis. It is comprised of two subunits, the chloroplast encoded large subunit (RBCL) and the nuclear encoded small subunit (RBCS). There are two RBCS genes (*RBCS1* and *RBCS2*) that make up a multigene family in Chlamydomonas (Khrebtukova and Spreitzer, 1996). The mRNA of *RBCS2* co-localizes with cytosolic ribosomes randomly throughout the cytoplasm, and supports the model for posttranslational import into the chloroplast (Uniacke and Zerges, 2009). The mRNA that encodes RBCL was found within the chloroplast and was concentrated to the perimeter of

the pyrenoid, the site of $CO_2$ fixation in algae. RBCL is localized to the pyrenoid through a co-translational mechanism and is an example of subcellular mRNA localization within an organelle.

D1 is a chloroplast encoded core protein of the photosystem II complex involved in the electron transport chain of the light-dependent reaction of photosynthesis. D1 is commonly damaged by intense environmental light. To maintain proper photosystem II function, damaged D1 protein is continually replaced with a newly synthesized protein (Järvi et al., 2015). The newly synthesized protein is localized to the existing photosystem II complex in the thylakoid membrane through D1 mRNA localization in a translation-dependent mechanism (Uniacke and Zerges, 2009). In contrast, during de novo photosystem II assembly D1 protein is targeted to the thylakoid membrane through D1 mRNA in a translation independent manner (Uniacke and Zerges, 2009). For either circumstance, the D1 mRNA was found to co-localize with chloroplast ribosomes thereby indicating localized translation and is another example of subcellular mRNA localization within an organelle.

#### 1.3.1.2 Endoplasmic reticulum

The most extensive area of plant subcellular mRNA localization study has been focused on the mRNAs that encode the seed storage proteins in rice and *Zea mays* (maize) endosperm cells (Crofts et al., 2004; Okita and Choi, 2002). These studies are the only examples of fluorescence *in situ* hybridization of subcellular mRNA localization in higher plant cells, and uses a technique called *in situ* PCR amplification to amplify the target mRNA for visualization. The ER plays an important role in synthesizing storage

proteins during seed development in plants. These seed storage proteins are metabolized by the growing embryo as a nutrient source. Three major storage proteins have been studied for mRNA localization: the alcohol soluble prolamines, and the salt-soluble globulins and glutelins (Choi et al., 2000; Li et al., 1993; Okita and Choi, 2002; Washida et al., 2004, 2012) (Figure 1.3). Prolamines form intracisternal inclusion granules called protein bodies (PB) in the ER lumen, while globulins and glutelins are stored in protein storage vacuoles (PSV). Prolamine is targeted to the PB in the ER lumen by localizing its mRNA to the PB-ER subdomain in both rice and maize (Choi et al., 2000; Li et al., 1993; Washida et al., 2004). In rice, the prolamine mRNA is targeted to the PB-ER surface through *cis* elements on the 3' UTR and on the coding region, and movement of the ribonucleoprotein particle is in a translationally repressed state (Choi et al., 2000; Hamada et al., 2003b). Four *cis*-elements are responsible for localizing prolamine mRNA in maize; one in the 3' UTR and three within the coding sequence of the mRNA (Washida et al., 2009a). The presence of localization sequences within the coding region indicates that maize prolamine mRNA is also translationally repressed during transport (Washida et al., 2009a). The dependence on translational arrest for proper transcript localization occurs in other eukaryotic systems (Gu et al., 2004; Macdonald, 2004). Live cell imaging techniques were used to determine the movement patterns of prolamine mRNA in rice (Hamada et al., 2003a). Multiple copies of the prolamine mRNA move together as one unit along actin filaments in unidirectional stop and go movements towards the cortical region of the cell. The movement is characteristic of a mechanism involving cytoskeletal motors.

Rice glutelin seed storage protein is transported by the cisternal ER for storage in the PSV (Figure 1.3). Glutelin targeting to the cisternal ER is facilitated by the

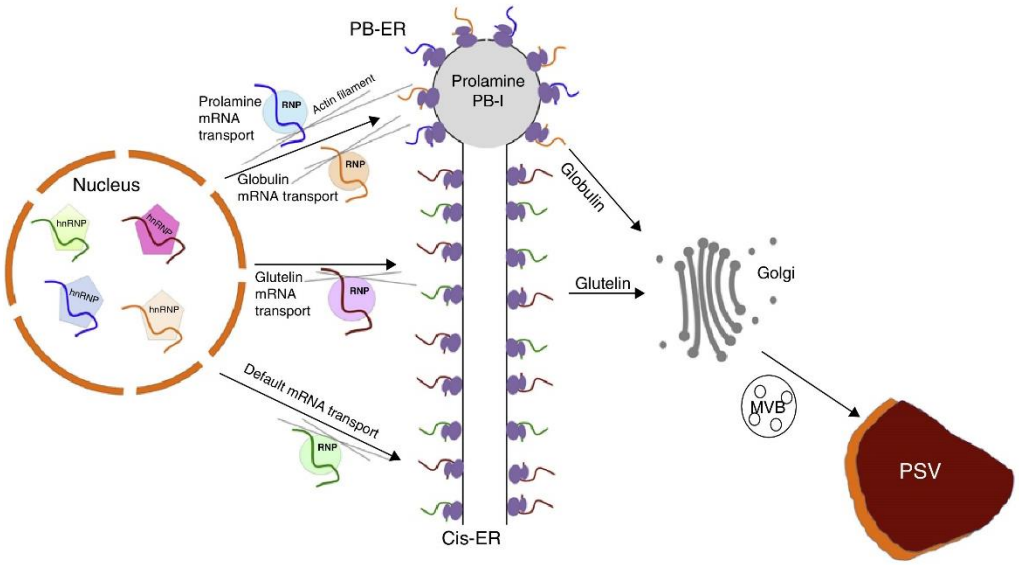


**Figure 1.3 Subcellular mRNA localization of seed storage mRNAs in rice endosperm cells**

Three mRNAs, prolamine mRNA (blue curve) globulin mRNA (orange curve) and glutelin mRNA (red curve), are components of individual RNPs upon export from the nucleus. Prolamine and globulin mRNAs travel to the PB-ER via actin filaments (grey lines) where both proteins are synthesized. Prolamine protein accumulates to form PB-I (grey circle) while the globulin protein is transported to the PSV via the Golgi apparatus. The glutelin mRNA is transported via actin filaments to the Cisternal ER (Cis-ER) where glutelin protein is synthesized. The glutelin protein is then transported to the PSV via the Golgi apparatus. The default mRNA transport (green RNP) refers to the targeting of mRNAs that lack *cis* elements to the Cis-ER. Adapted from Tian and Okita (2014).

localization of its cognate RNA to the cisternal ER by three *cis*-elements containing two conserved sequences amongst each other (Li et al., 1993; Washida et al., 2009b). Two of the *cis*-elements are found in the 5' and 3' end of the coding sequence, while one is found in the 3' UTR (Washida et al., 2009b). Conserve sequences among the *cis* elements are indicative of a sequence based RNA recognition signal for glutelin mRNA localization (Washida et al., 2009b).

Rice globulin seed storage protein is stored in the PSV similar to glutelin. However, globulin mRNA does not target to the cisternal ER but rather to the PB-ER (Washida et al., 2012). The globulin protein localizes to the periphery of the PB and is packaged into Golgi-associated dense vesicles (Figure 1.3). If the globulin mRNA is mis-localized to the cisternal ER, improper packaging of globulin and glutelin into the PSV results. This suggests that localization of seed storage protein mRNAs to separate ER subdomains functions to prevent undesirable protein interactions that prevent proper import into PSV (Washida et al., 2012).

### *1.3.2 Other Examples of Subcellular mRNA localization*

Despite the increasing evidence for a subcellular mRNA localization involvement in protein compartmentalization during embryo development, research in plants has been limited to two studies in the brown alga *Fucus distichus* (fucus) that focused on total mRNA and actin mRNA distribution (Bouget et al., 1995, 1996). The fucus zygote will form a polar axis 8 to 10 hours after fertilization when exposed to light. This results in cell division and the development of the rhizoid cell on the shaded side of the embryo and the thallus cell on the other side (Bouget et al., 1995). During embryogenesis, the total

mRNA of the zygote forms a concentration gradient highest at the thallus pole resulting in the majority of the total mRNA residing in the thallus cell after cytokinesis (Bouget et al., 1995). After the first cell division actin mRNA no longer concentrates to the thallus pole but concentrates at the cell plate for the first two divisions of the rhizoid (Bouget et al., 1996). The movement of total mRNA to the thallus pole is dependent on axis formation and microfilaments. However, the localization of actin mRNA to the cell plate requires only that cell plate formation occurs. This suggest that targeting of actin mRNA to the cell plate could occur through cytoplasmic streaming and mRNA anchoring to the cell plate (Bouget et al., 1996).

Cell plate formation in higher plants requires a GTPase called phragmoplastin, the GTP-binding proteins (ROP1 and RAN2), and a phragmoplastin-interaction protein (PHIP1) (Ma et al., 2008). RAN2 mRNA is localized to the phragmoplast during cell division in *Nicotiana tabacum* (tobacco) and PHIP1 is the RNA-binding protein that functions to localized RAN2 mRNA during cytokinesis (Ma et al., 2008).

Trichoplasts are polarized epidermal cells with tubular extensions that develop into root hairs. Actin filaments mediate the development of cell tip extensions by forming dense F-actin meshworks (Geitmann and Emons, 2000; Miller et al., 1999). This meshwork is stabilized by an actin binding protein called profilin which accumulates at the cell tip extension of the root hair (Baluska et al., 2000). In maize, profilin-encoding *ZmPRO4* mRNA localizes to the growing extension by interacting with the actin filaments themselves (Baluska et al., 2000). Localized translation at the extending tip allows for efficient and rapid localization of ZmPRO4 protein to properly stabilize the dynamic actin meshwork in the expanding trichoblast.

Tracheary elements are water-conducting vessels in xylem that develop from procambial cells that expand along their longitudinal axis prior to cell death (Fukuda, 1996). Expansin proteins loosen the cell wall to allow for the longitudinal axis expansion (Im et al., 2000). The mRNAs that encode three different expansin proteins in *Zinnia elegans* (ZeExp1, ZeExp2 and ZeExp3) localize tightly to the apical (ZeExp1 and ZeExp3) and the basipetal (ZeExp2) end of developing xylem cells (Im et al., 2000). The mechanism for localizing expansin mRNAs has not been determined. However, by restricting the localization of these mRNAs to the site of future growth, the expansin protein will only be expressed where cell wall loosening is required.

Carbonic anhydrase (CA) is a catalytic zinc metalloenzyme that reversibly converts $CO_2$ to $HCO_3^-$ in most living systems (Moroney et al., 2001). In algae, CA is needed to convert $HCO_3^-$ from the aqueous environment to $CO_2$ for photosynthesis (Serikawa et al., 2001). The unicellular macroalga *Acetabularia acetabulum* has high CA activity at the apical portion of the giant cell which corresponds with the concentration gradient of two CA encoding mRNAs (*AaCA1* and *AaCA2*) (Serikawa et al., 2001). This suggests that the CA enzyme is concentrated to the site of activity within the cytoplasm through mRNA localization.

These studies indicate that subcellular mRNA localization is a mechanism used by various plant systems during cell development, differentiation and division. However, no subsequent studies have been published to further investigate these claims or to understand how these transcripts are localized and none of these studies used fluorescence *in situ* hybridization techniques.

### 1.4 Objectives of This Thesis

The limited knowledge of subcellular mRNA localization in higher plants highlights the need for a method to study subcellular mRNA localization in a model plant system. This would provide a means to identify additional examples of localized mRNAs in plant cells and would provide tools for downstream analysis on the mechanisms responsible for mRNA localization. Although it is clear that subcellular mRNA localization has an important role in eukaryotic cell function, the frequency of this process in higher plants is not known.

Hypothesis:

Subcellular mRNA localization is a mechanism used by higher plants to localize proteins to specific regions of the cytoplasm and to organelle surfaces as a form of post-transcriptional gene regulation.

The specific objectives of this thesis research were to:

1) Establish a fluorescence WISH protocol in the model plant Arabidopsis that could be used to perform a large scale analysis of subcellular mRNA localization. Once established, the initiation of the large scale analysis would be carried out.
2) Optimize single RNA molecule *in situ* hybridization techniques in Arabidopsis to visualize the subcellular mRNA localization of target mRNAs in a quantitative manner for the first time in plant cells.

# CHAPTER 2. MATERIALS AND METHODS

## 2.1 Arabidopsis Seedling and Cell Culture Growth Conditions

Wild type Arabidopsis seedlings (Columbia, Col-0) were grown on half-strength Murishige and Skoog (MS) media (PhytoTechnology Laboratory), 1% (w/v) sucrose, agar (Caisson Labs) plates (pH 5.7). Approximately 45 seeds were placed in two rows per plate and incubated vertically in the dark at 4°C for 48-60 hours followed by exposure to 16 hours of light, 8 hours of dark at 22°C for 6 days.

Arabidopsis cell suspension cultures were subcultured weekly in liquid medium consisting of 0.44% (w/v) MS media, 0.05 µg/ml kinetin, 0.5 µg/ml 1-naphthaleneacetic acid and 3% (w/v) sucrose (pH 5.7). Four milliliters of one week-old cell culture was pipetted into 40 ml of fresh liquid medium. Cultures were grown in the dark, shaking at 170 rpm on an orbital shaker at room temperature (RT). Cell cultures that were used for *in situ* hybridization were harvested six days after their subculture date.

## 2.2 Riboprobe Synthesis

### *2.2.1 PCR Amplification of DNA Template*

Riboprobes were synthesized from DNA templates that were produced using polymerase chain reaction (PCR) amplification of wild type cDNA. PCR was performed using the following program: one cycle at 95°C for 4 min, 30 cycles at 94°C for 35 sec, one cycle at 54°C for 35 sec, one cycle at 72°C for 50 sec, one cycle at 72°C for 3 min, ending at 4°C. The PCR master mix contained 1X Taq reaction buffer (Lamda Biotech), 0.8 mM dNTP, 1.5 mM $MgCl_2$, 4% (v/v) DMSO, 0.1 µM of each primer and 5 units of

Taq DNA polymerase (Lamda Biotech). Primers were designed to amplify a unique segment of the target gene and incorporate the T7 or T3 RNA polymerase binding site (Table 2.1). The segments amplified were unique to the target mRNA and usually resided within the 3' untranslated region (UTR) of the gene. All amplified DNA templates were electrophoresed on 1% agarose gels, gel eluted (QIAquick Gel Extraction Kit, QIAGEN) and sequenced (University of Calgary, University Core DNA services). DNA template concentration and purity were determined by spectrophotometry (NanoDrop 1000, Thermo Scientific).

### *2.2.2 In vitro Transcription*

*In vitro* transcription was performed using the DNA templates described in Section 2.2.1 to produce riboprobes that were labelled with either digoxigenin (DIG) or biotin (Hejátko et al., 2006). The 10X NTP mix used for *in vitro* transcription contained 10 mM of ATP, CTP and GTP, 6.5 mM of UTP and 3.5 mM of either DIG-11-UTP (Roche) or Biotin-16-UTP (Roche). The reaction mixture contained 300-500 ng of DNA template, 1X NTP mix, 20 U RNasin (Roche) and either 10 U T3 RNA polymerase (Roche) and T3 transcription buffer (Roche) or 10 U T7 RNA polymerase (Life Technologies) and T7 transcription buffer (Life Technologies). The reaction was carried out at 37°C for 120 min. The T3 and T7 RNA polymerase was used to amplify the sense and the antisense riboprobes, respectively. Riboprobe quality and quantity was determined using 2% agarose gel electrophoresis and spectrophotometry. Riboprobes greater than 150 bp in length were shortened to approximately 150 bp using hydrolysis following the protocol from Hejatko et al. (2006).

**Table 2.1 PCR primer sequences for DNA template amplification**

| mRNA Target | Primer | Sequence (5'-3') | Region Amplified [i] | Size (bp) |
|---|---|---|---|---|
| abnormal inflorescence meristem (AIM-1) At4g29010 | Forward | GAG **AAT TAA CCC TCA CTA AAG GGA GA*** G TAT ATG CAG AAG GAG AGG CTG | 13 to 190 | 177 |
| | Reverse | GGA *TAA TAC GAC TCA CTA TAG GGA GA** C TTT ATG AAA CTG ACG TCA CTA CAA AC | | |
| breaking of asymmetry in the stomatal lineage (BASL) At5g60880 | Forward | GAG **AAT TAA CCC TCA CTA AAG GGA GA**C AGC CAT GGC TTC ACA GTG GAC | -791 to -10 | 781 |
| | Reverse | GGA *TAA TAC GAC TCA CTA TAG GGA GA* C ATT GGA ACC CTA AAG CAA CTG GC | | |
| light dependent NADPH protochlorophyllide reductase (PORB) At4g27440 | Forward | GAG **AAT TAA CCC TCA CTA AAG GGA GA**C TCT CGG TAC CAA TCG AAG AAA TC | 31 to 142 | 111 |
| | Reverse | GGA *TAA TAC GAC TCA CTA TAG GGA GA* C CAA GCA ATC TAC ACT CAA CAG AC | | |
| light harvesting complex of photosystem II 5 (LHCB5) At4g10340 | Forward | GAG **AAT TAA CCC TCA CTA AAG GGA GA**C AGC TGG TTT CAT CAT TCC TGA AG | -467 to -337 | 130 |
| | Reverse | GGA *TAA TAC GAC TCA CTA TAG GGA GA* G GGA TGT TCT TGC CAA AGT AGT TC | | |
| magnesium chelatase subunit H/CHLH (GUN5) At5g13630 | Forward | GAG **AAT TAA CCC TCA CTA AAG GGA GA**C GCT TGT GTA TTC TCC ATT CAC TC | -4,136 to -3,979 | 157 |
| | Reverse | GGA *TAA TAC GAC TCA CTA TAG GGA GA* C CGT TTC CAG ATA CAG CAG ATT TC | | |
| mitochondrial malate dehydrogenase (mMDH-1) At1g53240 | Forward | GAG **AAT TAA CCC TCA CTA AAG GGA GA**C AGT GAT TAA ACC GAG TTT ACT CG | -3 to 289 | 295 |
| | Reverse | GGA *TAA TAC GAC TCA CTA TAG GGA GA* C TGA GAA ACA GAA AGT ATG GTG AC | | |
| peroxisomal malate dehydrogenase (pMDH-1) At2G22780 | Forward | GAG **AAT TAA CCC TCA CTA AAG GGA GA**A GAG ACT CGA TCG TGA ATA AAC AC | 0 to 565 | 565 |
| | Reverse | GGA *TAA TAC GAC TCA CTA TAG GGA GA* C TCA CAA GAT CAT CTT AGT CTA AGA G | | |
| ribulose bisphosphate carboxylase large subunit (RBCL) AtCg00490 | Forward | GAG **AAT TAA CCC TCA CTA AAG GGA GA**G ACC GAG ATC TTT GGA GAT GAT TC | - 268 to -123 | 145 |
| | Reverse | GGA *TAA TAC GAC TCA CTA TAG GGA GA* T GCA AGA TCA CGT CCC TCA TTA C | | |
| ribulose bisphosphate carboxylase small subunit (RBCS1A) At1g67090 | Forward | GAG **AAT TAA CCC TCA CTA AAG GGA GA**C ACG GAT TTG TGT ACC GTG AG | -234 to -54 | 180 |
| | Reverse | GGA *TAA TAC GAC TCA CTA TAG GGA GA* G GTG TTG TCG AAT CCG ATG ATC | | |

*The extension for T3 RNA polymerase binding site is bolded and T7 RNA polymerase binding site italicized; bp = base pair; [i]Relative to the stop codon on cDNA. Negative numbers are in the coding region.

*2.2.3 Dot Blots*

Riboprobe labelling efficiency and quality was determined by dot blot analysis using a protocol similar to that described previously (Zimmerman et al., 2013). Riboprobes were diluted in DEPC treated dd$H_2O$ to 2 ng/ul, 500 pg/ul, and 100 pg/ul. One microliter of each dilution was pipetted onto a dry nylon membrane (Amersham Hybond –N+) and immediately UV crosslinked (UVC-508 Ultraviolet Crosslinker) 10 cm from the light source at 0.1 J/$cm^2$ followed by a brief wash in TBST (50 mM Tris pH 7.5, 150 mM $NaCl_2$, 0.05% Tween-20 (Sigma)). The membrane was blocked in 5% (w/v) skim milk powder in TBST for 30 min before incubating 30 min in diluted anti-DIG-POD Fab fragments (Roche) antibody (anti-DIG-HRP). The antibody was diluted 1:1000 in 5% (w/v) skim milk powder in TBST. The membrane was washed twice for 15 min in TBST followed by processing with SuperSignal West Pico Chemiluminescent Substrate (Thermo Scientific) as per the manufacturer's instructions. The membrane was placed in an autoradiography cassette (Fisher) and exposed to X-ray film (Biomax, Kodak) in the dark for 1 hour, followed by film processing.

## 2.3 Whole Mount *in situ* Hybridization (WISH)

A florescence WISH protocol was developed to detect mRNAs at the subcellular level in Arabidopsis cotyledons. This was adapted from multiple protocols (Basyuk et al., 2000; Uniacke and Zerges, 2009; Uniacke et al., 2011; Lécuyer et al., 2008; Pavlova et al., 2010; Khrustaleva and Kik, 2001; Vargas et al., 2011; de Almeida Engler et al., 1998; Küpper et al., 2007; Rozier et al., 2014; Hejátko et al., 2006). The following is the final optimized protocol.

*2.3.1 WISH Using Arabidopsis Seedlings*

2.3.1.1 Fixation

Five days post-germination (dpg) seedlings with roots removed were fixed in 4% (w/v) paraformaldehyde (Sigma), 15% (v/v) DMSO, and 0.1% (v/v) Tween-20 in 1X PBS (130 mM NaCl, 7 mM $Na_2HPO_4$, 3 mM $NaH_2PO_4$, pH 7.4) at a 1:1 ratio with n-heptane in 50 ml falcon tubes. A stock solution of 10% (w/v) paraformaldehyde in DEPC treated $H_2O_2$ was made fresh by heating the mixture to about 60°C (no boiling) while stirring vigorously. NaOH was added to the heated solution to raise the pH to 7.4. Once dissolved, the solution was placed on ice to cool. Fixation was performed at RT under vacuum for 15 min followed by 75 min of mixing on a vertical rotary mixer at low speed. To reduce autofluorescence, two methanol washes were performed for 20 min at -20°C followed by three ethanol washes for 5 min at RT. Seedlings were stored overnight in ethanol at -20°C.

2.3.1.2 Permeabilization and Hybridization

The shoot cuticle was removed by submerging the samples in an equal mixture of xylene and ethanol for 15 min. Shoots were treated with 1% $H_2O_2$ in methanol for 30 min to inactivate endogenous peroxidase activity. Samples were rehydrated by washing for 10 min each in 75% ethanol in DEPC treated water, 50% ethanol in 1X PBS, and 25% ethanol in 1X PBS prior to suspending the seedlings in 1X PBS. A cell wall digestion step was performed to further permeabilize the tissue (modified from Rozier et al., 2014). A 6X cell wall digestion solution containing 0.5% (w/v) cellulase (Yakult Honsha) and 0.25% pectolyase Y23 (Bioworld) in DEPC treated dd$H_20$ was passed through a 0.2 µm

filter and stored in aliquots at -20 °C. One aliquot was diluted to a 1X cell wall digestion solution using PBS containing 0.1% Tween-20 (PBST), heated to 55°C for 10 min, and cooled to RT before use. Shoots were digested for 6 min in 1X cell wall digestion solution at RT.

A second fixation step was then performed for 30 min with gentle shaking in fixative described above minus heptane. Shoots were incubated in Proteinase K (60 µg/ml) (Roche) in PBS for 15 min at 37°C. Proteinase K activity was inactivated by incubating shoots in 2 mg/ml glycine for 5 min, followed by two 10 min PBST washes. Shoots were fixed again for 20 min before being lightly scored with a sterile razor blade and carefully transferred to 48 well microtiter plates for hybridization. Shoots were incubated in pre-hybridization solution containing 50% (v/v) formamide (Sigma), 5X SSC, 0.1% (v/v) Tween-20 and 0.1 mg/ml heparin (Sigma) for 1 hour at 55°C. Overnight hybridization at 55°C was carried out in pre-hybridization solution supplemented with 1 mg/ml of denatured herring sperm DNA (Sigma) and 20-100 ng/ml of denatured DIG-labelled riboprobe. The microtiter plate was sealed tightly with plastic wrap and taped to limit evaporation. The herring sperm DNA stock (10 mg/ml) was previously sheared by passing through a 16-18 gauge needle, aliquoted and stored at -20°C until needed. Prior to adding to the hybridization solution, an aliquot of the herring DNA stock was warmed to 94°C for 5 min and placed immediately on ice to denature the DNA. The riboprobe was denatured by heating to 70°C for 10 min and then placing on ice.

2.3.1.3 Probe Washes and Antibody Incubation

A series of washes were performed at 55°C with increasing stringency, starting with 10 min, 60 min and 20 min washes in 50% (v/v) formamide, 2X SSC, and 0.1% (v/v) Tween-20. Samples were then washed for 20 min in 2X SSC, 0.1% (v/v) Tween-20 followed by two washes for 20 min in 0.2X SSC, 0.1% (v/v) Tween-20 and three 10 min washes in PBST. Samples were blocked at RT in a solution containing 10% (v/v) normal goat serum (Sigma) in PBST before incubation in 1:100 diluted anti-DIG-HRP overnight in the dark at room temperature. The antibody was diluted in 2% bovine serum albumin (BSA) and 1.5% normal goat serum in PBST.

2.3.1.4 Tyramide Amplification

Shoots were washed eight times, 20 min each in PBST to ensure that excess antibody was removed from the samples in order to reduce background staining. The fluorescently labeled tyramide used in this project was synthesized and generously donated by Dr. Peter Vize (Vize et al., 2009). Washed seedlings were incubated in tyramide-FITC or tyramide-CY3 diluted 1:10,000 in amplification buffer (0.1% (w/v) thimerosal (Sigma), 10 mM $Na_2HPO_4$, 2 mM $KH_2PO_4$) supplemented with 0.0015% $H_2O_2$ for 15 min. Three quick rinses followed by two 30 min washes in PBST was performed before mounting the shoots in Vectashield (Vector Labs) on 25 x 75 x 1 mm diamond white glass microscope slides (Globe Scientific Inc.) in preparation for imaging.

2.3.1.5 Colourmetric Visualization

For colorimetric staining, all steps were the same as Section 2.3.1.3 until the blocking stage where the seedlings were incubated for 90 min in blocking buffer containing 1% (w/v) BSA in PBST. Anti-digoxigenin-AP, Fab fragments (Roche) antibody (anti-DIG-AP) was diluted 1:2,000 in 1% (w/v) BSA in PBST and incubated with seedlings overnight in the dark. Excess antibody was removed as described in Section 2.3.1.4. The shoots were then incubated twice for 10 min in alkaline phosphatase buffer (ALP) containing 0.1 M Tris-HCl, pH 9.5, 0.1 M NaCl, 50 mM $MgCl_2$, 0.1% Tween-20. ALP was made with fresh $MgCl_2$ because it is unstable (Hejátko et al., 2006). Staining was performed in ALP buffer supplemented with 2 mM levamisole (Sigma), 1125 µg/ml NBT (Roche) in 70% (v/v) N, N dimethylformamide (DMF), and 875 µg/ml BCIP (Roche) in 70% (v/v) DMF. The length of the staining period varied with each probe, ranging from 50-120 min. Shoots were washed in 100% ethanol followed by 15 min in 50% ethanol before mounting in 50% (v/v) glycerol on microscope slides in preparation for imaging.

*2.3.2 Single RNA Molecule WISH on Arabidopsis Seedlings*

Multiple singly labelled probe (MSLP) sets were purchased from Biosearch Technologies. These probe sets contained 48 antisense oligonucleotide probes that were 20 nucleotides long and each containing a single fluorophore. These probes were complementary to unique sequences on the target mRNA (Table 2.2). The RBCS1A probe set was fluorescently labelled with Cal Fluor Red 610 with a maximum excitation/emission of 590 nm/610 nm. The ACT7 probe set was fluorescently labelled

with FITC with a maximum excitation/emission of 495 nm/519 nm. The BASL probe set was fluorescently labelled with Cy3 with a maximum excitation/emission of 550 nm/570 nm.

RNAscope Fluorescent Multiplex Kit was purchased from Advance Cell Diagnostics (ACD). The kit uses branched DNA (bDNA) technology and contains paired oligonucleotide probes designed to target unique sequences of the target mRNA in tandem and three amplifying buffers which dramatically increase signal and decrease background to achieve single molecule visualization (Table 2.2). The last amplification buffer, AMP4-FL, contained probes labelled with Atto 550 (excitation/emission of 554 nm/ 580 nm) or Alexa 488 (excitation/emission of 490 nm/ 525 nm). Further details on the bDNA approach are described in Chapter 4.

2.3.2.1 Multiple Singly Labelled Probes (MSLP)

The fixation and permeabilization was performed on 5 dpg shoots as described above in Section 2.3.1.1 and 2.3.1.2, except the scoring step was omitted. Prior to hybridization samples were incubated in wash buffer (2X SSC, 10% formamide in DEPC treated dd$H_2O$) for 5 min at 37°C. Hybridization was performed overnight in microtiter plates at 37°C in buffer containing 10% (w/v) dextran sulfate, 2X SSC, and 10% formamide supplemented with 250 nM of Custom Stellaris MLSP probe sets. Samples were washed twice for 30 min in wash buffer at 37°C and mounted in Vectashield solution on microscope slides in preparation for imaging.

**Table 2.2 Single molecule fluorescence *in situ* hybridization oligonucleotide probes**

| mRNA target | Probe Type |
|---|---|
| actin 7 (ACT7) | MSLP |
| alanine aminotransferase-1 (AlaAT1) | bDNA |
| breaking of asymmetry in the stomatal lineage (BASL) | MSLP |
| ribulose bisphosphate carboxylase small subunit (RBCS1A) | MSLP |
| ribulose bisphosphate carboxylase small subunit (RBCS1A) | bDNA |

MSLP = multiple singly labelled probes; bDNA = branched DNA technology

2.3.2.2 Branched DNA (bDNA) technology

The fixation and permeabilization was carried out on 5 dpg shoots as described above in Section 2.3.1.1 and 2.3.1.2 except the light scoring step was omitted. Overnight hybridization in a microtiter plate was carried out at 40°C as per manufacturer's instructions using the solutions provided (RNAscope Fluorescent Multiplex Kit, ACD). Amplification and washing times recommended in the manufacturer's instructions were extended (Table 2.3) because of the multiple tissue layers in a whole mount sample. Sufficient time was needed for probe penetration during amplification and for removal of unbound amplifiers during washing. Samples were mounted in Vectashield on microscope slides in preparation for imaging.

*2.3.3 bDNA Using Arabidopsis Protoplasts and Cell Culture*

2.3.3.1 Protoplasts

A cell wall enzyme solution was made by heating 20 mM MES pH 5.7, 0.4 M mannitol, and 7 mM $CaCl_2$ to 70°C for 5 min then adding 1.5% (w/v) cellulase, 0.2% (w/v) pectolyase Y23 to the mixture and incubating at 55°C for 10 min. The solution was cooled to RT before adding 5 mM β-mercaptoethanol and 0.1% (w/v) BSA. Media was removed from light grown Arabidopsis suspension culture and replaced with cell wall enzyme solution and incubated for 4 hours in the dark at RT. After 4 hours of incubation, an equal volume of W5 buffer (2 mM MES pH 5.7, 154 mM $NaCl_2$, 125 mM $CaCl_2$, 5 mM KCl in DEPC treated dd$H_2O$) was added to the enzyme solution/cell mixture and centrifuged (Micromase, IEC) at 100 g for 3 min. The pellet was resuspended in W5 solution and placed on ice for 30 min.

**Table 2.3 RNAscope fluorescent multiplex kit amplification protocol modifications**

| Step | Solution | Suggested Time (min) | Actual Time (min) |
|---|---|---|---|
| Pre-amplifier hybridization | Amp 1-FL | 30 | 120 |
| Wash | 1 X wash buffer | 2 | 45 |
| Signal enhancement | Amp 2-FL | 15 | 60 |
| Wash | 1 X wash buffer | 2 | 45 |
| Amplifier hybridization | Amp3-FL | 30 | 120 |
| Wash | 1 X wash buffer | 2 | 45 |
| Label probe | Amp4-FL | 15 | 60 |
| Wash | 1 X wash buffer | 2 | 45 |

2.3.3.2 Fixation and Permeabilization of Protoplasts

Protoplasts were pelleted by centrifugation at 100 g for 3 min and fixed in a 1:1 mixture of 8% paraformaldehyde and 2X MMG (8 mM MES pH 5.7, 0.8 M mannitol, 30 mM $MgCl_2$ in DEPC treated $ddH_2O$) for 10 min. The cells were washed twice with 1X MMG followed by treatment with 0.3% (v/v) Triton X-100 (Sigma) in PBS for 10 min. The protoplasts were washed twice in PBS and placed onto Superfrost plus 25 X 75 X 1 mm microscope slides (VWR). The protoplasts were washed three times for 5 min in 100% (v/v) methanol at -20 °C and submerged in 70% (v/v) ethanol at 4°C overnight. Protoplasts were rehydrated by washing in 50% (v/v) ethanol in PBS for 5 min, followed by one 10 min PBS wash. Pretreat 3 from the RNAscope Fluorescent Multiplex Kit was diluted 1:15 in PBS and placed on the protoplasts for 10 min followed by three short washes in PBS.

2.3.3.3 Fixation and Permeabilization of Cultured Cells

Media was removed from light grown Arabidopsis suspension culture and replaced with cell wall enzyme solution and incubated for 30 min in the dark at RT. The cells were pelleted by centrifugation at 200 g for 3 min. and fixed in a 1:1 ratio of 8% paraformaldehyde and 2X MMG for 10 min. The cells were washed twice with 1X MMG and then incubated in methanol twice at -20°C for 10 min each. Cells were stored at 4°C overnight in 100% ethanol. Cells were rehydrated by washing in 50% ethanol in PBS for 5 min, followed by one 10 min wash in PBST and then placed on Superfrost plus slides. Samples were exposed to Pretreat 3 diluted 1:15 in PBS for 10 min followed by three short washes in PBST. A negative control RNase treatment was performed using 0.2

µg/ml RNase A in PBST and incubating at 37 °C for 10 min followed by three PBST washes.

2.3.3.4 Hybridization and Amplification using Protoplasts and Cultured Cells

The hybridization, amplification steps and imaging using protoplasts and cultured cells were carried out using the RNAscope Fluorescent Multiplex Kit following the manufacturer's instructions for cultured adherent cells.

*2.3.4 MLSP using Cultured Cells*

Media was removed from light grown Arabidopsis suspension culture and replaced with cell wall enzyme solution and incubated for 30 min in the dark at RT. The cells were pelleted by centrifugation at 200 g for 3 min and fixed in a 1:1 ratio of 8% paraformaldehyde and 2X MMG for 10 min. The cells were washed three times with 1X MMG then incubated in 60 µg/ml proteinase K in PBS for 3 min. Cells were washed for 5 min with glycine and twice in PBS. Cells were resuspended in 70% ethanol overnight at 4°C. Two methanol washes at – 20°C for 10 min were performed, followed by one 2 min wash in 50 % ethanol in PBS and one 10 min wash in PBS. Cells were incubated in wash buffer for 5 min at 37°C. Hybridization was performed for 4 hours at 37°C in buffer containing 10 % (w/v) dextran sulfate, 2X SSC, and 10% formamide supplemented with 250 nM of Custom Stellaris MLSP probe sets (Biosearch Technologies). Samples were washed twice for 30 min in wash buffer at 37°C before imaging.

*2.3.5 Dual Labelling WISH with Tyramide Amplification*

2.3.5.1 Fixation, Permeabilization and Hybridization

Shoots 5 dpg were fixed and permeabilized as described in Section 2.3.1.1 and 2.3.1.2. Hybridization conditions were as described in Section 2.3.1.2 except that in addition to the 20-100 ng/ml of the DIG-labelled riboprobe, 20-100 ng/ml of biotin-labelled riboprobe targeting a different mRNA was also added.

2.3.5.2 Washing and Antibody Incubation

Samples were washed and the first round of antibody incubation was performed as described in Section 2.3.1.3 using anti-DIG-HRP. The following day the samples were processed for tyramide amplification as described in Section 2.3.1.4 using tyramide-FITC until the last wash step. Samples were then incubated in 0.3% $H_2O_2$ for 30 min to inactivate the HRP attached to the anti-DIG-HRP (Pinaud et al., 2008). A 30 min wash in PBST was performed to remove the $H_2O_2$ before repeating the antibody incubation, tyramide amplification and washing process above using anti-Biotin-HRP and tyramide-CY3. Samples were mounted in Vectashield on microscope slides in preparation for imaging.

## 2.4 *In situ* Hybridization on Sectioned Arabidopsis Seedlings

A protocol described previously (Jackson, 1991) was modified for the fixation, infiltration, embedding, and colorimetric *in situ* hybridization.

*2.4.1 Fixation and Infiltration*

Five dpg seedlings with roots removed were fixed in chilled 50% (v/v) ethanol, 5% (v/v) acetic acid and 3.7% (w/v) paraformaldehyde in DEPC treated dd$H_2O$ for a total of 4 hours. The first two hours of fixation was performed in a vacuum oven (Precision Scientific, National Appliance Company) attached to a vacuum pump (DualSeal 1400, Welch) at 20 mmHg for one hour and 27 mmHg for the second hour. Seedlings were fixed on ice in fresh fixative for the remaining two hours. Shoots were dehydrated gradually on ice using the following ethanol wash series: two washes for 30 min in 50% (v/v) ethanol, one wash for 30 min each in 60% (v/v) ethanol, 70% (v/v) ethanol, and 85% (v/v) ethanol. Shoots were stored at 4°C overnight in 95% (v/v) ethanol with 0.1% Eosin Y (Sigma) to stain the tissue.

Samples were incubated at RT in 100% (v/v) ethanol followed by a wash series of xylene:ethanol to gradually permeate the samples in 100% (v/v) xylene. This allowed for the paraffin wax to dissolve and encompass the samples completely. Each wash was performed at RT for 30 min in 10 ml of 25% (v/v), 50% (v/v), 75% (v/v) and 100% (v/v) xylene in ethanol. Twenty Paraplast Plus chips (McCormick Scientific) were added to the seedlings in 100% (v/v) xylene and incubated at RT overnight.

Samples were placed in a 42°C oven to melt the remaining wax. Paraplast plus chips were added every 10-15 min until they would no longer dissolve. At that point the seedlings were moved to a 60°C oven for two hours. Half of the xylene:wax mixture was replaced with 100% melted paraplast plus chips and incubated for another two hours at 60°C then stored in 100% wax overnight at 60°C. Two 100% wax exchanges were

performed six hours apart and stored overnight at 60°C. The vial caps were left open to allow residual xylene to evaporate off the sample.

*2.4.2 Embedding and Sectioning*

Wax molds approximately 10 x 5 x 2 cm were hand made using paper cards. One 20 ml vial containing 20 shoots was emptied into each mold and filled to the top with melted paraffin. Using hot metal tools, seedlings were carefully arranged in 6 groups of 2-3 and positioned properly. The molds were floated in ice cold water for 30 min to minimize air pocket formation as the wax solidifies. Samples were then allowed to solidify for a couple hours at RT before being stored at 4°C. The paper molds were removed and the wax was cut into cubes separating the 6 groups. The wax was trimmed to create a 2 mm boarder around the seedlings. Each cube was mounted onto plastic holders filled with wax by melting the wax of the cube and of the holder together. This was allowed to cool at RT for several hours. The blocks were stored at 4°C until needed.

Sections were made using a microtome (MT-920, Research and Manufacturing Company) with a thickness of 5 µm. Special care was taken to insure the microtome and surrounding area was RNase free. The resulting ribbons were floated on top of DEPC treated water on Superfrost plus 25 x 75 x 1 mm microscope slides on a slide warmer (Fisher) set at 60°C. Slides were carefully monitored until the ribbons had completely flattened and stretched out. Water was drained from the slides before placing on a slide warmer at 40°C to completely dry overnight. Once dried the slides were stored at 4°C.

*2.4.3 Clearing and Hybridization*

Slides were processed in 80 ml glass coplin jars for the remainder of the protocol unless indicated otherwise. The wax was removed by washing twice for 10 min in xylene. Shoots were hydrated using an ethanol series of 1 min washes in 100% (v/v), 95% (v/v), 90% (v/v), 80% (v/v) + 0.85% (w/v) NaCl , 60% + 0.85% (w/v) NaCl, and 30% (v/v) + 0.85% (w/v) NaCl. Proteinase digestion was carried out in 100 mM Tris, pH 7.5, 50 mM EDTA with 1 µg/ml proteinase K at 37°C for 30 min. The digestion was stopped using 2 mg/ml glycine in PBS. Post fixation was performed with 4% (w/v) formaldehyde in PBS followed by an acetylation step using 1.3% (v/v) triethanolamine (Sigma), 0.3% acetic anhydride (Sigma) pH 8 in PBS. The samples were dehydrated prior to hybridization using the same ethanol series above (minus xylene) to allow for better penetration of the probe. If the riboprobes were to be visualized using tyramide amplification then a wash with 100% (v/v) methanol at -20°C for 15 min followed by a 15 min incubation at RT in 1% $H_2O_2$ in methanol was carried out. The hybridization solution contained 50% (v/v) formamide (Sigma), 10% (w/v) dextran sulfate (Sigma), 1X hybridization salts (100 mM Tris pH 7.5, 10 mM EDTA pH 8, 3 M NaCl), 1X Denhardt's solution (Sigma), and 0.5 mg/ml tRNA. Prior to hybridization, 0.5-1 µl of riboprobe was diluted in 50% (v/v) formamide in DEPC water to a final volume of 37.5 µl and heated to 80°C for 2 min then put on ice. The diluted probe was added to 112.5 µl of pre-warmed hybridization solution and placed directly onto the slides and covered with coverslips (22 x 40 # 1.5, Fisher). A plastic container containing autoclaved paper towel soaked in 2X SSC and 50% (v/v) formamide was pre heated to 55°C. The slides were placed in the tightly sealed container

and placed in a plastic bag containing water soaked Kimwipes to maintain humid conditions and left at 55°C overnight.

*2.4.4 Washing and Antibody Incubation*

Coverslips were removed by washing in 2X SSC at 55°C for several minutes. Slides were washed 4 times for 30 min each in 0.2X SSC at 55°C, once for 5 min in 0.2X SSC at 37 °C, once for 5 min in 0.2X SSC at RT and once for 5 min in PBS, then stored overnight at 4°C in PBS. A blocking solution containing 1% (w/v) blocking agent (Roche) in maleic acid buffer (100 mM maleic acid pH 7.5, 150 mM NaCl) was added 1 ml per slide and incubated for 45 min at RT. The solution was drained and replaced by 1 ml of BSA wash solution (1% (w/v) BSA, 0.3% Triton –X100, 100 mM Tris HCl pH 7.5, 150 mM NaCl) and incubated for 45 min. The antibody used (anti-DIG-HRP or anti-DIG-AP) was diluted at 1:1250 in BSA wash solution and 250 µl applied to each slide. A coverslip was added and the samples were left for 90 min at RT. Coverslips were removed by washing in BSA wash solution, and the slides were then washed three times for 20 min each in BSA wash solution.

*2.4.5 Colourmetric Visualization*

Slides were washed twice for 15 min in TNM-50 (100 mM Tris pH 9.5, 100 mM NaCl, 50 mM $MgCl_2$). One milliliter of staining solution (0.1 mg/ml NBT, 0.1 mg/ml BCIP in TNM-50) was added to the slides, covered with a coverslip and incubated in the dark for 3.5 hours or longer. Samples were monitored and staining was stopped with 1X TE pH 8.0 (100 mM Tris pH 8.0, 10 mM EDTA pH 8.0) once the purple precipitate

appeared lightly in the sense controls. Samples were mounted in 50% (v/v) glycerol for imaging.

*2.4.6 Tyramide Amplification*

Slides were washed twice for 15 min in PBS. Tyramide-FITC was diluted 1:10,000 in amplification buffer (0.1% (w/v) thimerosal, 10 mM $Na_2HPO_4$, 2 mM $KH_2PO_4$) supplemented with 0.0015% $H_2O_2$. 1 ml of this solution was applied to each slide and incubated for 10 min. Three 5 min washes in PBS were performed followed by mounting in Vectasheild in preparation for imaging.

**2.5 Imaging**

Specimens were analyzed using either a Plan Fluotar 40X objective lens, a Plan APO 63X oil immersion objective lens, or a HCX PL Fluotar 100X oil immersion objective lens attached to an epifluorescence microscope (Leica, DMR Germany). The filter sets used were 31002-TRITC (RFP) and 31001-FITC (GFP). Images were captured with a cooled CCD camera (Retiga 1350 EX, QImaging, BC, Canada) and processed using Volocity software (Version 4.0, Improvision, Waltham, MA). Specimens were also imaged using a 63X oil immersion lens attached to an inverted laser scanning confocal microscope (Leica, Germany, Model TCS-SP2). Image processing for confocal microscopy was performed with Leica Application Suite Advance Fluorescence (Leica Microsystems). Adobe Photoshop software (Version 6.3, Adobe Systems Incorporated, San Jose, CA) was used to assemble figures and to enhance images by adjusting contrast, pseudo coloration and resolution.

# CHAPTER 3. SUBCELLULAR TRANSCRIPT LOCALIZATION IN ARABIDOPSIS

## 3.1 Introduction

Subcellular mRNA localization in higher plants has not been well characterized, with the majority of studies focused on rice and maize seed storage protein mRNA targeting to the ER. A protocol for detecting mRNAs at the subcellular level using fluorescence whole mount *in situ* hybridization (WISH) in higher plants has not been established to date but would be useful for identifying additional examples of plant subcellular mRNA localization. Here, a novel protocol was established that has the resolution to observe the localization of abundant mRNAs in Arabidopsis seedling cotyledon cells. This protocol used fluorescence WISH with digoxigenin labelled riboprobes (Figure 3.1). The goal was to design a protocol that could be used in a global analysis of mRNA localization in higher plants. Optimization of several steps in the WISH protocol was performed in an attempt to preserve the mRNA integrity and position in the cell. Increasing probe access into tissue, lowering autofluorescence, eliminating non-specific signals, and amplifying the fluorescent signal to acceptable levels of detection were also challenges that required optimization. This chapter summarizes the fluorescence WISH protocol in Arabidopsis cotyledons and reports the subcellular mRNA localization results of three transcripts that encode ribulose bisphosphate carboxylase small subunit (RBCS1A), ribulose bisphosphate carboxylase large subunit (RBCL) and light harvesting complex of photosystem II 5 (LHCB5) in Arabidopsis using this approach.

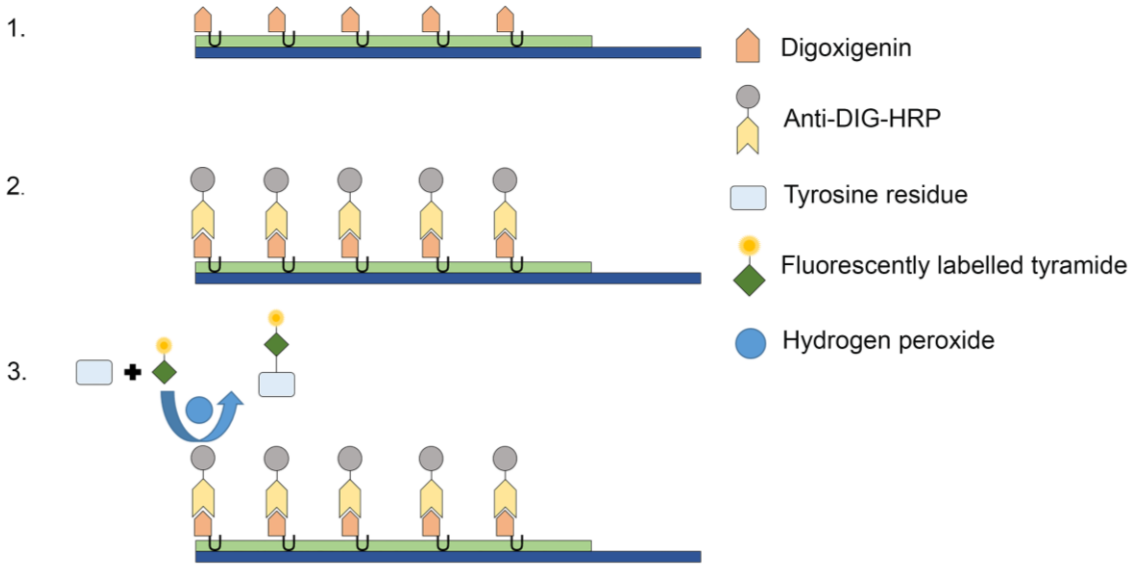


**Figure 3.1 Indirect labelling using tyramide signal amplification**

1) The riboprobe (green) containing digoxigenin labelled uridines (orange) hybridizes to the target mRNA (dark blue). 2) Digoxigenin specific antibodies (yellow) coupled to horseradish peroxidase (grey) binds to the digoxigenin labelled uridines. 3) In the presence of hydrogen peroxide (blue) horseradish peroxidase will modify the fluorescently labelled tyramide (dark green) into a radical that covalently binds to a nearby tyrosine reside (light blue). Multiple tyramide molecules will precipitate at each horseradish peroxidase enzyme to create an amplified signal.

## 3.2 Results

### *3.2.1 Riboprobe Synthesis For in situ Hybridization*

Riboprobes were synthesized by *in vitro* transcription using template DNA that contained an RNA polymerase binding site, as described in Section 2.2.2. The template DNA was amplified from cDNA using PCR, as described in Section 2.2.1. Nine different templates were amplified and the DNA quality was tested by agarose gel electrophoresis. Each amplified DNA template contained the T7 and T3 RNA polymerase binding sites and was the expected size on agarose gels (Figure 3.2). Antisense RNA probes were transcribed using T7 RNA polymerase and sense probes were synthesized using T3 RNA polymerase. A total of 18 riboprobes were synthesized. Nine were antisense probes and nine were sense probes. The riboprobes were electrophoresed on 2% agarose gels to determine if the *in vitro* transcription was successful. The sharp band observed at the bottom of each lane corresponded to tRNA that was used as a carrier during the precipitation of the riboprobes after synthesis (Figure 3.3). The smeared riboprobe RNA signal likely corresponded to folded versions of the riboprobe on these non-denaturing gels. These gels could not be used to determine specific riboprobe length because the RNA was not denatured and the molecular weight marker was DNA. An RNase digestion assay was performed on the RBCL riboprobes to ensure that the strong diffused signal observed in Figure 3.2 was RNA and not DNA. The *in vitro* transcription product exposed to RNase A was degraded whereas DNase I did not affect the *in vitro* transcription product (Figure 3.4).

The labelling efficiency of all 18 riboprobes was tested using dot blots (Figure 3.5). All riboprobes were detected when 2.0 μg of the riboprobe was dot blotted. The

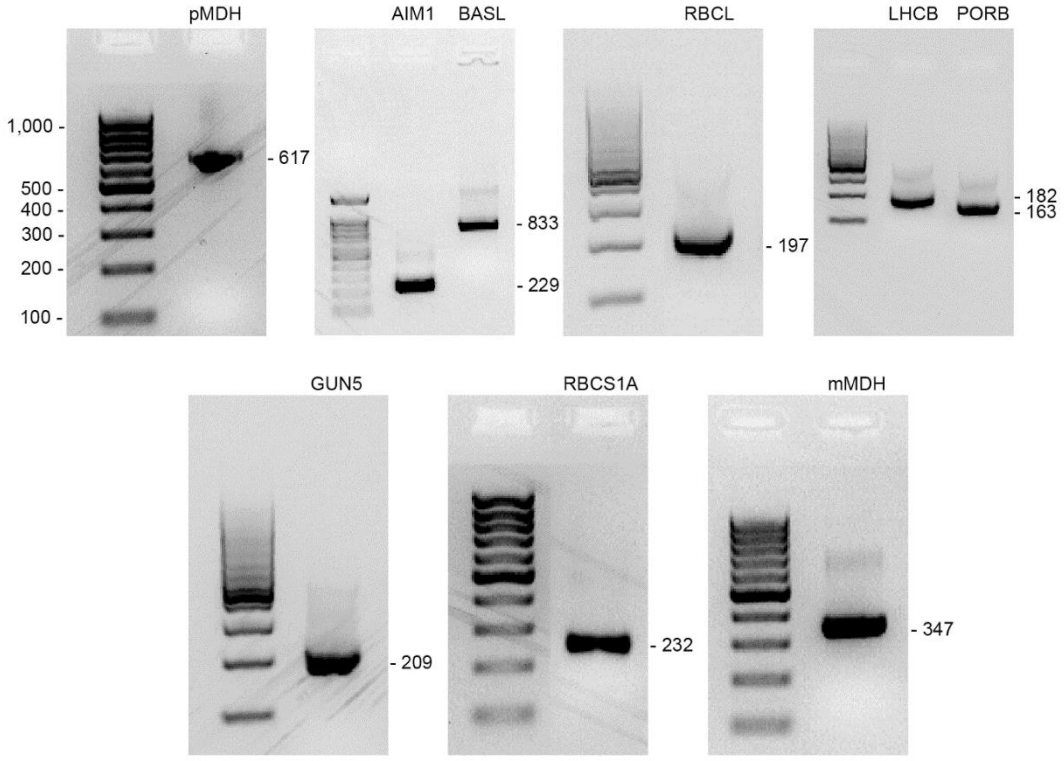


**Figure 3.2 Agarose gel electrophoresis of PCR amplified DNA templates**

Each DNA template was amplified from cDNA to incorporate RNA polymerase binding sites for *in vitro* transcription. Eight microliters of each PCR product was run on a 2% agarose gel containing ethidium bromide at 106 V for 25-30 min. The band sizes for the 100 bp ladder are indicated on the top left gel. The band size of each PCR product is indicated (base pairs). pMDH, peroxisomal malate dehydrogenase; AIM1, abnormal inflorescence meristem; BASL, breaking of asymmetry in the stomatal lineage; RBCL, ribulose bisphosphate carboxylase large subunit; LHCB, light harvesting complex of photosystem II 5; PORB, light depended NADPH protochlorophyllide reductase; GUN5, magnesium chelatase subunit H/CHL H; RBCS1A, ribulose bisphosphate carboxylase small subunits; mMDH, mitochondrial malate dehydrogenase.

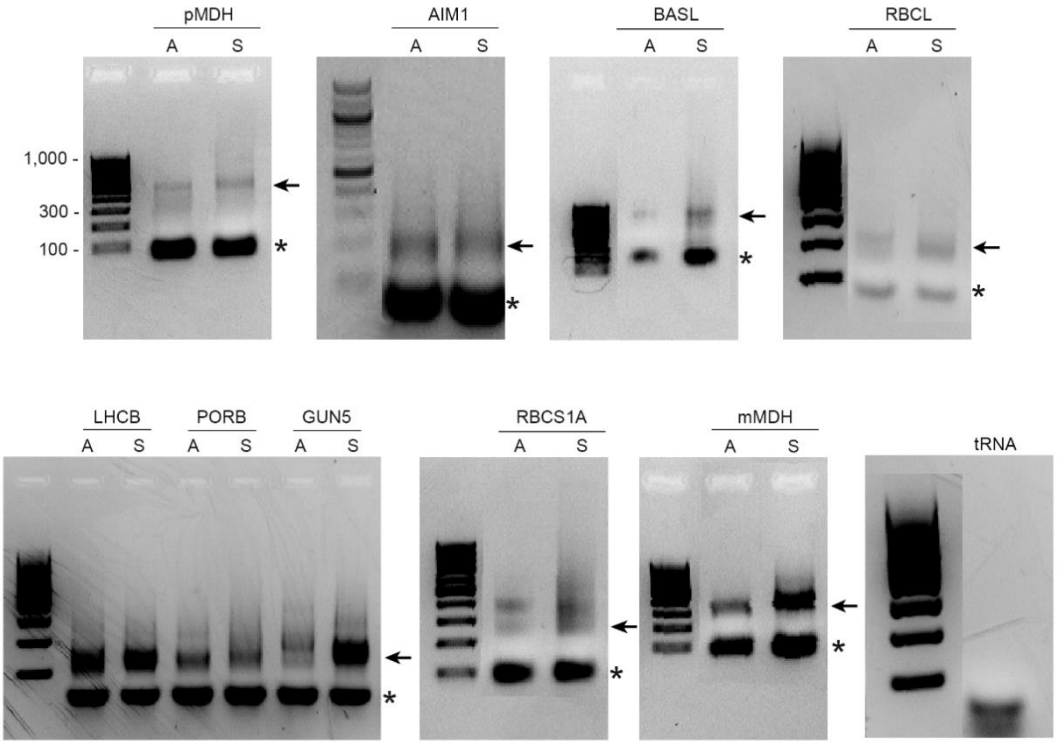


**Figure 3.3 Agarose gel electrophoresis of digoxigenin labelled riboprobes synthesized by *in vitro* transcription**

Riboprobes were transcribed from PCR amplified DNA templates using T7 RNA polymerase (antisense probe) or T3 RNA polymerase (sense probe). Eight microliters of each *in vitro* transcription reaction was run on a 2% agarose gel containing ethidium bromide at 106 V for 30 min. The band sizes for the DNA ladder is shown in base pairs on the top left gel. The arrows identify the smeared riboprobe band and the asterisks identify the tRNA used to precipitate the riboprobe. A, antisense riboprobe; S, sense riboprobe.

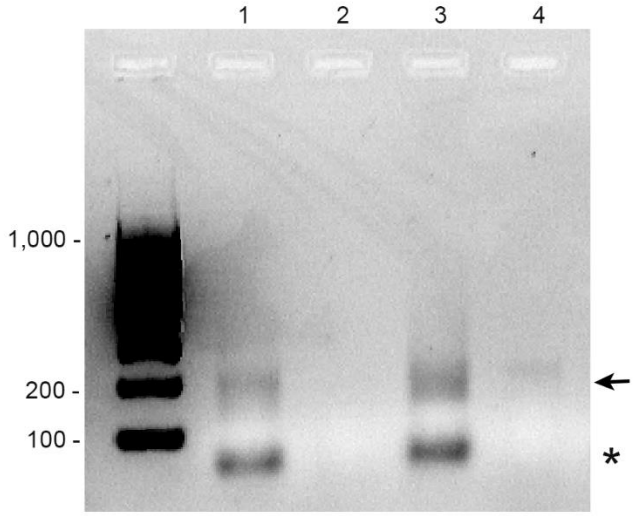


**Figure 3.4 Agarose gel electrophoresis of digoxigenin labelled riboprobes treated with RNase A and DNase I**

A 2% agarose gel stained with ethidium bromide and electrophoresed for 35 min at 106 V with a 100 bp ladder. Band sizes are indicated in base pairs. Lane 1, RBCL antisense riboprobe treated with DNase 1; Lane 2, RBCL antisense riboprobe treated with RNase A; Lane 3, RBCL sense probe treated with DNase 1; Lane 4, RBCL sense probe treated with RNase A. The arrows identify the riboprobe band and the asterisks indicates tRNA used to precipitate the riboprobe.

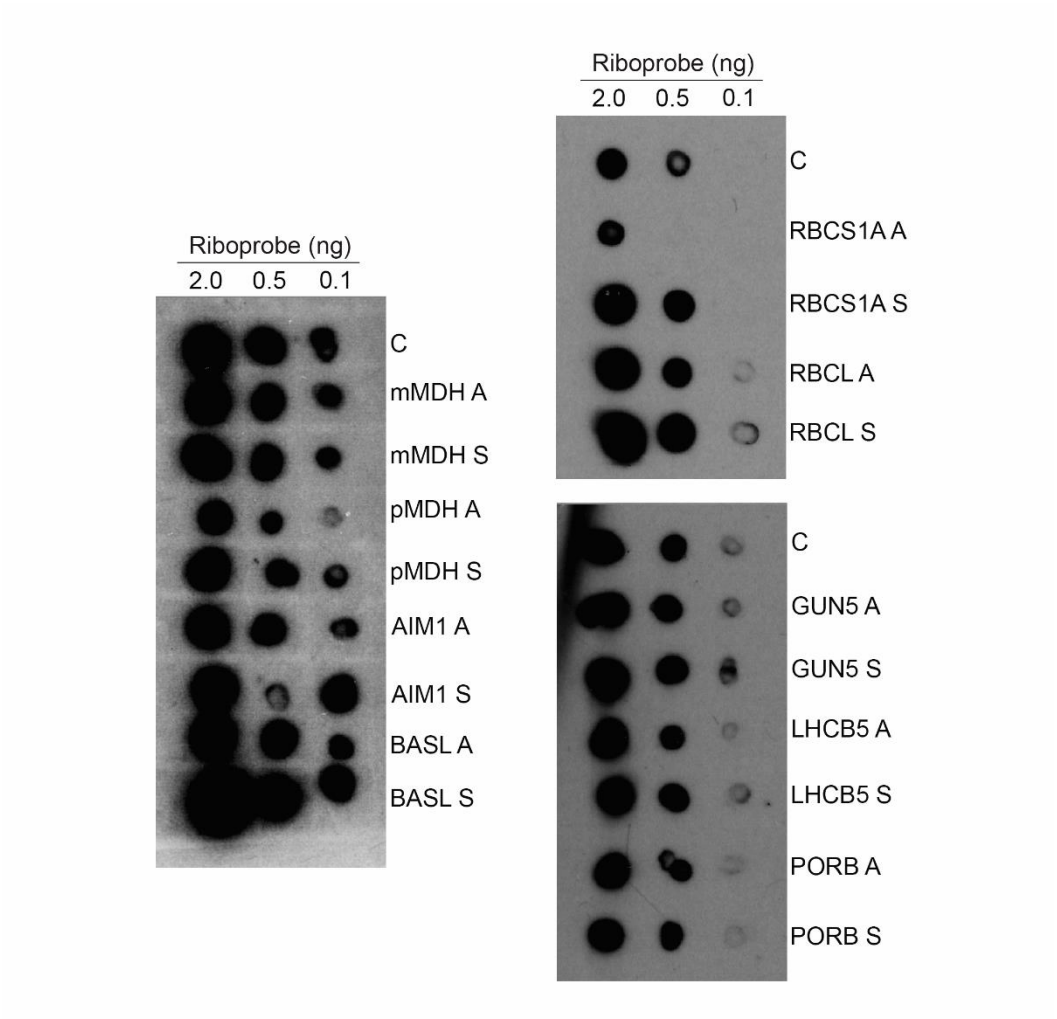


**Figure 3.5 Labelling efficiency of digoxigenin labelled riboprobes**

Dot blot analysis was performed to determine digoxigenin incorporation into riboprobes. Decreasing amounts of riboprobes were blotted onto a dry nylon membrane (2.0 ng, 0.5 ng and 0.1ng) and immediately UV crosslinked. The nylon membrane was incubated with anti-DIG-HRP antibody and imaged using chemiluminescence detection. Three separate dot blots where performed each with the same positive control. C, positive control Hoxa11 digoxigenin labelled riboprobe from mouse; A, antisense riboprobe; S, sense riboprobe.

RBCS1A antisense probe was not detected at the 0.5 μg loading, and all riboprobes except the RBCS1A antisense and sense probes were observed at a 0.1 μg loading. The positive control for each dot blot was an antisense probe designed to detect Hoxa11 mRNA from mouse (Gift of Dr. John Cobb) (Neufeld et al., 2014). The detection efficiency of Hoxa11 differed between the three dot blot experiments.

Biotin labelled riboprobes were synthesized to target either RBCL or RBCS1A using the same DNA templates that were used for digoxigenin labelled riboprobes. The products from *in vitro* transcription were electrophoresed on agarose gels to determine quality (Figure 3.6). Similar to the digoxigenin probes (Figure 3.3) the sharp bands at the bottom of the gel correspond to tRNA and the strong diffuse signal observed is the biotin labelled riboprobe (Figure 3.6). Dual labelling experiments using both biotin and DIG labelled riboprobes were attempted as described in Section 2.3.4 to target both RBCL and RBCS1A in the same cell. Dual labelling was never achieved, and neither the biotin labelled nor the DIG labelled riboprobes produced any signal when used together (data not show).

### *3.2.2 Fluorescence WISH in Cotyledons*

#### 3.2.2.1 Developing the Fluorescence WISH Protocol

Incorporation of components of different fluorescence *in situ* hybridization protocols that have been established for animals and plants (Basyuk et al., 2000; Uniacke and Zerges, 2009; Uniacke et al., 2011; Lécuyer et al., 2008; Pavlova et al., 2010; Khrustaleva and Kik, 2001; Vargas et al., 2011; de Almeida Engler et al., 1998; Küpper et al., 2007; Rozier et al., 2014) were used to modify an existing WISH protocol for

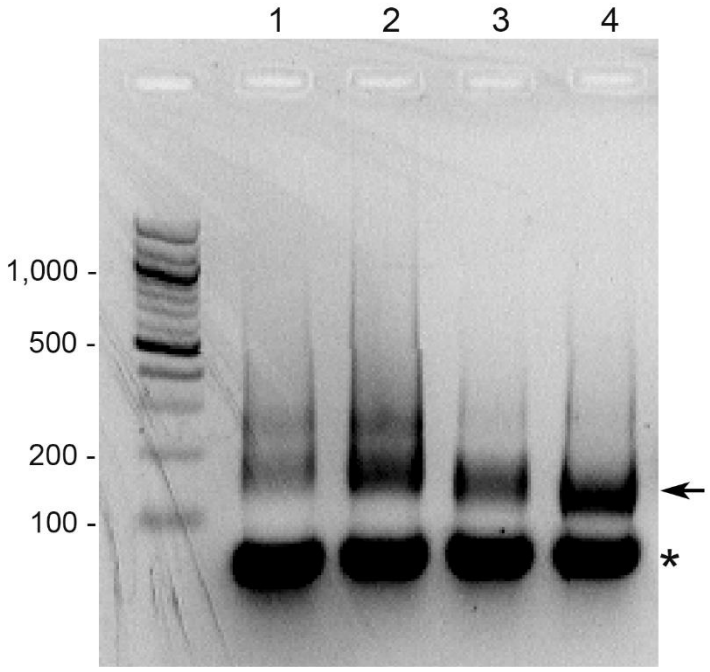


**Figure 3.6 Agarose gel electrophoresis of biotin labelled riboprobes synthesized by *in vitro* transcription**

Riboprobes were transcribed from PCR amplified DNA templates using T7 RNA polymerase (antisense) or T3 RNA polymerase (sense). Eight µl of each *in vitro* transcription product was electrophoresed on a 2% agarose gel containing ethidium bromide at 106 V for 30 min. Lane 1, RBCS1A antisense probe; Lane 2, RBCS1A sense probe; Lane 3, RBCL antisense probe; Lane 4, RBCL sense probe. A standard 100 bp ladder was use and the band sizes are indicated in base pairs. The arrow indicates the presence of the riboprobe. The asterisk indicates tRNA used to precipitate the riboprobes during *in vitro* transcription.

Arabidopsis (Hejátko et al., 2006) to establish a protocol for detecting subcellular mRNA localization in Arabidopsis cotyledons. The main parameters that were adjusted were the fixation, permeabilization, clearing, and antibody incubation steps. Table 3.1 provides a summary of experiments that were performed for optimization of the fluorescence WISH protocol. Most of the individual optimization experiments were performed more than once. Fixation time was adjusted from 45 min to 90 min and the use of a vacuum desiccator was incorporated to enhance infiltration of the fixative. The optimization of fixation conditions resulted in an enhanced preservation of the tissue as determined by morphological examination (Figure 3.7). Cell permeabilization was increased with the incorporation of a cell wall digestion step, using a proteinase K treatment at 37°C, and by gently scoring the tissue with a razor blade immediately prior to hybridization. Clearing was enhanced by increasing the methanol incubation time from 5 min to 20 min, and by decreasing the incubation temperature from 25°C to – 20°C. Those adjustments resulted in dramatically reduced autofluorescence levels in both the GFP and RFP filter channels (Figure 3.7B). Additionally, modifying the blocking solution composition and the solution used to dilute the anti-DIG-HRP was shown to dramatically reduce non-specific interactions. The use of 10% normal serum as the blocking reagent and the addition of 2% BSA with 1.5% normal serum when diluting the antibody (compared to 1% BSA) also significantly reduced non-specific fluorescent signal (Figure 3.7C).

**Table 3.1 Troubleshooting whole mount fluorescence *in situ* hybridization in *Arabidopsis thaliana***

| Test # | Fixation | Permeabilization and Clearing | Hybridization | Antibody | Visualization | Results |
|---|---|---|---|---|---|---|
| 1 | 4% paraformaldehyde, 15% DMSO, 0.1% Tween-20 in PBS, pH 7.4 15 min with heptane | 1:1 EtOH:xylene 30 min<br>125 µg/ml proteinase K 15 min | 50% formamide, 5 x SSC, 0.1% Tween-20, 0.1 mg/ml heparin, 1 mg/ml herring DNA O/N 55 °C | block 90 min in 1% BSA in PBST<br>1:100 Anti-DIG-HRP: block buffer | TSA kit # 12 | under fixed<br>strong autofluorescence<br>signal in -ve controls |
| 2 | 4% paraformaldehyde, 15% DMSO, 0.1% Tween-20 in PBS, pH 7.4 20 min with heptane | 1:1 EtOH:xylene 30 min<br>125 µg/ml proteinase K 15 min | 50% formamide, 5 x SSC, 0.1% Tween-20, 0.1 mg/ml heparin, 1 mg/ml herring DNA O/N 55 °C | block 1% BSA in PBST 90 min<br>1:100 Anti-DIG-HRP: block buffer | TSA kit # 12 | under fixed<br>strong autofluorescence<br>signal in -ve controls |
| 3 | 4% paraformaldehyde, 15% DMSO, 0.1% Tween-20 in PBS, pH 7.4 45 min with heptane | 1:1 EtOH:xylene 30 min<br>125 µg/ml proteinase K 15 min | 50% formamide, 5 x SSC, 0.1% Tween-20, 0.1 mg/ml heparin, 1 mg/ml herring DNA O/N 55 °C | block 1% BSA in PBST 90 min<br>1:100 Anti-DIG-HRP: block buffer | TSA kit # 12 | under fixed<br>strong autofluorescence<br>signal in -ve controls |
| 4 | 4% paraformaldehyde, 15% DMSO, 0.1% Tween-20 in PBS, pH 7.4 45 min with heptane under desiccator vacuum | 1:1 EtOH:xylene 15 min<br>60 µg/ml proteinase K 15 min<br><br>2 x 10 min MeOH -20°C<br>2.5% RNase control | 50% formamide, 5 x SSC, 0.1% Tween-20, 0.1 mg/ml heparin, 1 mg/ml herring DNA O/N 55 °C | 0.3% $H_2O_2$ in PBS 30 min<br>block in BA 60 min<br>1:100 Anti-DIG-HRP: BA 2 hours, | 1:1,000 tyramide-FITC 15 min<br><br>2 x 5 min, 3 x 60 min PBST, O/N 4°C | poor cell morphology<br>autofluorescence greatly reduced<br>strong signal in -ve controls<br>Rnase treated cells look like untreated |
| 5 | 4% paraformaldehyde, 15% DMSO, 0.1% Tween-20 in PBS, pH 7.4 90 min with heptane | 1:1 EtOH:xylene 30 min<br>125 µg/ml proteinase K 15 min | 50% formamide, 5 x SSC, 0.1% Tween-20, 0.1 mg/ml heparin, 1 mg/ml herring DNA O/N 55 °C | block 1% BSA in PBST 90 min<br>1:100 Anti-DIG-HRP: block buffer O/N | TSA kit # 12 | mesophyll good morphology<br>epidermis poor morphology<br>medium autofluorescence<br>no signal observed |
| 6 | | 1:1 EtOH:xylene 15 min 125 µg/ml proteinase K 15 min | | | 1:100 tyramide-FITC or cy3 15 min<br>3 x PBST wash<br>1 x 5 min PBST | mesophyll good morphology<br>epidermis fair morphology<br>strong background fluorescence<br><br>cy3 > background then FITC |
| 7 | | | | | 1:100 tyramide-FITC or cy3 15 min<br>3 x PBST wash<br>2 x 15 min PBST | mesophyll good morphology<br>epidermis fair morphology<br>strong background fluorescence<br><br>cy3 > background then FITC |

**Table 3.1 Troubleshooting whole mount fluorescence *in situ* hybridization in *Arabidopsis thaliana* (continued )**

| Test # | Fixation | Permeabilization and Clearing | Hybridization | Antibody | Visualization | Results |
|---|---|---|---|---|---|---|
| 8 | 4% paraformaldehyde, 15% DMSO, 0.1% Tween-20 in PBS, pH 7.4 90 min with heptane | 1:1 EtOH:xylene 15 min 150 µg/ml proteinase K 15 min extra 3 min MeOH RT | 50% formamide, 5 x SSC, 0.1% Tween-20, 0.1 mg/ml heparin, 1 mg/ml herring DNA O/N 50 °C | block 1% BSA in PBST 90 min 1:100 Anti-DIG-HRP: block buffer 2 hours RT, O/N 4°C | 1:100 tyramide-FITC 15 min 5 min, 20 min PBST | mesophyll good morphology epidermis fair morphology strong background fluorescence<br><br>-ve controls diffuse signal compared to antisense |
| 9 | | | 50% formamide, 5 x SSC, 0.1% Tween-20, 0.1 mg/ml heparin, 1 mg/ml herring DNA O/N 55 °C | 0.3% $H_2O_2$ in PBS 30 min block in BA 60 min 1:100 Anti-DIG-HRP: BA 2 hours, O/N 4°C | 1:1,000 tyramide-FITC 15 min 2 x 5 min, 3 x 60 min, O/N 4°C PBST | mesophyll good morphology epidermis poor morphology strong background fluorescence<br><br>-ve control and antisense similar patterns |
| 10 | 4% paraformaldehyde, 15% DMSO, 0.1% Tween-20 in PBS, pH 7.4 105 min with heptane | | 50% formamide, 5 x SSC, 0.1% Tween-20, 0.1 mg/ml heparin, 1 mg/ml herring DNA O/N 50 °C | | 1:100 tyramide-FITC or cy3 15 min 2 x 5 min, 3 x 60 min, O/N 4°C | mesophyll good morphology epidermis poor morphology very strong background fluorescence<br>-ve control and antisense similar patterns |
| 11 | 4% paraformaldehyde, 15% DMSO, 0.1% Tween-20 in PBS, pH 7.4 with heptane under desiccator vacuum 15 min, rotary 75 min | 1:1 EtOH:xylene 15 min 60 µg/ml proteinase K 15 min 2 x 10 min MeOH -20°C | 50% formamide, 5 x SSC, 0.1% Tween-20, 0.1 mg/ml heparin, 1 mg/ml herring DNA O/N 55 °C | | 1:100 tyramide-FITC 15 min 2 x 5 min, 3 x 60 min, O/N 4°C PBST | RBCS1A signal observed epidermis good morphology medium background fluorescence<br>sense controls similar to antisense for other probes |
| 12 | 4% paraformaldehyde, 15% DMSO, 0.1% Tween-20 in PBS, pH 7.4 with heptane under desiccator vacuum 15 min, rotary 15 min | | | | | RBCS1A localization observed but signal weak epidermis poor morphology<br><br>high background fluorescence |

**Table 3.1 Troubleshooting whole mount fluorescence *in situ* hybridization in *Arabidopsis thaliana* (continued)**

| Test # | Fixation | Permeabilization and Clearing | Hybridization | Antibody | Visualization | Results |
|---|---|---|---|---|---|---|
| 13 | 4% paraformaldehyde, 15% DMSO, 0.1% Tween-20 in PBS, pH 7.4 with heptane under desiccator vacuum 15 min, rotary 75 min | 1:1 EtOH:xylene 15 min 60 µg/ml proteinase K 15 min 2 x 10 min MeOH -20°C | 50% formamide, 5 x SSC, 0.1% Tween-20, 0.1 mg/ml heparin, 1 mg/ml herring DNA O/N 55 °C with adjusted probe concentrations (~100 ng/ml) | 0.3% $H_2O_2$ in PBS 30 min block in BA 60 min 1:100 Anti-DIG-HRP: BA 2 hours, O/N 4°C | 1:25,000 tyramide-FITC 15 min 2 x 5 min, 3 x 60 min, O/N 4°C PBST | cell morphology good RBCS1A localization observed but signal weak high background fluorescence |
| 14 | | no xylene 60 µg/ml proteinase K 15 min 2 x 10 min MeOH -20°C maceration before hybridization 1% $H_2O_2$ in MeOH 30 min 0.08% cellulase, 0.04% pectolyase in PBST 10 min | | block in BA 60 min 1:100 Anti-DIG-HRP: BA 2 hours, O/N 4°C | 1:25,000 vs 1:10,000 tyramide-FITC 15 min 2 x 5 min, 3 x 60 min, O/N 4°C PBST | signal observed in -ve controls along cut site 1:25,000 signal very weak high background fluorescence sample without cell wall enzymes had stronger antisense signal |
| 15 | | 1:1 EtOH:xylene 15 min 60 µg/ml proteinase K 15 min 37 °C 2 x 10 min MeOH -20°C maceration before hybridization 1 % $H_2O_2$ in MeOH 30 min 0.08% cellulase, 0.04% pectolyase in PBST 10 min | | block in BA 60 min 1:100 Anti-DIG-HRP: BA preabsorbed with plant extract 2 hours, O/N 4°C had a -ve control w/o antibody | 1:10,000 tyramide-FITC 15 min 2 x 5 min, 3 x 60 min, O/N 4°C PBST | RBCS1A localization observed sense has strong signal along cut site -ve control w/o antibody no background fluorescence and low autofluorescence |
| 16 | | | | block in 10% normal goat serum in PBST 60 min 1:100 Anti-DIG-HRP in 2% BSA, 1.5% normal goat serum in PBST with vs without plant extract | | RBCS1A location observed strongly and sense no signal -ve control no signal other probes no signal no difference between plant extract treatments |

**Table 3.1 Troubleshooting whole mount fluorescence *in situ* hybridization in *Arabidopsis thaliana* (continued)**

| Test # | Fixation | Permeabilization and Clearing | Hybridization | Antibody | Visualization | Results |
|---|---|---|---|---|---|---|
| 17 | 4% paraformaldehyde, 15% DMSO, 0.1% Tween-20 in PBS, pH 7.4 with heptane under desiccator vacuum 15 min, rotary 75 min | 1:1 EtOH:xylene 15 min 60 µg/ml proteinase K 15 min 37 °C 2 x 10 min MeOH -20°C maceration before hybridization 1 % $H_2O_2$ in MeOH 30 min 0.08% cellulase, 0.04% pectolyase in PBST 6 min | 50% formamide, 5 x SSC, 0.1% Tween-20, 0.1 mg/ml heparin, 1 mg/ml herring DNA O/N 55 °C with adjusted probe concentrations (~100 ng/ml) | block in 10% normal goat serum in PBST 60 min 1:100 Anti-DIG-HRP in 2% BSA, 1.5% normal goat serum preabsorbed with plant extract | 1:10,000 tyramide-FITC 15 min 2 x 5 min, 2 x 30 min PBST | same as above plus RBCL signal observed signal strongest at cut site morphology better with short cell wall digestion |
| 18 | | | | | 1:10,000 tyramide-FITC 1 hour vs 1:100 15 min 2 x 5 min, 2 x 30 min PBST | both visualization treatments resulted in strong background staining from tyramide |
| 19 | | 1:1 EtOH:xylene 15 min vs none 60 µg/ml proteinase K 15 min 37 °C 2 x 20 min MeOH -20°C maceration before hybridization 1 % $H_2O_2$ in MeOH 30 min 0.08% cellulase, 0.04% pectolyase in PBST 10 min | | block in 10% normal goat serum in PBST 60 min 1:100 Anti-DIG-HRP in 2% BSA, 1.5% normal goat serum preabsorbed with no plant extract | 1:10,000 tyramide-FITC 15 min 2 x 5 min, 2 x 30 min PBST | at cut site RBCS1A and RBCL signal observed -ve controls good LHCB low cytosolic signal observed xylene treatments had > signal |
| 20 | | 1:1 EtOH:xylene 15 min 60 µg/ml proteinase K 15 min 37 °C 2 x 20 min MeOH -20°C maceration after fixation vs freeze-thaw after hydration 1 % $H_2O_2$ in MeOH 30 min 0.08% cellulase, 0.04% pectolyase in PBST 10 min | | | | both maceration and freeze thaw had signals in -ve controls<br><br>RBCS1A signal observed<br><br>RBCL and LHCB not observed |

**Table 3.1 Troubleshooting whole mount fluorescence *in situ* hybridization in *Arabidopsis thaliana* (continued)**

| Test # | Fixation | Permeabilization and Clearing | Hybridization | Antibody | Visualization | Results |
|---|---|---|---|---|---|---|
| **21** | 4% paraformaldehyde, 15% DMSO, 0.1% Tween-20 in PBS, pH 7.4 with heptane under desiccator vacuum 15 min, rotary 60 min, vacuum 15 min, O/N at 4 ℃ rotary | 1:1 EtOH:xylene 15 min 60 µg/ml proteinase K 15 min 37 °C 2 x 20 min MeOH -20°C maceration after fixation vs before hybridization 2 % $H_2O_2$ in MeOH 30 min 0.08% cellulase, 0.04% pectolyase in PBST 6 min | 50% formamide, 5 x SSC, 0.1% Tween-20, 0.1 mg/ml heparin, 1 mg/ml herring DNA O/N 55 °C with adjusted probe concentrations (~100 ng/ml) | block in 10% normal goat serum in PBST 60 min 1:100 Anti-DIG-HRP in 2% BSA, 1.5% normal goat serum preabsorbed with no plant extract | 1:10,000 tyramide-FITC 15 min 2 x 5 min, 2 x 30 min PBST | **both maceration treatments had good -ve controls**<br>**Strong signal observed for maceration before hybridization**<br><br>**LHCB low cytosolic pattern observed that wasn't in sense control**<br>**RBCS1A and RBCL signal observed** |
| 22 | 4% paraformaldehyde, 15% DMSO, 0.1% Tween-20 in PBS, pH 7.4 under pump vacuum atmosphere 25 ° 2 x 15 min, then with heptane on rotary 120 min | | | | | fixation was not successful<br>morphology poor<br>no signal observed |
| 23 | 4% paraformaldehyde, 15% DMSO, 0.1% Tween-20 in PBS, pH 7.4 with heptane under pump vacuum atmosphere 25 ° 15 min, then with heptane on rotary 60 min, vacuum 15 min, rotary 30 min | 1:1 EtOH:xylene 15 min 60 µg/ml proteinase K 15 min 37 °C 2 x 20 min MeOH -20°C maceration before hybridization 1 % $H_2O_2$ in MeOH 30 min 0.08% cellulase, 0.04% pectolyase in PBST 6 min | | | | possible over fixation<br>morphology good<br>no signal observed |
| 24 | Fixed in FAA containing 50 % EtOH, 5 % acetic acid , 3.7 % paraformaldehyde under under desiccator vacuum for 60 min | 1:1 EtOH:xylene 15 min 60 µg/ml proteinase K 15 min 37 °C maceration before hybridization 0.08% cellulase, 0.04% pectolyase in PBST 6 min 2 x 10 min, O/N -20°C MeOH | | | | sense and -ve controls good<br><br>autofluorescence increase with FAA<br><br>signal observed for RBCS1A, RBCL in multiple cells<br>LHCB signal in few cells |

O/N = overnight; BA = blocking reagent from TSA kit # 12 ( ThermoFisher); -ve = negative; RT = room temperature. For reagent full names see methods and materials.

The bolded trial number and results indicates final optimized protocol

**Figure 3.7 Optimization of the whole mount fluorescence *in situ* hybridization procedure in Arabidopsis cotyledons**

A) Cotyledons fixed with 4% formaldehyde for 45 min without a vacuum showed a compromised morphology (i) whereas cotyledons fixed with 4% formaldehyde for 90 min with a vacuum showed a preserved morphology (ii). B) Autofluorescence of mesophyll cells in the GFP channel when treated with methanol at room temperature (i). Autofluorescence of mesophyll cells in the GFP channel when treated with methanol at -20°C (ii). Autofluorescence of mesophyll cells in the RFP channel when treated with methanol at room temperature (iii). Autofluorescence of mesophyll cells in the RFP channel when treated with methanol at – 20°C (iv). C) A negative control (no probe) with a 1% BSA blocking step used prior to antibody incubation (i). A negative control (no probe) with a 10% normal goat serum blocking step used prior to antibody incubation. Size bars, 10 μm. All images were captured using a 40X objective lens on an epifluorescence microscope.

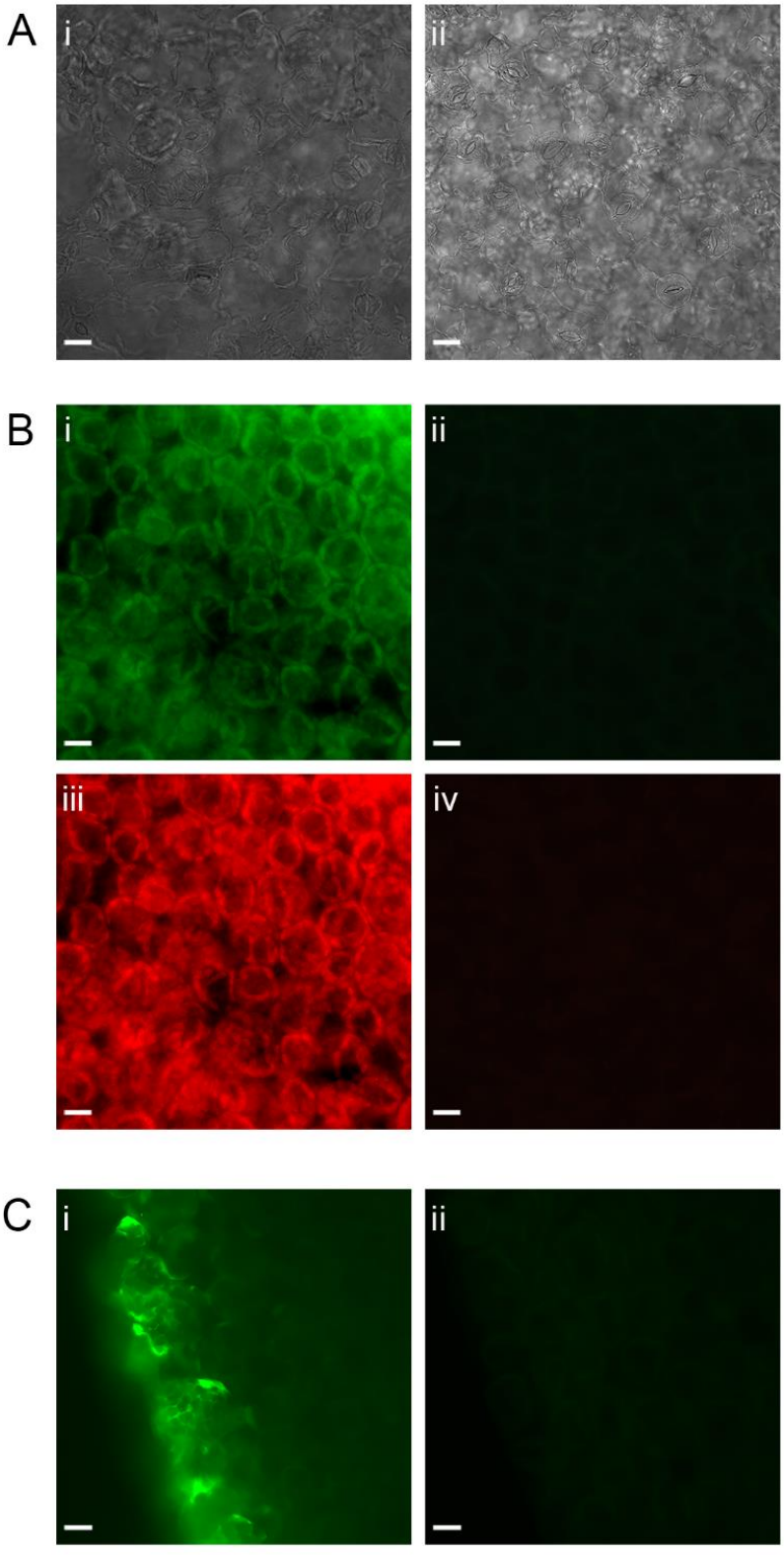
A
i
ii
B
i
ii
iii
iv
C
i
ii

3.2.2.2 Subcellular Detection of mRNAs Encoding Chloroplast Proteins

The protocol described in Section 2.3.1 was used to successfully determine the subcellular localization of three mRNAs that encode chloroplast proteins: RBCS1A, RBCL and LHCB5 (Figure 3.8). A cytosolic pattern was observed for the RBCS1A antisense probe, and was consistent in all mesophyll cells that displayed a fluorescent signal (Figure 3.8A). A strong fluorescent signal was observed throughout the cytoplasm and was absent in the chloroplasts and the vacuole. This labelling pattern was observed in 12 separate experiments using three seedlings in each experiment. This fluorescence pattern was never observed when the RBCS1A sense probe was used (Figure 3.8B). The fluorescent antisense RBCL probe signal was restricted to the chloroplast in the mesophyll cells that were closest to the maceration site in four experiments, each containing three different seedlings (Figure 3.8C). A ring type pattern of fluorescence on the inner side of the chloroplast membrane was observed (Figure 3.8C, inset). When the RBCL sense probe was used, this fluorescence pattern was never observed (Figure 3.8D). LHCB5 mRNA fluorescent signal was observed in 2 to 3 mesophyll cells near the cut sites in three separate experiments (Figure 3.8E). A cytosolic, punctate signal was observed that was concentrated at the periphery of chloroplasts. This pattern was not always observed in all three seedlings per experiment. When the LHCB5 mRNA sense probe was used, the fluorescence signal was low (Figure 3.8F). However, in one experiment the LHCB5 sense probe displayed punctate signals similar to that observed for the antisense probe in two cells, although the frequency of puncta was much lower (data not shown).

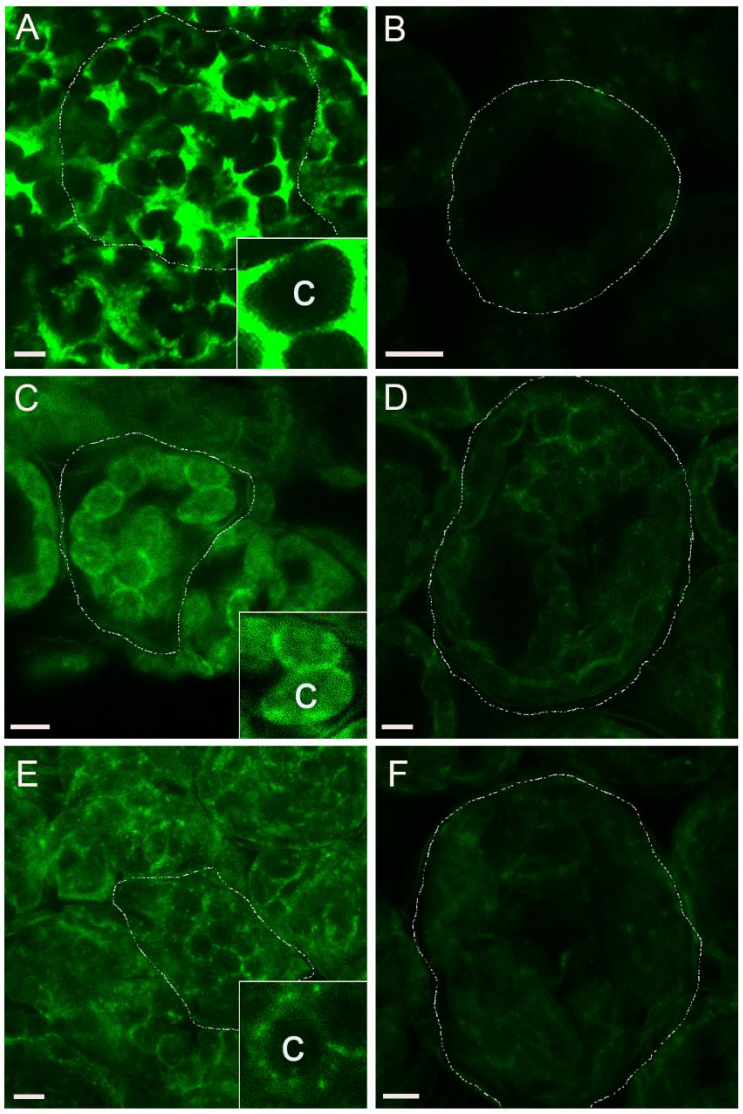


**Figure 3.8 The subcellular localization of mRNAs that encode chloroplast proteins in Arabidopsis cotyledons using fluorescence WISH**

Fluorescence WISH was performed on 5 days post-germination cotyledons using digoxigenin labelled riboprobes. Optical sections of mesophyll cells were imaged using a 63X oil immersion lens attached to an inverted laser scanning confocal microscope. All probes were visualized by tyramide signal amplification using tyramide-FITC A) RBCS1A mRNA subcellular localization. Inset shows a magnified image of chloroplast and surrounding cytoplasm. B) RBCS1A sense negative control probe. C) RBCL mRNA subcellular localization. Inset showing a magnified image of chloroplasts and surrounding cytoplasm. D) RBCL sense negative control probe. E) LHCB5 mRNA subcellular localization. Inset showing the magnified image of a chloroplast to observe signal pattern F) LHCB5 sense probe negative control. Size bars = 5 μm; c, chloroplast. Cell boundary is highlighted in white.

*In situ* hybridization of paraffin embedded and sectioned true leaf tissue was performed as described in Section 2.4 to verify results obtained from the whole mount protocol. The same riboprobes were used and visualized by either colourmetric or tyramide signal amplification. Both the RBCS1A and RBCL had prominent signals in mesophyll cells of young leaves using colourometric staining, with similar patterns that highlighted the chloroplast (Figure 3.9C, F). The RBCS1A riboprobe signal prominently labelled chloroplasts, with some signal detected in the cytosol (Figure 3.9C). The RBCL riboprobe labelling of chloroplasts was more intense than that observed with the RBCS1A probe, and there was less detectable cytosolic labelling using the RBCL probe (Figure 3.9C, F). The sections were void of any signal when using the sense probes (Figure 3.9B, E). As expected, both antisense probes did not produce a signal in the epidermal layer of the leaf (Figure 3.9A, D) because the Rubisco enzyme is not produced in epidermal pavement cells. This technique did not detect LHCB5 mRNA, as the LHCB5 antisense probe did not produce a colour signal (data not shown).

When the riboprobes were visualized on sectioned leaves using tyramide signal amplification, the subcellular patterns observed for RBCS1A and RBCL were consistent with the patterns observed using fluorescence WISH (compare Figures 3.8 and 3.10). Merging the chloroplast autofluorescence (CAF) signal in the RFP channel with the RBCS1A signal clearly showed the cytosolic pattern of RBCS1A fluorescence and the absence of RBCS1A signal in the chloroplast (Figure 3.10A). This was in contrast to the colourmetric visualization of the RBCS1A probe signal shown in Figure 3.10C. The merged image of the CAF signal and the RBCL signal shows co-localization of the chloroplast signal (Figure 3.10B). Localizing LCHB5 using tyramide signal amplification

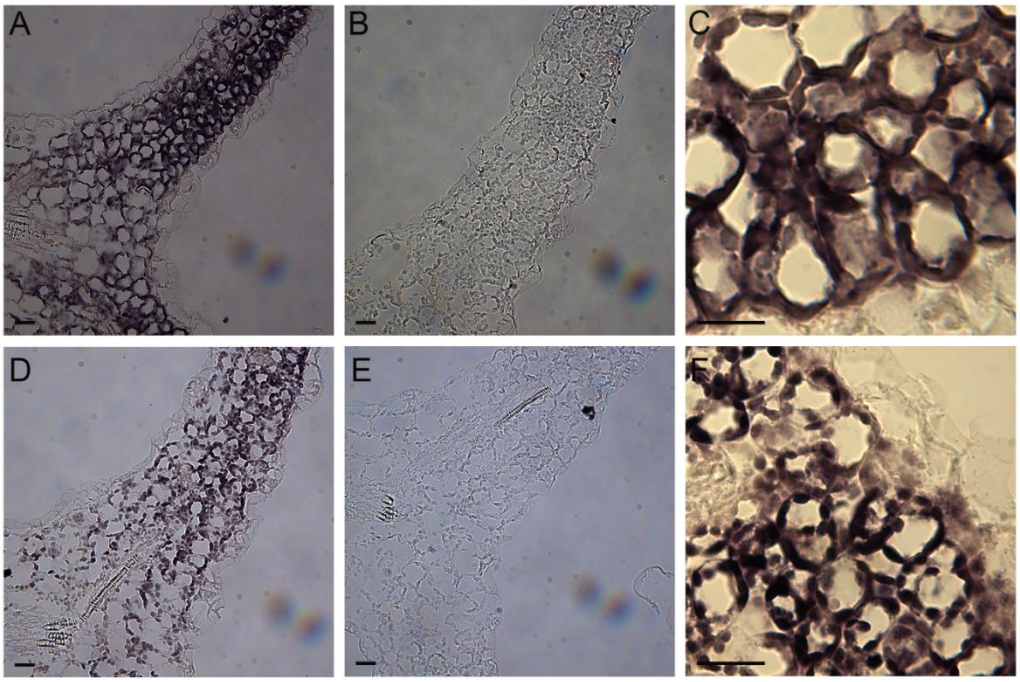


**Figure 3.9 *In situ* hybridization of sectioned true leaves of Arabidopsis seedlings**

Five dpg seedlings were fixed and embedded in paraffin wax and sectioned at 5 μm thickness. Digoxigenin riboprobes were visualized using alkaline phosphatase detection. Images were taken with a 40X objective lens (A, B, D, E) or a 100X oil immersion objective lens (C, F) on an epifluorescence microscope. A) RBCS1A antisense probe; B) RBCS1A sense probe; C) RBCS1A antisense probe at a higher magnification; D) RBCL antisense probe; E) RBCL sense probe; F) RBCL antisense probe at a higher magnification. Size bar = 10 μm.

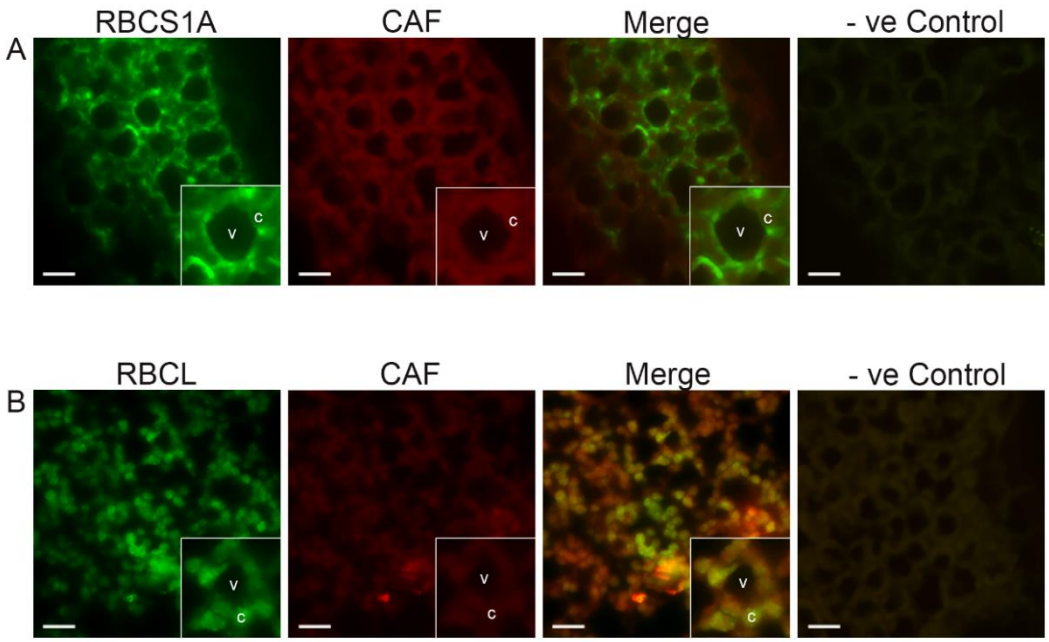


**Figure 3.10 Fluorescence *in situ* hybridization on sections of true leaves from Arabidopsis seedlings**

Five dpg seedlings were fixed and embedded in paraffin wax and sectioned to 5 μm thickness. Digoxigenin riboprobes were visualized using tyramide signal amplification with tyramide-FITC. Images were taken with a 40X objective lens on an epifluorescence microscope. A) The signal observed using the RBCS1A antisense probe alone, by visualizing the chloroplast autofluorescence in the RFP channel (CAF), and the merge of both RBCS1A antisense signal with CAF. The negative control shows RBCS1A sense probe signal merged with the CAF signal. B) The signal observed using the RBCL antisense probe, by visualizing the CAF signal in the RFP channel, and the merge of both RBCL antisense signal with the CAF signal. The negative control shows RBCL sense probe signal merged with the CAF signal. Size bar, 10 μm; c, chloroplast; v, vacuole.

method on sectioned leaf tissue was not successful, as the antisense and sense probes both displayed generic background fluorescence (data not shown.)

*In situ* hybridization of leaf sections was performed with colorimetric detection using the six riboprobes that were unsuccessful with WISH (AIM-1, pMDH-1, mMDH-1, PORB, GUN5 and BASL). These hybridizations were carried out only once. Only one riboprobe, GUN5, displayed a signal in true leaves (Figure 3.11). The subcellular localization of GUN5 is not reliable, but it appears the transcript is expressed in the mesophyll cells. The remaining riboprobes did not display a signal unless the reaction time was increased to two days. After this long incubation period, the sense probe also displayed the identical signal to the antisense probes after the long exposure (data not shown).

### 3.3 Discussion

The fluorescence WISH protocol that was established for subcellular localization in this chapter was successful using three riboprobes. Although probes to nine different mRNAs were used, only RBCS1A, RBCL and LHCB5 mRNA was detected (Figure 3.8). The subcellular localization of these three mRNAs in Arabidopsis has not been reported to date. RBCS1A mRNAs are localized randomly in the cytosol of cotyledons and mesophyll cells of young true leaves (Figure 3.8, 3.10). This pattern was observed numerous times in whole mount samples and was consistent when performing the optimized *in situ* hybridization technique on leaf sections (Figure 3.10). In addition, these results agree with published work that demonstrated randomly localized cytosolic mRNAs encoding the small subunits of Rubisco in Chlamydomonas

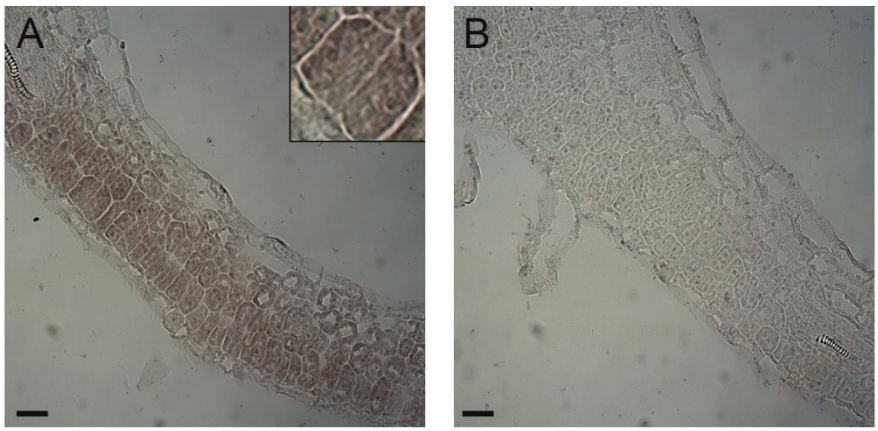


**Figure 3.11 *In situ* hybridization with colourmetric detection of GUN5 mRNA on sections of true leaves of Arabidopsis seedlings**

Five dpg seedlings were fixed and embedded in paraffin wax and sectioned to 5 μm thickness. Digoxigenin labelled riboprobes were visualized using alkaline phosphatase. Images were taken with a 40X objective lens on an epifluorescence microscope. A) GUN5 antisense probe. Inset showing a magnified image of two cells B) GUN5 sense probe.

(Uniacke and Zerges, 2009). RBCL mRNA was detected within chloroplasts in a diffuse pattern with distinct concentrated clusters (Figure 3.8, Figure 3.10). These clusters were not due to DNA fluorescence because the DNA is double stranded and thus cannot hybridize to the riboprobes. Also, no punctate labeling was observed using the sense riboprobe. RBCL is encoded by a chloroplast gene, so visualizing the transcript within the chloroplast served as a good control for successful *in situ* hybridization staining. In Chlamydomonas, RBCL mRNA localized to the perimeter of the pyrenoid, to the area of carbon fixation within the chloroplast (Uniacke and Zerges, 2009). In Arabidopsis, RBCL mRNA was expected to be distributed randomly throughout the chloroplast because carbon fixation occurs throughout the stroma. However the RBCL *in situ* hybridization signal was concentrated near the inner membrane of the chloroplast (Figure 3.8, inset). It is possible that the large subunit is translated near the chloroplast membrane, which is the site of $CO_2$ diffusion into the organelle. This would allow the Rubisco protein to be translated and concentrated near areas of high $CO_2$ levels.

The LHCB5 mRNA fluorescent WISH signal was localized in distinct punctate structures that appeared to be enriched at the periphery of chloroplasts in mesophyll cells (Figure 3.8, inset). Tyramide signal amplification does not have the resolution for single mRNA imaging, suggesting these punctate structures contain multiple LHCB5 mRNAs and are likely a type of ribonucleoprotein particle (RNP). This result is preliminary because the pattern was observed in a limited number of samples, and the attempts to corroborate the localization of LHCB5 using the established paraffin section *in situ* hybridization protocol was not successful. In addition, sense controls for both LHCB5

and other transcripts occasionally had punctate signals in a few cells that were less frequent and weaker than those punctate observed for LHCB5 antisense probe. However, if authentic, this localization pattern is in agreement with published work that demonstrated that LHCB5 mRNAs in wheat and Chlamydomonas is concentrated at the cytosolic face of chloroplasts (Marrison et al., 1996; Uniacke and Zerges, 2009). Localizing the LHCB5 mRNA to the periphery of the chloroplast would be an efficient mechanism to concentrate the LHCB5 protein for import into the organelle, perhaps in a co-translational manner. In Chlamydomonas, LHCB5 mRNA co-localizes with cytoplasmic ribosomes in a translation dependent manner (Uniacke and Zerges, 2009). Protein targeting to organelles through mRNA localization in a translation dependent manner has been commonly observed in other eukaryotic systems (Weis et al., 2013).

The protocol of Hejatko et al. (2006) served at the basis for the optimized fluorescence WISH procedure developed in this study. The protocol was optimized from a tissue-level staining approach using colourmetric detection, as reported in the Hejatko et al. (2006) study, to a subcellular method here using fluorescence detection. The results for *in situ* hybridization on leaf sections highlights the need to use a tyramide amplification technique rather than a colourmetric detection approach (Figure 3.9). Consistent with the results presented here, the purple precipitate created from alkaline phosphatase is diffusible in the cytosol, and it cannot be effectively used to determine subcellular localization as was shown elsewhere (Lécuyer et al., 2007). The staining pattern of alkaline phosphatase for both RBCS1A and RBCL are similar with signal around the chloroplast as well as in the cytosol in mesophyll cells (Figure 3.10). When the same riboprobes were used with tyramide signal amplification, distinct subcellular

patterns were observed (Figure 3.8, 3.10). The fluorescent signal obtained from tyramide signal amplification is covalently bound immediately adjacent to the site of the catalyst enzyme localization, resulting in a stable, non-diffusing signal that allows for accurate determination of the mRNA location pattern within the cell.

The main parameters that were modified from the Hejatko et al. (2006) protocol involved fixation, permeabilization, clearing and antibody incubation (Figure 3.7). Each plant tissue and cell type required specific optimization due to different structural organization and chemical composition of the cell. For example, if samples are under-fixed, the morphology of the cells will be compromised and the localization of the mRNAs will not be properly preserved. In Figure 3.7 the morphology of under-fixed vs optimally fixed epidermal cells were compared, and showed that without extended fixation times and the incorporation of a vacuum infiltration step, the cell boundaries of pavement cells were compromised and stomata became unevenly spaced. If a sample is over-fixed, the morphology of the cell will not be affected but the extensive crosslinking of the tissue could prevent the probe from accessing the mRNA target. When fixation times extended greater than 90 min or when a strong vacuum was used, the signal was lost in mesophyll cells, indicating that the tissue was over-fixed (Table 3.1). Finding a balance between properly fixed cells was essential to this research. The inability to localize the six mRNAs is not likely due to fixation problems, because three riboprobes were successful in penetrating the tissue and hybridizing to their target mRNA.

A proteinase K treatment can be used to partially digest crosslinked proteins to increase tissue permeability and remove RNA-binding proteins that could mask the mRNA target. The major modification that was made compared to the Hejátko et al.

(2006) protocol involved increasing the proteinase K incubation temperature to 37°C (Table 3.1). Cell membranes and plant specific structures, such as the cell wall and cuticle, also influence cell permeabilization. A cell wall digestion step was incorporated here, as described in a different protocol (Rozier et al., 2014). The successful detection of RBCS1A, RBCL and LCHB5 mRNAs (Figure 3.8) indicated that the tissues and cells were permeabilized sufficiently to allow riboprobe access without compromising mRNA preservation or cell morphology. The riboprobe was designed to be around 150-300 bp or hydrolyzed into small fragments, and contained the same 2:3 ratio of digoxigenin labelled versus unlabeled uridines (Figure 3.3, 3.5). Therefore, all of the probes should have had equal access to their target. Also, the RBCL riboprobe had to enter into the fixed and permeabilized chloroplast to reach its target. Lastly, localizing the mRNAs using *in situ* hybridization of sectioned tissue, where wall and cell membrane permeabilization was not an issue, was only successful with the RCBCS1A and RBCL riboprobes. Therefore, it is likely that the whole mount samples were permeabilized adequately and the lack of success was not due to restricted riboprobe access. The labelling efficiency of the nine riboprobes were all fairly comparable with every riboprobe displaying a signal when 2.0 ng of riboprobe was loaded onto the dot blot. This was well below the 10-50 ng used during hybridization (Figure 3.5). The signal strength of all nine riboprobes were equal or greater than to the control Hoxa11, a riboprobe that displayed a reliable signal in WISH of mouse embryos (Neufeld et al., 2014).

RBCS1A is highly expressed in both cotyledons and true leaves in Arabidopsis seedlings (Winter et al., 2007). The target transcript with the next highest absolute abundance in those organs is LHCB5, followed by GUN5, PORB, RBCL, mMDH-1,

AIM-1, pMDH-1 and BASL, respectively. The RBCS1A riboprobe targeted all four RBCS subunits, each with an absolute expression level of 5493.39 (Winter et al., 2007). This riboprobe produced the strongest and most reliable hybridization signal out of the three successful riboprobes, suggesting that the abundance of target mRNA could be a factor for successful visualization. However, RBCL has only one subunit with an absolute mRNA expression level of 1369.13. This is similar to mMDH-1 and lower then GUN5 and PORB. The optimized protocol was able to localize RBCL reliably but was not successful for mMDH-1, GUN5 or PORB. This suggests that target mRNA abundance is not limiting. However, the RBCL mRNA is concentrated within chloroplasts and this would result in a concentrated tyramide signal. mRNA targets that are spread throughout the cytosol might create a diffuse signal that cannot be easily detected above the background noise.

Tyramide amplification used in *in situ* hybridization experiments was employed previously in the Arabidopsis inflorescence apex to determine the tissue level expression of CLAVATA3, WUSHEL and ARABIDOPSIS HISTIDINE PHOSPHOTRANSFER PROTEIN mRNA (Rozier et al., 2014). This is the only published example of *in situ* hybridization in higher plants that used tyramide amplification. The absolute abundance of three of these mRNAs in the inflorescence apex are less than 20 (Winter et al., 2007), which is much lower than the values of the target mRNAs in this thesis. The inflorescence apex is a meristematic region that develops into floral organs. Meristem tissue is made up of undifferentiated and cytoplasmically dense cells that lack chloroplasts. Therefore, it is possible that the autofluorescence in the floral meristem is lower than in cotyledons and leaf tissue. Perhaps the amplification system is not sensitive

enough to detect moderate to low abundant transcripts in plant cells where autofluorescence is high. This would explain the difficulty in visualizing the target transcripts in the present research. Substantial effort was made to lower background noise from autofluorescence, endogenous peroxidase activity and non-specific antibody interactions while increasing signal by increasing tyramide concentration and staining time (Table 3.1). The transcript abundance levels determined in Winter et al. (2007) were based on microarray data. The eFP Arabidopsis browser developed by Winter et al. (2007) is a useful tool for determining where a transcript is expressed throughout development and within different tissues. However, microarray techniques have been described as lacking sensitivity and abundance results should be used as guidelines and not concrete evidence. Therefore it is possible that the absolute values used to determine transcript abundance of the target mRNAs using the browser are not necessarily the same levels found in the cell types used here.

Traditionally, *in situ* hybridization of plant cells was performed without fluorescent imaging due to the challenges of autofluorescence in the tissue. Cell wall components, membranes, extracellular matrix, pigments and other secondary metabolites all have fluorescent properties with an emission spectrum ranging from 400-800 nm (Talamond et al., 2015). This becomes especially problematic when probing transcripts that were not abundant. Methanol is commonly used to clear pigments from tissue, with treatments times varying from a few minutes to overnight (Hejátko et al., 2006; Küpper et al., 2007). In research presented in this chapter, the duration of the methanol washes was not as important as the temperature of the methanol incubation step (Table 3.1). A drastic reduction of autofluorescence in both the RFP and GFP channels was observed in

samples treated with methanol at -20 °C compared to room temperature (Figure 3.7). However, some autofluorescence remained and may have prevented visualization of lightly labelled mRNAs.

To determine if background autofluorescence was the main problem in achieving a detectable signal, the riboprobes were used on sectioned tissue using *in situ* hybridization with colourmetric detection. The signal obtained for RBCS1A and RBCL was strong and staining could be observed with the naked eye after 1 hour of stain development (Figure 3.9). No signal was observed for the remaining seven probes except for the faint signal observed for the antisense GUN5 probe after overnight stain development (Figure 3.11). This *in situ* hybridization experiment was only performed once per riboprobe on three different paraffin sectioned seedlings. GUN5 mRNA is the second most abundant transcript (after LHCB5) out of the seven transcripts targeted in Arabidopsis true leaves (Winter et al., 2007). Therefore, if the *in situ* techniques were limited by transcript abundance, a signal should have been observed for the LHCB5 probe using colorimetric detection. In contrast, the rapid development of signal observed with RBCS1A riboprobes versus the weak and slow signal observed with the GUN5 probe could indicate that transcript abundance is a real issue for detection. It will be necessary to repeat this experiment before coming to any firm conclusions about LHCB5 and GUN5 mRNA labeling using this approach.

GUN5 has been observed to localize to the periphery of chloroplasts in sectioned Arabidopsis leaves using colorimetric detection (Gibson et al., 1996). The results from the research presented in this thesis suggested that GUN5 is localized throughout the cytosol and shows no strong indication that GUN5 localizes to the periphery of

chloroplast (Figure 3.11). However, as mentioned before, this colourmetric technique is unreliable for subcellular localization which makes both Gibson et al. (1996) and our subcellular results questionable. In addition, the samples used here were embedded in different medium than Gibson et al. (1996), and sections were 5 μm instead of 7 μm in thickness.

Another parameter that was adjusted was the blocking and antibody incubation steps. The conditions for antibody incubation need to be considered carefully to avoid non-specific interactions that result in high background fluorescence. The conditions described by Hejátko et al. (2006) were not stringent enough for the samples used in the present study, as these resulted in high background (Figure 3.7C). The background fluorescence in these samples completely masked any signal from the riboprobes, except for RBCS1A, making subcellular localization impossible. The blocking buffer used to prepare the sample prior to antibody incubation was adjust to 10% normal serum and the antibody dilution buffer was changed to 1.5% normal serum with 2% BSA (Table 3.1). This adjustment greatly reduced the nonspecific interactions and resulted in drastically lower background fluorescence (Figure 3.7D). Once this parameter was changed it was possible to localize RBCL and LHCB5 mRNA at the subcellular level. However this adjustment did not aid in observing a signal for the remaining six riboprobes.

It is unclear exactly which parameter(s) requires further adjusting in the protocol established in this thesis to allow for subcellular mRNA localization at a global scale. It is likely that transcript abundance and tissue autofluorescence are important factors when using tyramide amplification techniques. Troubleshooting experiments using organs with higher transcript levels might be a solution. Using cell types with a dense cytoplasm and

low vacuole size, such as those found in meristem tissue, might also aid in visualizing mRNA targets because signals would be more concentrated. Lastly, using this established protocol with other fluorescence visualization techniques that have higher sensitivity could eliminate transcript abundance limitations.

# CHAPTER 4. SINGLE MOLECULE FLUORESCENCE *IN SITU* HYBRIDIZATION IN ARABIDOPSIS

## 4.1 Introduction

Single molecule fluorescence *in situ* hybridization is a sensitive technique that allows researchers to image single mRNAs independent of mRNA concentration. In Chapter 3 it was demonstrated that the fluorescence WISH technique using tyramide amplification was not effective in visualizing most of the transcripts that were analyzed in Arabidopsis cotyledons. In the results presented in this chapter, two single molecule fluorescence imaging techniques were incorporated into the WISH protocol that was established in Chapter 3 in an effort to increase the success of WISH labeling, as well as establishing single molecule imaging in plants. These two single molecule imaging techniques were a branched DNA (bDNA) probe approach and a multiple singly labelled probe (MSLP) approach (Figure 4.1). The bDNA probe kit from Advance Cell Diagnostics contained paired target probes (up to ten), pre-amplifiers, amplifiers and labelled probes. The paired target probes hybridize to the target mRNA to create a binding platform for the pre-amplifiers. Multiple amplifiers hybridize to one pre-amplifier and become a binding site for the labelled probes. This creates a branched structure that contains numerous fluorophores, which dramatically increases the signal strength. The MSLP probe sets were ordered from Biosearch Technologies and contained 48 probes that were complimentary to tandem sequences on the target mRNA. Each probe was 20 nt long and had a single fluorophore attached to the 5' end. The

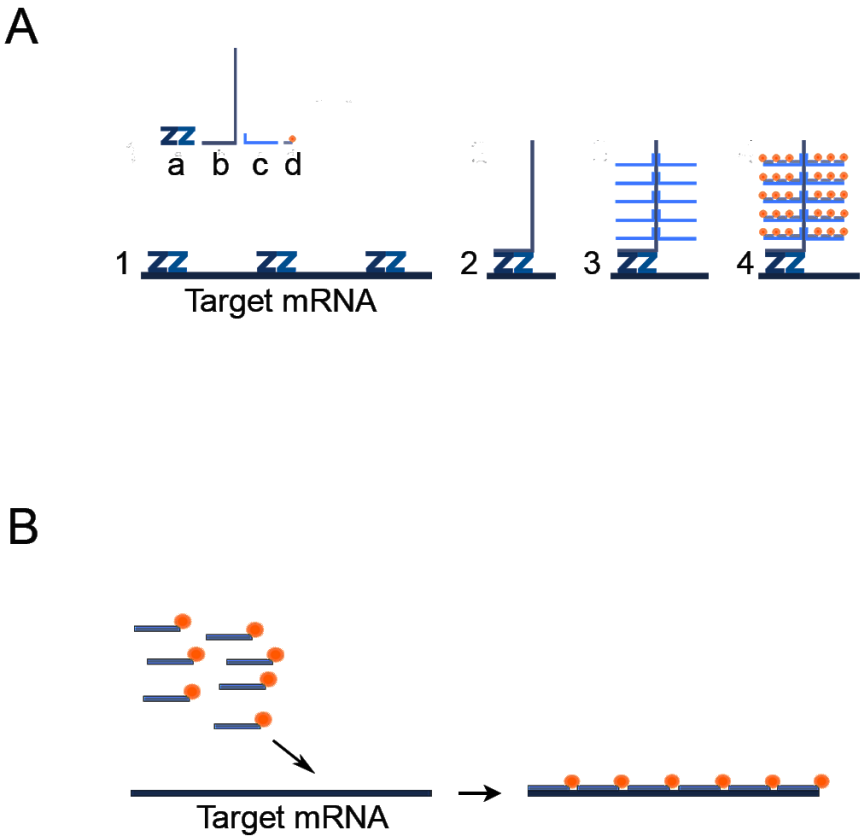


**Figure 4.1 Single molecule *in situ* hybridization visualization techniques**

A) Branched DNA technology from Advance Cell Diagnostic. 1) The paired target probes (a) bind in pairs along the target mRNA. 2) The pre-amplifiers (b) hybridize to the target probe pairs. These pre-amplifiers will not bind unless both target probes have hybridized to the target in tandem. 3) The multiple amplifiers (c) hybridize to one pre-amplifier to create a branched structure. 4) Multiple label probes (d) that each contain one fluorophore bind to each amplifier to produce an amplified, punctate signal. B) Multiple singly labelled oligonucleotide probe sets from Biosearch Technologies. Each probe is 20 nt long and contains one terminal fluorophore. There are 48 probes in one set that bind in tandem to the target mRNA. Only when the majority of the probes bind to a single mRNA will a punctate signal be observed.

major limitation to single molecule fluorescence *in situ* hybridization as a technique for a large scale analysis of subcellular mRNA localization is that it is costly. Neither of these techniques have yet been successfully used in higher plants for fluorescent imaging and only one study has been published that used a bDNA technique with colourmetric detection to localize two different mRNAs at the tissue level in paraffin embedded sections of maize leaves (Bowling et al., 2014). Results obtained using both techniques are discussed in this chapter along with the optimization experiments that were performed in whole mount seedlings, suspension culture cells and protoplasts.

## 4.2 Results

### *4.2.1 bDNA in situ Hybridization*

#### 4.2.1.1 The Use of bDNA Probes in Whole Mount Arabidopsis Seedlings

The protocol established for WISH in Chapter 3 was extended for use with bDNA probes from ACD as described in Section 2.3.2.2. Three different cytosolic transcripts were targeted; RBCS1A, alanine aminotransferase-1 (AlaAT1) and Ent-copalyl disphosphate synthase (GA1). Optimization of the manufacturer's instructions were necessary, as this technology was designed for cultured mammalian cells and sectioned mammalian tissue. Details of the various optimization conditions that were tested are listed in Table 4.1. When the manufacturer's instructions were followed, high background staining was observed in the form of moving punctate signals. Post-hybridization washing times were extended from 5 min to 15 min, and amplification

**Table 4.1 Troubleshooting bDNA whole mount *in situ* hybridization on *Arabidopsis thaliana* seedlings**

| Test # | Fixation | Permeabilization | Hybridization | Wash | Results |
|---|---|---|---|---|---|
| 1 | 4% paraformaldehyde, 15% DMSO, 0.1% Tween-20 in PBS, pH 7.4 with heptane under desiccator vacuum 15 min, rotary 75 min | 2 x 15 min MeOH -20°C<br>1:1 EtOH:xylene 15 min<br>proteinase K 60 µg/ml 15 min | APM except O/N | APM | +ve and -ve controls same pattern<br>RBCS1A punctate signal<br>a lot of moving punctate signals observed for all |
| 2 | | | | APM with wash time increased to 15 min each.<br>Amp hybridization times doubled | non-specific signal in -ve control<br>low punctate signal observed with and without movement RBCS1A<br>cell morphology good |
| 3 | | 3 x 20 min MeOH -20°C<br>1:1 EtOH:xylene 15 vs 30 min<br>proteinase K 60 µg/ml 15 min | | APM with wash time increased to 15 min each | no signal observed for RBCS1A<br>moving punctate signals in control<br>mesophyll morphology poor<br>no difference in xylene treatments |
| 4 | | 2 x 15 min MeOH -20°C<br>1:1 EtOH:xylene 30 min<br>proteinase K 60 µg/ml 15 min | | APM with wash time increased to 15 min each.<br>Amp hybridization times fourfold | non-specific signal in -ve control<br>RBCS1A punctate signal in epidermis not moving<br>stationary punctate signals in RBCS1A and AlaAT1<br>moving punctate signals in all samples reduced |
| **5** | | 2 x 15 min MeOH -20°C<br>1:1 EtOH:xylene 30 min<br>proteinase K 60 µg/ml 15 min<br><br>0.08% cellulase, 0.04% pectolyase in PBST 5 min | | | **-ve control moving signal only**<br>**RBCS1A not in epidermis**<br>**RBCS1A stationary punctate in mesophyll**<br>**no moving RBCS1A signal**<br>**AlaAT1 signal moving**<br>**morphology good**<br>**signal intensity increased for all probes** |
| 6 | | 2 x 15 min MeOH -20°C<br>1:1 EtOH:xylene 30 min<br>proteinase K 100 µg/ml 20 min | | 0.2 X SSC, 0.01% Tween-20 15 min each.<br>Amp hybridization times fourfold | -ve control moving and non-moving punctate signal<br>punctate signal in mesophyll, RBCS1A not in epidermis<br>moving RBCS1A and AlaAT1<br>cell morphology good |
| 7 | Vacuumed and chilled 5% paraformaldehyde, 10% DMSO, 0.1% Tween-20, 0.08M EDTA in PBS, pH 11 under desiccator vacuum 40 min, rotary 10 min | 2 x 40 min MeOH, O/N RT<br>100% xylene 60 min<br>acetone washes<br>proteinase K 100 µg/ml 20 min | | | -ve control moving and non-moving punctate signal<br>stationary punctate signals in RBCS1A only<br>moving punctate signals for all probes<br>RBCS1A in epidermis<br>cell morphology poor |
| 8 | | 2 x 40 min MeOH, O/N RT<br>100% xylene 60 min<br>acetone washes<br>proteinase K 40 µg/ml 20 min | | APM with wash time increased to 15 min each.<br>Amp hybridization times fourfold | -ve control moving and non-moving punctate signal<br>moving punctate signal reduced<br>stationary punctate signals for RBCS1A and AlaAT1<br>cell morphology good |

O/N = over night; RT = room temperature; APM= as per RNAscope Fluorescent Multiplex Kit User Manual catalog # 320293; -ve = negative; +ve = positive; Amp = amplification

The bolded trial number and results indicates final optimized protocol

hybridization times were quadrupled and resulted in a decrease of background staining. The introduction of a cell wall digestion step further reduced the background staining and the frequency of moving signal. The RBCS1A probe shows multiple, punctate signals that were fixed throughout the cytoplasm of mesophyll cells (Figure 4.2A). The AlaAT1 signal showed punctate signals in the epidermal layer only (Figure 4.2A). Some AlaAT1 punctate signals were stationary while others were moving throughout the cell. The GA1 probe displayed faint moving punctate signals in the cytoplasm and the negative control 4-hydroxy-tetrahydrodipiconlinate reductase (DapB) target probe displayed brighter, punctate, moving signals in mesophyll cells (Figure 4.2B).

#### 4.2.1.2 *In situ* Hybridization Using bDNA Probes in Arabidopsis Cultured Cells

Suspension culture cells were fixed, permeabilized and hybridized as described in Section 2.3.3. Optimization of *in situ* hybridization protocols was performed on both cell culture and protoplasts in order to find the most appropriate cell type for visualizing the bDNA probes (Table 4.2). Fixation time and the use of permeabilization agents, such as Triton X-100 and cell wall digestion enzymes, were tested. Triton X-100 treatments (0.3% or higher) resulted in damaged cell morphology, and cell wall digestion was necessary to observe any punctate signal. Protoplasts were easily destroyed by centrifugation over 100 g making them difficult to pellet and wash. This resulted in the loss of the cells in the control sample for images shown in Figure 4.3. Both the suspension culture cells and protoplasts aggregated during the *in situ* hybridization, resulting in poorly marked cell boundaries and distorted cell morphology. The most

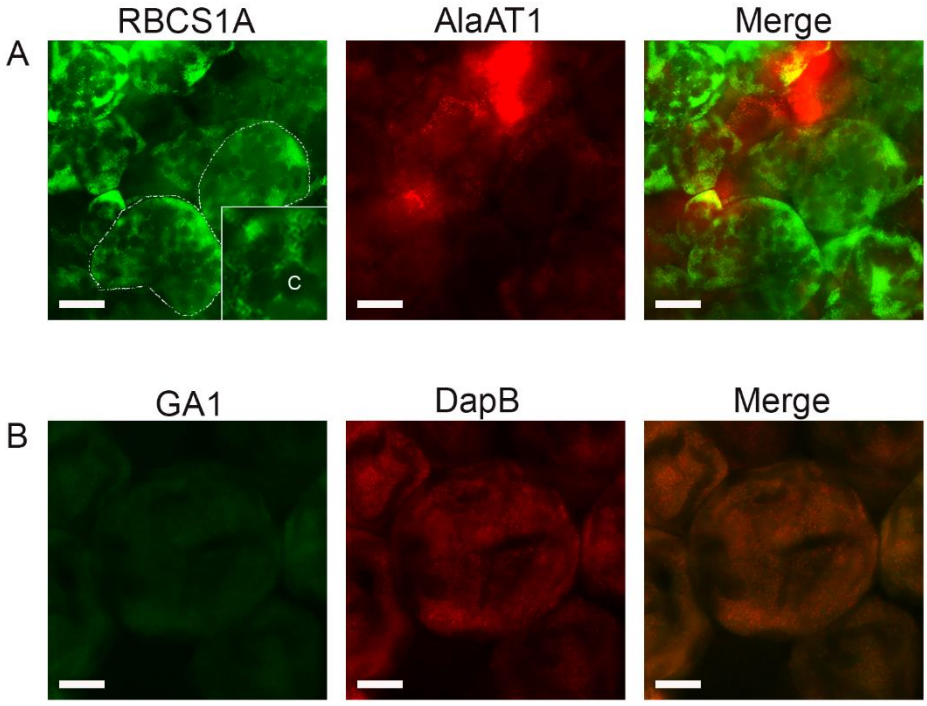


**Figure 4.2 Whole mount fluorescence *in situ* hybridization in Arabidopsis seedlings bDNA technology**

Dual labelling with RNAscope Fluorescent Multiplex kit in cotyledon cells visualized using a 100X oil immersion objective lens on an epifluorescence microscope. A) The signal observed using RBCS1A target probes and Alexa 488 labelled probes, AlaAT1 target probes and Atto 550 labelled probes, and the merge of the images. Inset is magnified image to show signal pattern of RBCS1A. B) The signal observed using GA1 target probes and Alexa 488 labelled probes, DapB target probes and Atto 550 labelled probes, and the merge of the images. Size bar = 10 μm. C, chloroplast.

**Table 4.2 Troubleshooting bDNA whole mount *in situ* hybridization on *Arabidopsis thaliana* cell culture**

| Test # | Fixation | Permeabilization | Hybridization | Wash | Results |
|---|---|---|---|---|---|
| 1 | DG culture in 4% paraformaldehyde pH 7.4 in 0.44% MS media, 0.05 µg/ml kinetin, 0.5 µg/ml 1-naphthaleneacetic acid, 3% sucrose 30 min rotary | 1% Triton X 100 10 min<br>2 x 10 min MeOH -20°C<br>1:15 pretreat 3 in PBS 10 min | APM | APM | cells appear fixed, good morphology<br>no signal observed |
| 2 | LG cell culture in 4% paraformaldehyde, pH 7.4 in 4 mM MES, 0.4 M mannitol, 15 mM $MgCl_2$ 10 min | 0.3 vs 0.03% Triton X 100 10 min<br>2 x 10 min MeOH -20°C<br>1:15 pretreat 3 in PBS 10 min<br>20 mM MES, 0.4 M mannitol, 7 mM CaCl2, 1.5% cellulase, 0.2% pectolyase Y23, 5 mM β-mercaptoethanol,0.1% BSA 10 vs 30 min | | | 0.3% cell clumps with poor morphology, few cells intact with signal<br>0.03% poor morphology and no signal<br>no difference between 10 and 30 min digestion |
| 3 | | 0.3% Triton X 100 vs 1:15 pretreat 3 in PBS 10 min<br>2 x 10 min MeOH -20°C<br>20 mM MES, 0.4 M mannitol, 7 mM CaCl2, 1.5% cellulase, 0.2% pectolyase Y23, 5 mM β-mercaptoethanol,0.1% BSA 30 min<br><br>RNase treatment control | | | pretreat 3 samples had better morphology then Triton X 100<br>large aggregates in RNase control<br>stationary, punctate signal observed for both RBCS1A and AlaAT1 |
| 4 | LG protoplast in 4% paraformaldehyde, pH 7.4 in 4 mM MES, 0.4 M mannitol, 15 mM MgCl2 10 min on slides | 0.3% Triton X 100 10 min<br>3 x 5 min MeOH -20°C<br>1:15 pretreat 3 in PBS 10 min<br>done on slides | | | poor morphology, cells clustering<br>punctate, stationary signal for RBCS1A an AlaAT1<br>-ve control very few punctate structures |
| 5 | LG protoplast in 4% paraformaldehyde, pH 7.4 in 4 mM MES, 0.4 M mannitol, 15 mM MgCl2 10 min in falcon tubes | 0.3% Triton X 100 10 min<br>4 x 5 min MeOH -20°C<br>1:15 pretreat 3 in PBS 10 min<br>done in falcon tubes | APM on APES slides | | poor morphology, cells clustering<br>RBCS1A and AlaAT1 punctate signals overlap<br>-ve control has punctate signals |

DG = dark grown; LG = light grown; pretreat 3 from RNAscope Fluorescent Multiplex Kit Cat # 320293; APM = as per RNAscope Fluorescent Multiplex Kit user manual

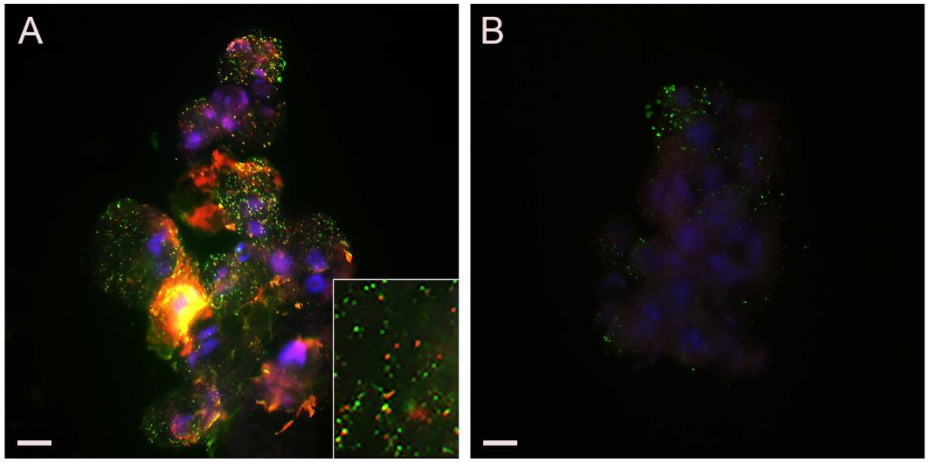


**Figure 4.3 Whole mount fluorescence *in situ* hybridization in Arabidopsis cell culture using bDNA technology**

Dual labelling with RNAscope Fluorescent Multiplex kit in light grown cell culture visualized using a 40X objective lens on an epifluorescence microscope. A) Signal obtained by RBCS1a target probes visualized with Alexa 488 labelled probes (green); signal obtained by AlaAT1 target probes visualized with Atto 550 labelled probes (red); DAPI stain (blue); inset shows a magnification of part of the cell culture cluster to show distinct punctate signals. B) Signal obtained when cell culture was treated with RNase A prior to probe hybridization. Size bar = 10 μm.

successful experiment using cell culture was shown in Figure 4.3. The punctate signals for both probes do not co-localize and were stationary (Figure 4.3A, inset). There was a higher number of RBCS1A punctate signals than AlaAT1 signal, and all punctate signals were stationary. A portion of the cells were treated with RNase A after fixing and prior to hybridization and resulted in a dramatic decrease in punctate signal abundance for both probes (Figure 4.3B). However, medium sized aggregate signals were still observed for RBCS1A target probes. This experiment was repeated once and resulted in punctate signals observed in the DapB negative control sample (data not shown).

A representative example of bDNA technology using protoplasts with controls is shown in Figure 4.4. The RBCS1A punctate signal is observed throughout the protoplast clump and in abundance compared to the AlaAT1 signal (Figure 4.4A). The two target probes produced stationary punctate signals that do not overlap. The GA1 target probe set displayed one punctate signal and the negative control DapB displayed two punctate signals throughout the entire protoplast clump (Figure 4.4B).

### *4.2.2 MSLP in situ Hybridization*

#### 4.2.2.1 MSLP *in situ* Hybridization in Whole Mount Arabidopsis Seedlings

The whole mount protocol established in Chapter 3 was modified to include the MSLP approach as described in Section 2.3.2.1 with little success. Optimizing efforts were mainly focused on proper hybridization conditions for the short length probes by modifying the Biosearch Technologies user manual for Custom Stellaris probe sets (Table 4.3). A hybridization reagent, dextran sulfate, appeared to distort cell morphology at recommended concentrations of 10% (w/v). Optimization experiments were not

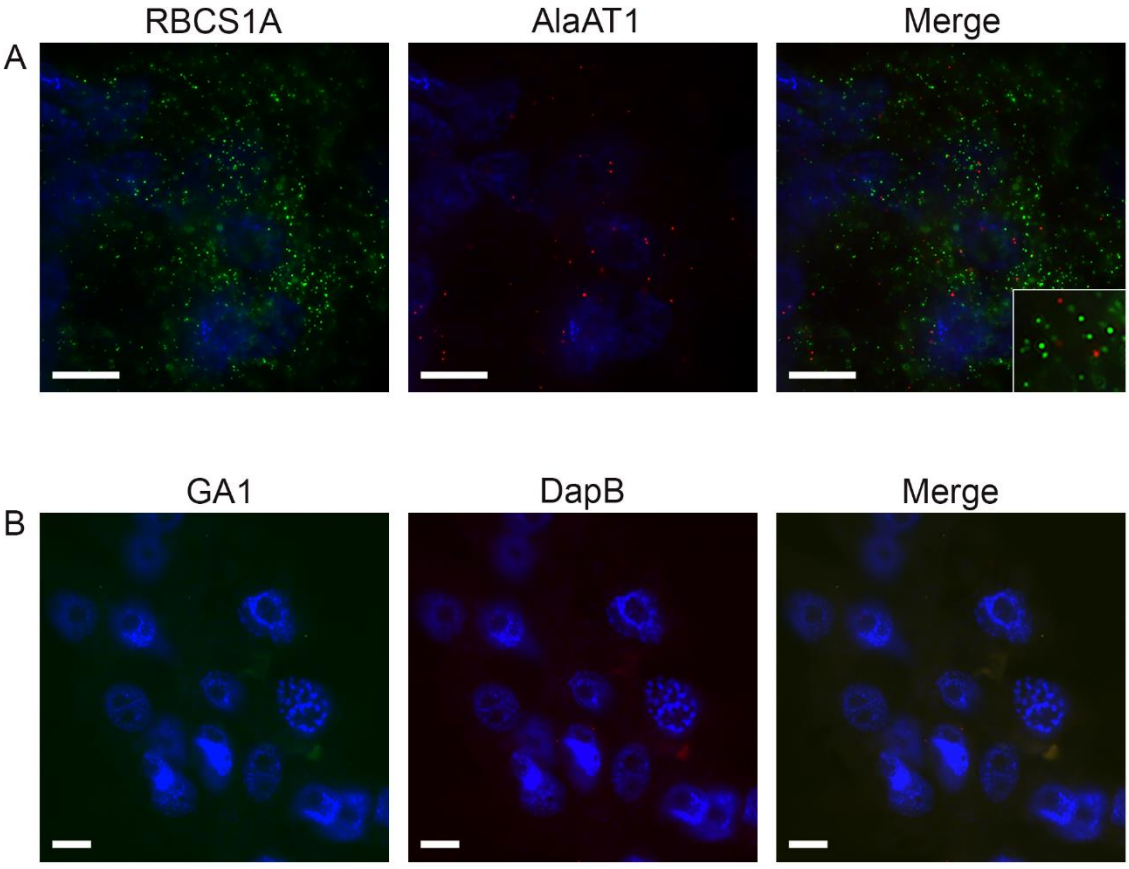


**Figure 4.4 Whole mount fluorescence *in situ* hybridization in Arabidopsis protoplasts using bDNA technology**

Dual labelling with RNAscope Fluorescent Multiplex kit in light grown cell culture protoplasts visualized using a 40X objective lens (A) or a 100X oil immersion objective lens on an epifluorescence microscope (B) A) Signal obtained by RBCS1A target probes visualized with Alexa 488 labelled probes; signal obtained by AlaAT1 target probes visualized with Atto 550 labelled probes; and the merge of both signals. Inset is a magnified image to show punctate signals B) The signal observed using GA1 target probes and Alex 488 labelled probes; using DapB target probes and Atto 550 labelled probes; and the merge of both signals. DAPI in blue. Size bar = 10 μm.

**Table 4.3 Troubleshooting MSLP whole mount *in situ* hybridization on *Arabidopsis thaliana* seedlings**

| Test # | Fixation | Permeabilization | Hybridization | Wash | Results |
|---|---|---|---|---|---|
| 1 | 4% paraformaldehyde, 15% DMSO, 0.1% Tween-20 in PBS, pH 7.4 with heptane for 90 min | 1:1 EtOH:xylene 15 min<br>proteinase K 125 µg/ml 15 min | 100 mg/ml dextran sulfate, 10% formamide in 2 X SSC O/N 37°C with 250 nM of probe | 2 x 30 min 2 X SSC, 10% formamide | morphology poor<br>no signal observed |
| 2 | | | 50% formamide, 5 X SSC, 0.1% Tween-20, 0.1 mg/ml heparin, 1 mg/ml herring DNA O/N 37°C with 250 nM of probe | as per Hejatko et al. 2006 | morphology good<br>BASL faint diffuse signal<br>strong autofluorescence |
| 3 | 4% paraformaldehyde, 15% DMSO, 0.1% Tween-20 in PBS, pH 7.4 with heptane for 100 min | 1:1 EtOH:xylene 15 min<br>proteinase K 60 µg/ml 15 min<br>extra 3 min MeOH wash RT | 10% formamide in 2 X SSC O/N 37°C with vs without 50 mg/ml dextran sulfate with 250 nM of probe | 2 x 30 min 2 X SSC, 10% formamide | sample with dextran sulfate had poor morphology compares to without<br>non-specific signal and strong autofluorescence |
| 4 | DG seedlings in 4% paraformaldehyde, 15% DMSO, 0.1% Tween-20 in PBS, pH 7.4 with heptane for 100 min | | 10% formamide in 2 X SSC O/N 37°C with 250 nM of probe | | morphology good<br>minimal autofluorescence<br>non-specific signal<br>cotyledon cells underdeveloped |
| 5 | Vacuumed and chilled 5% paraformaldehyde, 10% DMSO, 0.1% Tween-20, 0.08M EDTA in PBS, pH 11 under desiccator vacuum 30 min, rotary 15 min | 100% xylene for 60 min<br>proteinase K 40 µg/ml 20 min<br>2 x 40 min MeOH, O/N RT<br>acetone washes | 100 mg/ml dextran sulfate, 10% formamide in 2 X SSC O/N 37°C with 250 nM of probe | | no signal observed<br>distorted morphology |
| 6 | 4% paraformaldehyde, 15% DMSO, 0.1% Tween-20 in PBS, pH 7.4 with heptane under desiccator vacuum 15 min, rotary 75 min | 1:1 EtOH:xylene 30 min<br>proteinase K 60 µg/ml 15 min<br>2 x 15 min MeOH -20°C | 100 mg/ml dextran sulfate, 10% formamide in 2 X SSC O/N 37°C with 250 nM of probe | | minimal punctate signal observed in select cells probed with ACT7<br>distorted morphology |
| 7 | | | 25 mg/ml dextran sulfate, 10% formamide in 2 X SSC O/N 37°C with 250 nM of probe | | punctate signal observed in one cell probed with ACT7<br>morphology good<br>large aggregates observed |

**Table 4.3 Troubleshooting MSLP whole mount *in situ* hybridization on *Arabidopsis thaliana* seedlings (continued)**

| Test # | Fixation | Permeabilization | Hybridization | Wash | Results |
|---|---|---|---|---|---|
| 8 | 4% paraformaldehyde, 15% DMSO, 0.1% Tween-20 in PBS, pH 7.4 with heptane under desiccator vacuum 15 min, rotary 75 min | 1:1 EtOH:xylene 30 min proteinase K 60 µg/ml 15 min 2 x 15 min MeOH -20°C | 2 X SSC, 10% formamide O/N 37°C with 1.25 µM of probe | 2 x 30 min 2 X SSC | no signal observed |
| 9 | | | 2 X SSC, 5% formamide O/N 37°C with 1.25 µM of probe | | no signal observed |
| 10 | | | 2 X SSC, 2% formamide O/N 37°C with 1.25 µM of probe | | no signal observed |
| 11 | | | 5 X SSC, 10% formamide O/N 37°C with 1.25 µM of probe | | no signal observed<br>large aggregates observed |
| 12 | | | 5 X SSC, 5% formamide O/N 37°C with 1.25 µM of probe | | no signal observed<br>large aggregates observed |
| 13 | | | 5 X SSC, 2% formamide O/N 37°C with 1.25 µM of probe | | punctate signal observed for ACT7. About 10 per cell only in a few cells<br>large aggregates observed |
| 14 | | | 5 X SSC, 2% O/N 37°C with 1.25 µM of probe | | no signal observed<br>large aggregates observed |

O/N = overnight; RT= room temperature; For reagent full names see methods and materials.

successful in producing a signal, except when hybridization conditions were of low stringency (Table 4.3). When using these low stringency conditions, the ACT7 probe set produced punctate signals in the epidermal layer, mostly within pavement and meristimoid cells (Figure 4.5). There was no negative control for this experiment and the results could not be duplicated. No signal was observed when using the BASL or RBCS1A probe sets.

#### 4.2.2.2 MLSP *in situ* Hybridization Optimization in Arabidopsis Cultured Cells

An effort was made to localize ACT7 and RBCS1A in cell culture using MSLP as described in Section 2.3.4. Optimization was focused on fixation and hybridization conditions (Table 4.4). Dextran sulfate disrupted cell morphology when used at concentrations higher than 5% (w/v). However, no signal was obtained without dextran sulfate. One experiment resulted in a diffuse signal with the RBCS1A probe set used with light grown suspension culture that was not observed in dark grown culture (Figure 4.6). The observed signal appears to be concentrated around chloroplasts in the cytosol of one cell amongst the cluster of cells (Figure 4.6A). This experiment was only performed once with the RBCS1A probe, and the signal shown in Figure 4.6 was only observed in one cell cluster.

## 4.3 Discussion

Single molecule mRNA imaging is a relatively new and, powerful technique that has been used for mRNA subcellular localization studies in animal cells

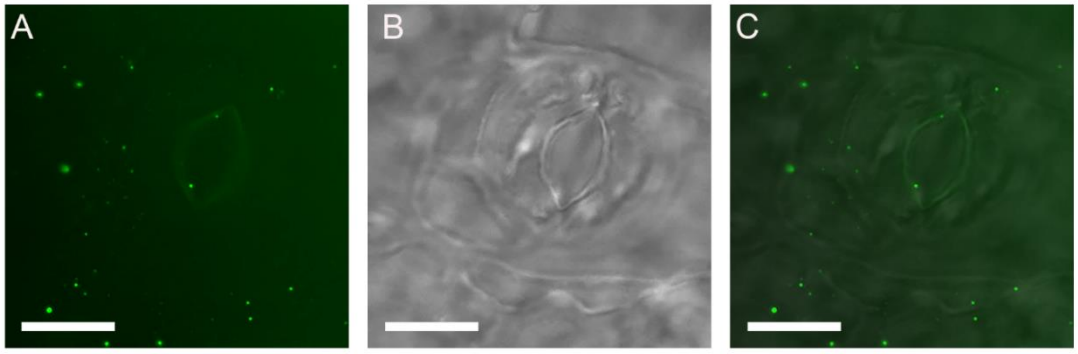


**Figure 4.5 Whole mount fluorescence in situ hybridization in Arabidopsis seedlings using multiple singly labelled probes**

A) The fluorescent signal observed in the epidermal layer using the Custom Stellaris MSLP ACT7 probe set. B) Bright field image of the epidermal layer C) A merge of A and B showing the location of the punctate signals. Images were using a 100X oil immersion objective lens on an epifluorescence microscope. Size bar = 10 μm

**Table 4.4 Troubleshooting MSLP whole mount *in situ* hybridization on *Arabidopsis thaliana* cell culture**

| Test # | Fixation | Permeabilization | Hybridization | Wash | Results |
|---|---|---|---|---|---|
| 1 | DG cell culture 4% paraformaldehyde, 15% DMSO in PBS, pH 7.4 with heptane 30 min rotary, 15 min stationary | 1:1 EtOH:xylene 5 min<br>2 x 10 min MeOH -20°C<br>proteinase K 60 µg/ml 5 min | 100 mg/ml dextran sulfate, 10% formamide in 2 X SSC O/N 37°C | 2 x 30 min 2 X SSC, 10% formamide | very poor morphology<br>no signal observed<br>mild autofluorescence |
| 2 | | no xylene<br>2 x 10 min MeOH -20°C<br>proteinase K 60 µg/ml 5 min | | | very poor morphology<br>no signal observed<br>mild autofluorescence |
| 3 | | no xylene<br>2 x 10 min MeOH -20°C<br>proteinase K 60 µg/ml 5 min<br>2 % Triton x 100 10 min | 10% formamide in 2 X SSC O/N 37°C with 0%, 5% or 10% dextran sulfate | | good morphology with no dextran sulfate<br>5-10% dextran sulfate cytoplasm pulled away from cell wall, lots of empty cells<br>no signal observed |
| 4 | DG cell culture 4% paraformaldehyde pH 7.4 in 0.44% MS media, 0.05 µg/ml kinetin, 0.5 µg/ml 1-naphthalenaeacetic acid, 3% sucrose 20 min rotary | 1% Triton x 100 10 min | | | good morphology with 0-5% dextran sulfate<br>burst cells for 10% dextran sulfate<br>no signal observed<br>high autofluorescence |
| 5 | LG cell culture 4% paraformaldehyde, pH 7.4 in 4 mM MES, 0.4 M mannitol, 15 mM $MgCl_2$ for 10 min | 2 x 10 min MeOH -20°C<br>proteinase K 60 µg/ml 3 min<br>20 mM MES, 0.4 M mannitol, 7 mM CaCl2, 1.5% cellulase, 0.2% pectolyase Y23, 5 mM β-mercaptoethanol,0.1% BSA 30 min | 100 mg/ml dextran sulfate, 10% formamide in 2 X SSC 4 hours 37°C | | cell membrane pulled away from wall in most cells<br>chloroplast bunching, cells clustered<br>diffuse signal observed for RBCS1A in one cluster<br>DG control had lower diffuse signal for RBCS1A |
| 6 | DG protoplast in 4% paraformaldehyde, pH 7.4 in 4 mM MES, 0.4 mannitol, 15 mM $MgCl_2$ for 60 min | 0.3% Triton x 100 10 min | 100 mg/ml dextran sulfate, 10% formamide in 2 X SSC O/N 37°C | | morphology poor in some cells<br>protoplast clumped together<br>very strong autofluorescence<br>no signal observed |
| 7 | DG protoplast in 4% paraformaldehyde, pH 7.4 in 4 mM MES, 0.4 mannitol, 15 mM $MgCl_2$ for 10 min | 0.3% vs no Triton x 100 10 min | | | morphology poor, protoplast clumped together<br>no difference between Triton treatments<br>very strong autofluorescence<br>no signal observed |
| 8 | | 0.3% Triton x 100 10 min<br>MeOH -20°C 10 min<br>proteinase K 60 µg/ml 5 min | | | no viable cells remained on slides<br>when cells were placed on poly-l coated cells<br>distortion occurred after > 15 min |

DG = dark grown; LG = light grown; O/N = overnight

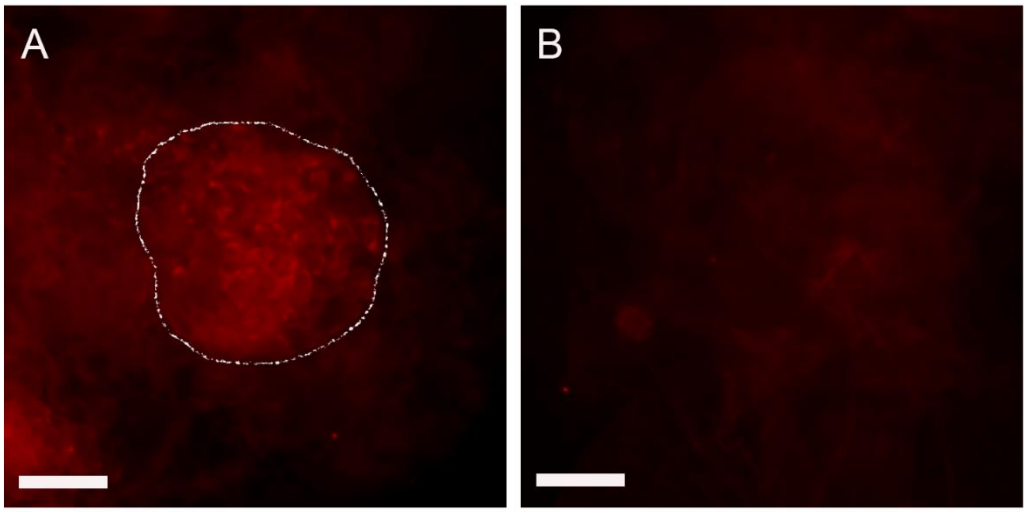


**Figure 4.6 Whole mount fluorescence *in situ* hybridization in Arabidopsis cell culture using Multiple Singly Labelled Probes**

A) Light grown suspension culture probed with RBCS1A probe set under RFP filter. B) Dark grown suspension culture probed with RBCS1A probe set under RFP filter. Images were with a 63X oil immersion objective lens on an epifluorescence microscope. Size bar = 10 μm. A cell boundary is outlined in white.

(Batish et al., 2012; Raj et al., 2008; McIsaac et al., 2013; Lyubimova et al., 2013; Vassilakopoulou et al., 2014; Liu et al., 2015; Tomas et al., 2014; Ziskin et al., 2012). To date, this technology has not been applied to plant model systems. In this chapter two different approaches were used to attempt fluorescence *in situ* hybridization of four different mRNAs at the single molecule resolution. Success was minimal for MSLP from Biosearch Technologies, and without a proper negative control probe any results that were obtained cannot be validated. The signal observed in cell culture using the RBCS1A probe set (Figure 4.6) was more reliable than the signal observed in whole cotyledons (Figure 4.5). This was because the dark grown cell culture conditions served as an appropriate negative control, since Rubsico protein is not expressed in non-photosynthetic cells. In dark grown cell culture, no signal was observed when using the RBCS1A probe set (Figure 4.6). The major problem with using a group of short probes for hybridization is the need for a crowding agent in the solution to increase hybridization efficiency. The manual for Custom Stellaris probes indicates the requirement for dextran sulfate as a crowding agent. This large molecule results in macromolecular crowding, causing a lower volume of solvent availability in the hybridization solution for the probe set. This allows for the probe set to be more "concentrated" to the mRNA target site. This is important with these short 20 nucleotide probes because the melting temperature of a probe is directly proportional to its length. It was shown that in the presence of dextran sulfate, both seedling epidermal cells and cultured cells became plasmolyzed (Table 4.3; Table 4.4). A combination of lowered permeabilization treatments and lowered dextran sulfate concentrations was attempted to determine if this crowding agent could be used without destroying morphology. The balance between good morphology and proper

hybridization conditions was never obtained. This could be the main reason MSLP sets were unsuccessful in Arabidopsis, as adequate permeabilization is crucial for probes to penetrate the cuticle, cell wall and cell membrane but it weakens the tissue to the point where the necessary crowding agent for efficient hybridization caused cell plasmolysis.

bDNA technology from ACD was more successful in achieving single molecule mRNA imaging in Arabidopsis than MSLP. A general cytosolic labelling pattern was observed using RBCS1A target probes that was similar to the pattern observed in Chapter 3 in seedling cotyledon mesophyll cells (Figure 4.2A). A different, less abundant fluorescence pattern was observed in the cytoplasm of epidermal cells using the target probes for AlaAT1 in the same sample (Figure 4.2A). AlaAT1 is an enzyme involved in carbon and nitrogen metabolism in plants. The protein is expressed it roots, shoots, leaves and cell culture but is predominantly found in vascular tissues (Miyashita et al., 2007). The protein is predicted to be located mainly in mitochondria and plastids, however, there is also evidence for cytosolic localization (Heazlewood et al., 2004; Kleffmann et al., 2004; Ito et al., 2011). The labeling of the epidermal cells using the AlaAT1 probe is questionable because some punctate structures were moving, suggesting a non-specific signal. The RBCS1A and AlaAT1 results (Figure 4.2) are preliminary, as the experiment was only performed once using the protocol that yielded these results. However, the negative control that targeted the bacterial mRNA DapB lacked signal and increases confidence that the AlaAT1 signal is authentic (Figure 4.2B). ACD provided us with an alternative probe set that targets Ga1 mRNA in Arabidopsis. The expression of Ga1 mRNA in Arabidopsis cotyledons is extremely low (Winter et al., 2007). However, the single molecules of Ga1 mRNA should have been resulved using this single molecule

approach (Figure 4.2 B; Figure 4.4 B). The lack of signal using the Ga1 target probes suggests that the bDNA probes may not be effectively labelling every mRNA in the cell.

The major problem that was encountered when using bDNA technology in whole mount samples was background staining (Table 4.1). Non-specific, punctate signal that moved freely within a cell was observed for all probe types when following the RNAscope Fluorescent Multiplex Kit User Manual. This problem was also experienced when the same kit and protocol was used in whole mount zebrafish embryos (Gross-Thebing et al., 2014). The Amp-1 oligonucleotide is large and bulky, and it acts as the scaffold for the branching system to build upon (Figure 4.1). This could make it difficult for Amp-1 to penetrate whole mount tissue. When the probe does penetrate the cell, it is difficult to remove. Subsequent amplification steps build a branching structure on these free scaffolds within the cell, making them impossible to remove and resulting in moving, punctate signals. A partial digestion of the cell wall was performed in order to permeabilize the tissue further in an attempt to remove the Amp-1 probe more effectively. This cell wall digestion step, combined with extended amplification hybridization and washing times, allowed for the successful detection of fixed RBCS1A mRNA target signal (Figure 4.2A). The fluorescent signal using the AlaAT1 probe was less convincing because some of the punctate signals observed were moving (Table 4.1). It will be necessary to repeat the WISH procedure to explore the effectiveness of this technique.

Suspension culture cells are easier to penetrate than cells within tissues because there is a lack of cuticle and tissue layers. When the bDNA technology was used on culture cells, the moving, non-specific signal was eliminated (Table 4.2). The fluorescent

pattern observed for RBCS1A and AlaAT1 target probes in culture cells (Figure 4.3) did not overlap, and the number of fluorescent puncta that were visible using the RBCS1A probe was much higher than that observed for the AlaAT1 probe. This is validation that the signals observed are representative of the respective target mRNAs. The larger punctate signals observed for RBCS1A are likely artifacts, as they were also observed in samples treated with RNase A (Figure 4.3B). In an effort to obtain a more reliable fluorescent signal in cultured cells, the cell wall was removed to create protoplasts. The fluorescent signal for RBCS1A and AlaAT1 were similar to Figure 4.3 in frequency and no co-localization was observed (Figure 4.4A). There was a lack of signal using the DapB target probe which indicates the signals observed for RBCS1A and AlaAT1 were not artifacts (Figure 4.4B). Similar to the whole mount results, no signal was evident using Ga1 target probe (Figure 4.4B). The experiments using cultures cells and protoplasts were difficult to replicate. The cells were easily damaged or lost during the extensive washings and hybridization steps. Determining the cell boundaries was also a challenge as both the protoplasts and the cell culture would cluster in large numbers during the procedure.

Single molecule imaging of mRNA is a useful tool for quantifying transcript abundance and for determining mRNA interactions with one another during localization (Batish et al., 2012). The development of reliable protocol using this technology in Arabidopsis would be highly beneficial to gain a better understanding of subcellular mRNA localization in higher plants. The results presented in this chapter are preliminary and additional work needs to be performed to create a reliable system. However, it appears that the successful use of bDNA technology in both protoplasts and whole mount

seedlings is possible and the results from this study are the first examples of single molecule imaging in plants. Using the bDNA *in situ* hybridization technology with paraffin embedded sections was never tested. This procedure would overcome any permeabilization problems since the wall and membrane are removed in sections. The extensive troubleshooting using the MSLP indicates this system is not compatible in Arabidopsis cotyledons and cell culture. Therefore, the research presented here suggests that the most promising technology for single molecule imaging of mRNA in higher plants is the bDNA technology from ACD.

# CHAPTER 5: GENERAL DISCUSSION

## 5.1 Overall Summary

Subcellular mRNA localization is an important process involved in post-transcriptional regulation in eukaryotes that functions to compartmentalize proteins within the cell. This process is involved in establishing polarity during oocyte and embryo development, protein targeting to organelles, and concentrating protein to specific areas of the cytoplasm in various eukaryotic cell types (Lécuyer et al., 2007; Bramham and Wells, 2007; Long et al., 1997; Uniacke and Zerges, 2009; Weis et al., 2013). The extent of subcellular mRNA localization in higher plants is unknown. The majority of work on higher plants has focused on the essential role of subcellular mRNA localization in the targeting of seed storage proteins in endosperm cells (Crofts et al., 2004; Washida et al., 2012). Other less extensively focused plant studies have indicated that subcellular mRNA localization is involved in polarized protein expression during xylem development, targeting proteins to chloroplasts to facilitate import, and in cell differentiation and division (Im et al., 2000; Gibson et al., 1996; Marrison et al., 1996; Ma et al., 2008; Baluska et al., 2000). The global survey of mRNA localization in the Drosophila embryo revealed that over 70% of the mRNAs in the developing embryo were localized non randomly (Lécuyer et al., 2007). This inspired us to perform a similar, although less extensive analysis using the model plant, Arabidopsis. To date, no protocol for subcellular mRNA localization using fluorescence WISH in higher plants has been published. A whole mount protocol would allow for a high throughput analysis and

provide three-dimensional resolution of mRNA localization in the plant cell. This thesis research project aimed to optimize a fluorescence WISH protocol to visualize subcellular mRNA localization in Arabidopsis cotyledon cells with the goal of performing a large scale analysis to determine the frequency of this process in higher plants.

In Chapter 3, a plant fluorescence WISH technique with tyramide signal amplification was described to localize mRNA at the subcellular level. Previously published animal and plant *in situ* hybridization protocols were combined, and this required optimization of various treatments affecting fixation, permeabilization, clearing, antibody specificity and probe visualization. Attention to detail at each of these steps was necessary to overcome the unique challenges presented by the structural and chemical composition of plant cells. Using this approach, three mRNAs that encode chloroplast proteins (RBCS1A, RBCL and LHCB5) were successfully visualized at the subcellular level. These results indicate that RBCS1A does not localize to chloroplasts through localization of its mRNA since the mRNA is randomly localized throughout the cytoplasm. In contrast, the LHCB5 mRNA was enriched at the periphery of the chloroplast, suggesting that mRNA localization assists in the targeting of LHCB5. As expected, RBCL mRNA was strictly localized within the chloroplast where it is encoded. The RBCL mRNA signal was enriched at the periphery of the stroma near the inner membrane of the chloroplast. The results obtained for all three transcripts are comparable to the subcellular localization of the transcripts in Chlamydomonas (Uniacke and Zerges, 2009). Fluorescence WISH using probes for six mRNAs that encode organelle targeted proteins or proteins involved in asymmetrical cell division (mMDH-1, pMDH-1, AIM1, PORB, GUN5, BASL) did not result in any observable signal. However, demonstrating

that two out of the three successful mRNA targets displayed asymmetric localization patterns indicates that this tyramide amplification approach can be used in fluorescence WISH experiments to identify subcellular localization of mRNAs in plant cells. This protocol requires further optimization in order to detect a broad range of mRNAs so that it can be used as a reliable platform for the global analysis of mRNA localization.

In Chapter 4 an effort was made to improve the WISH protocol by using single molecule fluorescence mRNA localization techniques. *In situ* single molecule mRNA fluorescence detection is a relatively new technique that has not been reported in plant cells. This approach is quantifiable and allows for the visualization of individual transcripts independent of their abundance in the cell. Two different single molecule mRNA localization techniques were used in Chapter 4. The first technique explored was multiple singly labelled probes (MSLP) using custom probes (Stellaris probes, Biosearch Technologies). Despite extensive optimization efforts, this technique was never successful in whole cotyledons or in cultured cells. The reason for the lack of success was unclear but could be related to the hybridization conditions necessary to achieve successful labelling resulted in compromised cell morphology. The second technique was branched DNA (bDNA) technology (RNAscope, Advanced Cell Diagnostics). Two transcripts, RBCS1A and AlaAT1, were targeted using this approach. Adjustments were made to the protocol in the RNAscope Fluorescent Multiplex kit manual to diminish the extensive non-specific background staining that was initially obtained. This modified technique produced results on the subcellular mRNA localization of RBCS1A in whole mount seedlings that were consistent with the results obtained using the tyramide approach described in Chapter 3. In protoplasts, cultured cells and whole mount

seedlings, punctate signals were observed for both RBCS1A and AlaAT1 targeted probes that appear to correspond to single mRNA molecules. To our knowledge, this is the first time single molecule imaging of mRNAs has been achieved in plant cells. The practicality of using single molecule mRNA localization techniques for a large scale project is not manageable because of the high cost associated with this technique. However, it could be used as a tool to provide greater depth in understanding the localization of a limited number of localized transcripts. Therefore, the experiments described in Chapter 4 demonstrate the feasibility of single molecule imaging in higher plants using the bDNA technique.

Developing a universal protocol to determine subcellular mRNA localization in higher plants would be an immensely valuable tool. It could be used to gain a better understanding of post-transcriptional control of gene expression during development and could also be used to visualize gene expression patterns during stress responses. This protocol would allow researchers to have a better understanding of protein compartmentalization and would be a strong tool for understanding expression patterns for endogenous genes. It could also aid in transgenic and mutagenic studies, as well as systems biology studies that look at expression of genes in single cells. The work presented in this thesis has provided a strong foundation for the establishment of a protocol that would be capable of a large scale analysis of subcellular mRNA localization in higher plants.

## 5.2 Future Directions

The protocol that was optimized in this thesis for subcellular mRNA localization in higher plants needs to be further developed to become more reliable and extensive. The level of transcript abundance may be a contributor factor that limited the ability to visualize the localization of several of the mRNAs studied here. In an effort to overcome this limitation, an alternative visualization techniques using single molecule *in situ* hybridization was used. Another way to overcome the low transcript abundance problem would be to perform *in situ* hybridization on other organs, tissues, or developmental stages that would be transcriptionally more active than seedling cotyledons. Designing riboprobes that target multiple subunit mRNAs, like the RBCS1A riboprobe designed in this thesis, might aid in increasing the signal to noise ratio. Whole mount samples were chosen over thin sectioned tissue mainly to create a protocol that was simple to use in any laboratory. *In situ* hybridization using paraffin embedded thin sections is technically demanding, time consuming and requires special equipment. However, throughout this project cell permeabilization and non-specific autofluorescence of whole tissue was problematic. Therefore, developing a protocol for subcellular mRNA localization using paraffin embedded and sectioned tissue might be the most logical option for global analysis. In addition, performing *in situ* hybridization of thin sections with bDNA technology was not attempted in this thesis. The limitations of bDNA technology in Arabidopsis was strongly influence by permeabilization of the whole mount tissue. Therefore, performing *in situ* hybridization of paraffin sectioned tissue with bDNA technology may be the best approach to visualizing single molecule mRNAs in Arabidopsis.

Further work to expand on the non-random mRNA localization results of LHCB5 and RBCL, as shown here, could be performed to determine the mechanisms for mRNA localization. In Chlamydomonas, translation inhibitors were used to determine whether localized mRNAs occurred through *cis*-elements on the mRNA or in a cotranslational manner through the nascent peptide (Uniacke and Zerges, 2009). Similar studies could be performed to determine if the localization pattern observed for LHCB5 and RBCL are dependent on translation in higher plant cells. If *cis*-elements on the mRNA are indeed involved in the localization of LHCB5 and RBCL mRNAs, deletion studies could be performed to determine the sequence(s) responsible for this localization (Hamada et al., 2003b). Live cell imaging techniques, such as the MS2 system, could be performed to understand the localization dynamics of these mRNAs. Incorporating cytoskeleton drugs into the live cell imaging studies would allow us to determine if the mRNA localization uses actin filaments or microtubules as structures that facilitate transport (Hamada et al., 2003a). Cytoskeleton drugs could also be incorporated into the WISH protocol to determine its role in localizing LHCB5.

It would also be important to know what RNA-binding proteins are interacting with the localizing mRNAs. This would give insight into the mechanisms responsible for mRNA localization, such as active transport. Proteins that interact with *cis*-elements within a localized mRNA could be identified using *in vivo* crosslinking and mass spectrometry approaches that have been used elsewhere (Sugimoto et al., 2012; Castello et al., 2013). These approaches not only identify authentic RNA-binding proteins, but can also determine the RNA sequence that these proteins bind to in the localized mRNA.

Overall, these studies would assist in determining the mechanisms (active transport, cytoplasmic streaming, or other methods) used to localize LHCB5 and RBCL.

## REFERENCES


**Akam, M.E.** (1983). The location of Ultrabithorax transcripts in Drosophila tissue sections. EMBO J. **2**: 2075–2084.

**de Almeida Engler, J., Van Montagu, M., and Engler, G.** (1998). Whole-mount in situ hybridization in plants. Methods Mol. Biol. **82**: 373–384.

**Apel, K., Santel, H.J., Redlinger, T.E., and Falk, H.** (1980). The protochlorophyllide holochrome of barley (Hordeum vulgare L.). Isolation and characterization of the NADPH:protochlorophyllide oxidoreductase. Eur. J. Biochem. **111**: 251–258.

**Bailey-Serres, J., Sorenson, R., and Juntawong, P.** (2009). Getting the message across: cytoplasmic ribonucleoprotein complexes. Trends Plant Sci. **14**: 443–453.

**Baluska, F., Salaj, J., Mathur, J., Braun, M., Jasper, F., Samaj, J., Chua, N.H., Barlow, P.W., and Volkmann, D.** (2000). Root hair formation: F-actin-dependent tip growth is initiated by local assembly of profilin-supported F-actin meshworks accumulated within expansin-enriched bulges. Dev. Biol. **227**: 618–632.

**Basyuk, E., Bertrand, E., and Journot, L.** (2000). Alkaline fixation drastically improves the signal of in situ hybridization. Nucleic Acids Res. **28**: E46.

**Batish, M., van den Bogaard, P., Kramer, F.R., and Tyagi, S.** (2012). Neuronal mRNAs travel singly into dendrites. Proc. Natl. Acad. Sci. **109**: 4645–4650.

**Belaya, K. and St Johnston, D.** (2011). Using the mRNA-MS2/MS2CP-FP system to study mRNA transport during Drosophila oogenesis. Methods Mol. Biol. **714**: 265–283.

**Bertrand, E., Chartrand, P., Schaefer, M., Shenoy, S.M., Singer, R.H., and Long, R.M.** (1998). Localization of ASH1 mRNA particles in living yeast. Mol. Cell **2**: 437–445.

**Van De Bor, V. and Davis, I.** (2004). mRNA localisation gets more complex. Curr. Opin. Cell Biol. **16**: 300–307.

**Bouget, F., Gerttula, S., Shaw, S., and Quatrano, R.** (1996). Localization of actin mRNA during the establishment of cell polarity and early cell divisions in Fucus embryos. Plant Cell **8**: 189–201.

**Bouget, F.Y., Gerttula, S., and Quatrano, R.S.** (1995). Spatial redistribution of poly(A)+ RNA during polarization of the Fucus zygote is dependent upon microfilaments. Dev. Biol. **171**: 258–61.

**Bowling, A.J., Pence, H.E., and Church, J.B.** (2014). Application of a novel and automated branched DNA in situ hybridization method for the rapid and sensitive localization of mRNA molecules in plant tissues. Appl. Plant Sci. **2**: 1400011.

**Bramham, C.R. and Wells, D.G.** (2007). Dendritic mRNA: transport, translation and function. Nat. Rev. Neurosci. **8**: 776–789.

**Bratu, D.P., Catrina, I.E., and Marras, S. a E.** (2011). Tiny molecular beacons for in vivo mRNA detection. Methods Mol. Biol. **714**: 141–157.

**Bratu, D.P., Cha, B.-J., Mhlanga, M.M., Kramer, F.R., and Tyagi, S.** (2003). Visualizing the distribution and transport of mRNAs in living cells. Proc. Natl. Acad. Sci. U. S. A. **100**: 13308–13313.

**Brendza, R.P., Serbus, L.R., Duffy, J.B., and Saxton, W.M.** (2000). A Function for Kinesin I in the Posterior Transport of oskar mRNA and Staufen Protein. Science **289**: 2120–2122.

**Bullock, S.L., Zicha, D., and Ish-Horowicz, D.** (2003). The Drosophila hairy RNA localization signal modulates the kinetics of cytoplasmic mRNA transport. EMBO J. **22**: 2484–2494.

**Castello, A., Horos, R., Strein, C., Fischer, B., Eichelbaum, K., Steinmetz, L.M., Krijgsveld, J., and Hentze, M.W.** (2013). System-wide identification of RNA-binding proteins by interactome capture. Nat. Protoc. **8**: 491–500.

**Choi, S.B., Wang, C., Muench, D.G., Ozawa, K., Franceschi, V.R., Wu, Y., and Okita, T.W.** (2000). Messenger RNA targeting of rice seed storage proteins to specific ER subdomains. Nature **407**: 765–767.

**Christensen, N.M., Oparka, K.J., and Tilsner, J.** (2010). Advances in imaging RNA in plants. Trends Plant Sci. **15**: 196–203.

**Chung, S. and Takizawa, P.** (2011). In vivo visualization of RNA using the U1A-based tagged RNA system. Methods Mol. Biol. **714**: 221–235.

**Crofts, A.J., Crofts, N., Whitelegge, J.P., and Okita, T.W.** (2010). Isolation and identification of cytoskeleton-associated prolamine mRNA binding proteins from developing rice seeds. Planta **231**: 1261–1276.

**Crofts, A.J., Washida, H., Okita, T.W., Ogawa, M., Kumamaru, T., and Satoh, H.** (2004). Targeting of proteins to endoplasmic reticulum-derived compartments in plants. The importance of RNA localization. Plant Physiol. **136**: 3414–3419.

**David, L.E., Fowler, C.B., Cunningham, B.R., Mason, J.T., and O'Leary, T.J.** (2011). The effect of formaldehyde fixation on RNA: Optimization of formaldehyde adduct removal. J. Mol. Diagnostics **13**: 282–288.

**Ding, D., Parkhurst, S.M., Halsell, S.R., and Lipshitz, H.D.** (1993). Dynamic Hsp83 RNA localization during Drosophila oogenesis and embryogenesis. Mol. Cell. Biol. **13**: 3773–3781.

**Donnelly, C.J., Fainzilber, M., and Twiss, J.L.** (2010). Subcellular communication through RNA transport and localized protein synthesis. Traffic **11**: 1498–1505.

**Femino, a M., Fay, F.S., Fogarty, K., and Singer, R.H.** (1998). Visualization of single RNA transcripts in situ. Science **280**: 585–590.

**Ferrandon, D., Elphick, L., Nüsslein-Volhard, C., and St Johnston, D.** (1994). Staufen protein associates with the 3′UTR of bicoid mRNA to form particles that move in a microtubule-dependent manner. Cell **79**: 1221–1232.

**Forrest, K.M. and Gavis, E.R.** (2003). Live imaging of endogenous RNA reveals a diffusion and entrapment mechanism for nanos mRNA localization in Drosophila. Curr. Biol. **13**: 1159–1168.

**Fukuda, H.** (1996). Xylogenesis : Initiation, progression, and cell death. Annu. Rev. Plant Biol. **47**: 299–325.

**Geitmann, a and Emons, a M.** (2000). The cytoskeleton in plant and fungal cell tip growth. J. Microsc. **198**: 218–245.

**Gibson, L.C.D., Marrison, J., Leechl, R.M., Jensenzt, P.E., Bassham, D.C., Cibson, M., and Hunter, C.N.** (1996). A putative Mg chelatase subunit from Arabidopsis thaliana cv C24.: 61–71.

**Gross-Thebing, T., Paksa, A., and Raz, E.** (2014). Simultaneous high-resolution detection of multiple transcripts combined with localization of proteins in whole-mount embryos. BMC Biol. **12**: 55.

**Gu, W., Deng, Y., Zenklusen, D., and Singer, R.H.** (2004). A new yeast PUF family protein, Puf6p, represses ASH1 mRNA translation and is required for its localization. Genes Dev. **18**: 1452–1465.

**Hachet, O. and Ephrussi, A.** (2004). Splicing of oskar RNA in the nucleus is coupled to its cytoplasmic localization. Nature **428**: 959–962.

**Hamada, S., Ishiyama, K., Choi, S.-B., Wang, C., Singh, S., Kawai, N., Franceschi, V.R., and Okita, T.W.** (2003a). The transport of prolamine RNAs to prolamine protein bodies in living rice endosperm cells. Plant Cell **15**: 2253–2264.

**Hamada, S., Ishiyama, K., Sakulsingharoj, C., Choi, S.-B., Wu, Y., Wang, C., Singh, S., Kawai, N., Messing, J., and Okita, T.W.** (2003b). Dual regulated RNA transport pathways to the cortical region in developing rice endosperm. Plant Cell **15**: 2265–2272.

**Heazlewood, J.L., Tonti-Filippini, J.S., Gout, A.M., Day, D. a, Whelan, J., and Millar, a H.** (2004). Experimental analysis of the Arabidopsis mitochondrial proteome highlights signaling and regulatory components, provides assessment of targeting prediction programs, and indicates plant-specific mitochondrial proteins. Plant Cell **16**: 241–256.

**Hejátko, J., Blilou, I., Brewer, P.B., Friml, J., Scheres, B., and Benková, E.** (2006). In situ hybridization technique for mRNA detection in whole mount Arabidopsis samples. Nat. Protoc. **1**: 1939–1946.

**Im, K.H., Cosgrove, D.J., and Jones, a M.** (2000). Subcellular localization of expansin mRNA in xylem cells. Plant Physiol. **123**: 463–470.

**Ito, J., Batth, T.S., Petzold, C.J., Redding-Johanson, A.M., Mukhopadhyay, A., Verboom, R., Meyer, E.H., Millar, a. H., and Heazlewood, J.L.** (2011). Analysis of the Arabidopsis cytosolic proteome highlights subcellular partitioning of central plant metabolism. J. Proteome Res. **10**: 1571–1582.

**Jackson, D.P.** (1991). In situ hybridization in plants B.D.J. Gurr, S J, McPherson, M J, ed (Oxford University Press: Oxford).

**Jacob, J., Todd, K., Birnstiel, M.L., and Bird, A.** (1971). Molecular hybridization of 3H-labelled ribosomal RNA with DNA in ultrathin sections prepared for electron microscopy. Biochim. Biophys. Acta - Nucleic Acids Protein Synth. **228**: 761–766.

**Jansen, R.P.** (2001). mRNA localization: message on the move. Nat. Rev. Mol. Cell Biol. **2**: 247–256.

**Jansen, R.-P. and Niessing, D.** (2012). Assembly of mRNA-protein complexes for directional mRNA transport in eukaryotes - an overview. Curr. Protein Pept. Sci. **13**: 284–293.

**Järvi, S., Suorsa, M., and Aro, E.-M.** (2015). Photosystem II repair in plant chloroplasts - Regulation, assisting proteins and shared components with photosystem II biogenesis. Biochim. Biophys. Acta **1847**: 900–9.

**Jensen, W.A.** (1962). Botanical Histochemistry D. Whitaker, R. Emerson, D. Kennedy, and G. Beadle, eds (W. H. Freeman and Company: Berkeley).

**Kehr, J. and Buhtz, A.** (2008). Long distance transport and movement of RNA through the phloem. J. Exp. Bot. **59**: 85–92.

**Khrebtukova, I. and Spreitzer, R.J.** (1996). Elimination of the Chlamydomonas gene family that encodes the small subunit of ribulose-1,5-bisphosphate carboxylase/oxygenase. Proc. Natl. Acad. Sci. U. S. A. **93**: 13689–13693.

**Khrustaleva, L.I. and Kik, C.** (2001). Localization of single-copy T-DNA insertion in transgenic shallots (Allium cepa) by using ultra-sensitive FISH with tyramide signal amplification. Plant J. **25**: 699–707.

**Kleffmann, T., Russenberger, D., von Zychlinski, A., Christopher, W., Sjölander, K., Gruissem, W., and Baginsky, S.** (2004). The Arabidopsis thaliana Chloroplast Proteome Reveals Pathway Abundance and Novel Protein Functions. Curr. Biol. **14**: 354–362.

**Kloc, M., Zearfoss, N.R., and Etkin, L.D.** (2002). Mechanisms of subcellular mRNA localization. Cell **108**: 533–544.

**Köhler, A. and Hurt, E.** (2007). Exporting RNA from the nucleus to the cytoplasm. Nat. Rev. Mol. Cell Biol. **8**: 761–773.

**Kragler, F.** (2013). Plasmodesmata: Intercellular tunnels facilitating transport of macromolecules in plants. Cell Tissue Res. **352**: 49–58.

**Küpper, H., Seib, L.O., Sivaguru, M., Hoekenga, O. a., and Kochian, L. V.** (2007). A method for cellular localization of gene expression via quantitative in situ hybridization in plants. Plant J. **50**: 159–175.

**Lange, S., Katayama, Y., Schmid, M., Burkacky, O., Brauchle, C., Lamb D.C., D.C., and Jansen, R.P.** (2008). Simultaneous transport of different localized mRNA species revealed by live-cell imaging. Traffic **9**: 1256–1267.

**Latham, V.M., Yu, E.H.S., Tullio, A.N., Adelstein, R.S., and Singer, R.H.** (2001). A Rho-dependent signaling pathway operating through myosin localizes β-actin mRNA in fibroblasts. Curr. Biol. **11**: 1010–1016.

**Lécuyer, E., Parthasarathy, N., and Krause, H.M.** (2008). Fluorescent in situ hybridization protocols in Drosophila embryos and tissues. Methods Mol. Biol. **420**: 289–302.

**Lécuyer, E., Yoshida, H., Parthasarathy, N., Alm, C., Babak, T., Cerovina, T., Hughes, T.R., Tomancak, P., and Krause, H.M.** (2007). Global analysis of mRNA localization reveals a prominent role in organizing cellular architecture and function. Cell **131**: 174–187.

**Li, X., Franceschi, V.R., and Okita, T.W.** (1993). Segregation of storage protein mRNAs on the rough endoplasmic reticulum membranes of rice endosperm cells. Cell **72**: 869–879.

**Liu, Y., Feng, J., Li, J., Zhao, H., Ho, T.-V., and Chai, Y.** (2015). An Nfic-hedgehog signaling cascade regulates tooth root development. Development.

**Long, R.M., Singer, R.H., Meng, X., Gonzalez, I., Nasmyth, K., and Jansen, R.P.** (1997). Mating type switching in yeast controlled by asymmetric localization of ASH1 mRNA. Science **277**: 383–387.

**Lyubimova, A., Itzkovitz, S., Junker, J.P., Fan, Z.P., Wu, X., and van Oudenaarden, A.** (2013). Single-molecule mRNA detection and counting in mammalian tissue. Nat. Protoc. **8**: 1743–58.

**Ma, L., Xie, B., Hong, Z., Verma, D.P.S., and Zhang, Z.** (2008). A novel RNA-binding protein associated with cell plate formation. Plant Physiol. **148**: 223–234.

**Macdonald, P.M.** (2004). Translational control: a cup half full. Curr. Biol. **14**: R282–3.

**Marín-González, E. and Suárez-López, P.** (2012). "And yet it moves": Cell-to-cell and long-distance signaling by plant microRNAs. Plant Sci. **196**: 18–30.

**Marrison, J.L., Schunmann, P., Ougham, H.J., and Leech, R.M.** (1996). Subcellular visualization of gene transcripts encoding key proteins of the chlorophyll accumulation process in developing chloroplasts. Plant Physiol. **110**: 1089–1096.

**Martone, M.E., Pollock, J. a, and Ellisman, M.H.** (1998). Subcellular localization of mRNA in neuronal cells. Contributions of high-resolution in situ hybridization techniques. Mol. Neurobiol. **18**: 227–246.

**McIsaac, R.S., Silverman, S.J., Parsons, L., Xu, P., Briehof, R., McClean, M.N., and Botstein, D.** (2013). Visualization and analysis of mRNA molecules using fluorescence in situ hybridization in Saccharomyces cerevisiae. J. Vis. Exp.: e50382.

**Meyer, S., Temme, C., and Wahle, E.** (2015). Messenger RNA turnover in eukaryotes: pathways and enzymes. Crit. Rev. Biochem. Mol. Biol. **39**: 197–216.

**Miki, T., Takano, K., and Yoneda, Y.** (2005). The role of mammalian Staufen on mRNA traffic: a view from its nucleocytoplasmic shuttling function. Cell Struct. Funct. **30**: 51–56.

**Miller, D.D., De Ruijter, N.C. a, Bisseling, T., and Emons, a. M.C.** (1999). The role of actin in root hair morphogenesis: Studies with lipochito-oligosaccharide as a growth stimulator and cytochalasin as an actin perturbing drug. Plant J. **17**: 141–154.

**Miller, M. and Olivas, W.** (2011). Roles of Puf proteins in mRNA degradation and translation. Wiley Interdiscip. Rev. RNA **2**: 471–92.

**Miller, S., Yasuda, M., Coats, J.K., Jones, Y., Martone, M.E., and Mayford, M.** (2002). Disruption of dendritict translation of CaMKIIα impairs stabilization of synaptic plasticity and memory consolidation. Neuron **36**: 507–519.

**Minagawa, J. and Takahashi, Y.** (2004). Structure, function and assembly of Photosystem II and its light-harvesting proteins. Photosynth. Res. **82**: 241–263.

**Miyashita, Y., Dolferus, R., Ismond, K.P., and Good, A.G.** (2007). Alanine aminotransferase catalyses the breakdown of alanine after hypoxia in Arabidopsis thaliana. Plant J. **49**: 1108–1121.

**Moore, M.J.** (2005). From birth to death: the complex lives of eukaryotic mRNAs. Science **309**: 1514–1518.

**Moroney, J. V., Bartlett, S.G., and Samuelsson, G.** (2001). Carbonic anhydrases in plants and algae: Invited review. Plant, Cell Environ. **24**: 141–153.

**Neufeld, S.J., Wang, F., and Cobb, J.** (2014). Genetic interactions between shox2 and hox genes during the regional growth and development of the mouse limb. Genetics **198**: 1117–26.

**Okita, T.W. and Choi, S.B.** (2002). mRNA localization in plants: Targeting to the cell's cortical region and beyond. Curr. Opin. Plant Biol. **5**: 553–559.

**Ovechkina, Y. and Wordeman, L.** (2003). Unconventional motoring: an overview of the Kin C and Kin I kinesins. Traffic **4**: 367–375.

**Paige, J.S., Wu, K.Y., and Jaffrey, S.R.** (2011). RNA mimics of green fluorescent protein. Science **333**: 642–646.

**Papenbrock, J., Mock, H.P., Tanaka, R., Kruse, E., and Grimm, B.** (2000). Role of magnesium chelatase activity in the early steps of the tetrapyrrole biosynthetic pathway. Plant Physiol. **122**: 1161–1169.

**Park, H.Y., Lim, H., Yoon, Y.J., Follenzi, A., Nwokafor, C., Lopez-Jones, M., Meng, X., and Singer, R.H.** (2014). Visualization of dynamics of single endogenous mRNA labeled in live mouse. Science **343**: 422–4.

**Pavlova, P., Tessadori, F., de Jong, H.J., and Fransz, P.** (2010). Immunocytological analysis of chromatin in isolated nuclei. Methods Mol. Biol. **655**: 413–432.

**Pinaud, R., Mello, C. V, Velho, T.A., Wynne, R.D., and Tremere, L.A.** (2008). Detection of two mRNA species at single-cell resolution by double-fluorescence in situ hybridization. Nat. Protoc. **3**: 1370–1379.

**Raj, A., van den Bogaard, P., Rifkin, S. a, van Oudenaarden, A., and Tyagi, S.** (2008). Imaging individual mRNA molecules using multiple singly labeled probes. Nat. Methods **5**: 877–879.

**Rozier, F., Mirabet, V., Vernoux, T., and Das, P.** (2014). Analysis of 3D gene expression patterns in plants using whole-mount RNA in situ hybridization. Nat. Protoc. **9**: 2464–2475.

**Sakakibara, H. and Oiwa, K.** (2011). Molecular organization and force-generating mechanism of dynein. FEBS J. **278**: 2964–2979.

**Santangelo, P.J., Nitin, N., and Bao, G.** (2005). Direct visualization of mRNA colocalization with mitochondria in living cells using molecular beacons. J. Biomed. Opt. **10**: 044025.

**Santangelo, P.J., Nix, B., Tsourkas, A., and Bao, G.** (2004). Dual FRET molecular beacons for mRNA detection in living cells. Nucleic Acids Res. **32**: e57.

**Schönberger, J., Hammes, U.Z., and Dresselhaus, T.** (2012). In vivo visualization of RNA in plants cells using the λn 22 system and a GATEWAY-compatible vector series for candidate RNAs. Plant J. **71**: 173–181.

**Serikawa, K. a, Porterfield, D.M., and Mandoli, D.F.** (2001). Asymmetric subcellular mRNA distribution correlates with carbonic anhydrase activity in Acetabularia acetabulum. Plant Physiol. **125**: 900–911.

**Shahbabian, K. and Chartrand, P.** (2012). Control of cytoplasmic mRNA localization. Cell. Mol. Life Sci. **69**: 535–552.

**Shepard, K. a, Gerber, a P., Jambhekar, a, Takizawa, P. a, Brown, P.O., Herschlag, D., DeRisi, J.L., and Vale, R.D.** (2003). Widespread cytoplasmic mRNA transport in yeast: identification of 22 bud-localized transcripts using DNA microarray analysis. Proc. Natl. Acad. Sci. U. S. A. **100**: 11429–11434.

**Shi, L.-X. and Theg, S.M.** (2013). The chloroplast protein import system: from algae to trees. Biochim. Biophys. Acta **1833**: 314–31.

**Strack, R.L., Disney, M.D., and Jaffrey, S.R.** (2013). A superfolding Spinach2 reveals the dynamic nature of trinucleotide repeat-containing RNA. Nat. Methods **10**: 1219–24.

**Sugimoto, Y., König, J., Hussain, S., Zupan, B., Curk, T., Frye, M., and Ule, J.** (2012). Analysis of CLIP and iCLIP methods for nucleotide-resolution studies of protein-RNA interactions. Genome Biol. **13**: R67.

**Takizawa, P. a, Sil, a, Swedlow, J.R., Herskowitz, I., and Vale, R.D.** (1997). Actin-dependent localization of an RNA encoding a cell-fate determinant in yeast. Nature **389**: 90–93.

**Talamond, P., Verdeil, J.-L., and Conéjéro, G.** (2015). Secondary metabolite localization by autofluorescence in living plant cells. Molecules **20**: 5024–5037.

**Tian, L. and Okita, T.W.** (2014). mRNA-based protein targeting to the endoplasmic reticulum and chloroplasts in plant cells. Curr. Opin. Plant Biol. **22C**: 77–85.

**Tomas, J., Reygner, J., Mayeur, C., Ducroc, R., Bouet, S., Bridonneau, C., Cavin, J.-B., Thomas, M., Langella, P., and Cherbuy, C.** (2014). Early colonizing Escherichia coli elicits remodeling of rat colonic epithelium shifting toward a new homeostatic state. ISME J. **9**: 1–13.

**Tyagi, S.** (2009). Imaging intracellular RNA distribution and dynamics in living cells. Nat. Methods **6**: 331–338.

**Tyagi, S. and Alsmadi, O.** (2004). Imaging native beta-actin mRNA in motile fibroblasts. Biophys. J. **87**: 4153–4162.

**Uniacke, J., Colón-Ramos, D., and Zerges, W.** (2011). FISH and immunofluorescence staining in Chlamydomonas. Methods Mol. Biol. **714**: 15–29.

**Uniacke, J. and Zerges, W.** (2009). Chloroplast protein targeting involves localized translation in Chlamydomonas. Proc. Natl. Acad. Sci. U. S. A. **106**: 1439–1444.

**Vargas, D.Y., Shah, K., Batish, M., Levandoski, M., Sinha, S., Marras, S. a E., Schedl, P., and Tyagi, S.** (2011). Single-molecule imaging of transcriptionally coupled and uncoupled splicing. Cell **147**: 1054–1065.

**Vassilakopoulou, M. et al.** (2014). In Situ Quantitative Measurement of HER2mRNA Predicts Benefit from Trastuzumab-Containing Chemotherapy in a Cohort of Metastatic Breast Cancer Patients. PLoS One **9**: e99131.

**Vize, P.D., McCoy, K.E., and Zhou, X.** (2009). Multichannel wholemount fluorescent and fluorescent/chromogenic in situ hybridization in Xenopus embryos. Nat. Protoc. **4**: 975–983.

**Wang, F., Flanagan, J., Su, N., Wang, L.C., Bui, S., Nielson, A., Wu, X., Vo, H.T., Ma, X.J., and Luo, Y.** (2012). RNAscope: A novel in situ RNA analysis platform for formalin-fixed, paraffin-embedded tissues. J. Mol. Diagnostics **14**: 22–29.

**Washida, H. et al.** (2009a). Identification of cis-localization elements of the maize 10-kDa ??-zein and their use in targeting RNAs to specific cortical endoplasmic reticulum subdomains. Plant J. **60**: 146–155.

**Washida, H., Kaneko, S., Crofts, N., Sugino, A., Wang, C., and Okita, T.W.** (2009b). Identification of cis-localization elements that target glutelin RNAs to a specific subdomain of the cortical endoplasmic reticulum in rice endosperm cells. Plant Cell Physiol. **50**: 1710–1714.

**Washida, H., Sugino, A., Doroshenk, K. a., Satoh-Cruz, M., Nagamine, A., Katsube-Tanaka, T., Ogawa, M., Kumamaru, T., Satoh, H., and Okita, T.W.** (2012). RNA targeting to a specific ER sub-domain is required for efficient transport and packaging of α-globulins to the protein storage vacuole in developing rice endosperm. Plant J. **70**: 471–479.

**Washida, H., Sugino, A., Messing, J., Esen, A., and Okita, T.W.** (2004). Asymmetric localization of seed storage protein RNAs to distinct subdomains of the endoplasmic reticulum in developing maize endosperm cells. Plant Cell Physiol. **45**: 1830–1837.

**Weis, B.L., Schleiff, E., and Zerges, W.** (2013). Protein targeting to subcellular organelles via mRNA localization. Biochim. Biophys. Acta - Mol. Cell Res. **1833**: 260–273.

**Wilkie, G.S. and Davis, I.** (2001). Drosophila wingless and Pair-Rule Transcripts Localize Apically by Dynein-Mediated Transport of RNA Particles. Cell **105**: 209–219.

**Winter, D., Vinegar, B., Nahal, H., Ammar, R., Wilson, G. V., and Provart, N.J.** (2007). An "Electronic Fluorescent Pictograph" Browser for Exploring and Analyzing Large-Scale Biological Data Sets. PLoS One **2**: e718.

**Yang, Y., Crofts, A.J., Crofts, N., and Okita, T.W.** (2014). Multiple RNA binding protein complexes interact with the rice prolamine RNA cis-localization zipcode sequences. Plant Physiol. **164**: 1271–82.

**Zarnack, K. and Feldbrügge, M.** (2010). Minireviews microtubule-dependent mrna transport in fungi. Eukaryot. Cell **9**: 982–990.

**Zhang, H.L., Eom, T., Oleynikov, Y., Shenoy, S.M., Liebelt, D.A., Dictenberg, J.B., Singer, R.H., and Bassell, G.J.** (2001). Neurotrophin-induced transport of a β-actin mRNP complex increases β-actin levels and stimulates growth cone motility. Neuron **31**: 261–275.

**Zimmerman, S.G., Peters, N.C., Altaras, A.E., and Berg, C. a** (2013). Optimized RNA ISH, RNA FISH and protein-RNA double labeling (IF/FISH) in Drosophila ovaries. Nat. Protoc. **8**: 2158–79.

**Zimyanin, V.L., Belaya, K., Pecreaux, J., Gilchrist, M.J., Clark, A., Davis, I., and St Johnston, D.** (2008). In vivo imaging of oskar mRNA transport reveals the mechanism of posterior localization. Cell **134**: 843–53.

**Ziskin, J.L., Dunlap, D., Yaylaoglu, M., Fodor, I.K., Forrest, W.F., Patel, R., Ge, N., Hutchins, G.G., Pine, J.K., Quirke, P., Koeppen, H., and Jubb, a. M.** (2012). In situ validation of an intestinal stem cell signature in colorectal cancer. Gut: 1012–23.

## APPENDIX 1

### License Agreement for Figure 1.1

NATURE PUBLISHING GROUP LICENSE TERMS AND CONDITIONS

Dec 21, 2015

This is an Agreement between Johanna Halbauer ("You") and Nature Publishing Group ("Nature Publishing Group"). It consists of your order details, the terms and conditions provided by Nature Publishing Group, and the payment terms and conditions.

**All payments must be made in full to CCC. For payment instructions, please see information listed at the bottom of this form.**

| | |
|---|---|
| License Number | 3773720359216 |
| License date | Dec 21, 2015 |
| Licensed Content Publisher | Nature Publishing Group |
| Licensed Content Publication | Nature Reviews Molecular Cell Biology |
| Licensed Content Title | mRNA localization: message on the move |
| Licensed Content Author | Ralf-Peter Jansen |
| Licensed Content Date | Apr 1, 2001 |
| Volume number | 2 |
| Issue number | 4 |
| Type of Use | reuse in a dissertation / thesis |
| Requestor type | academic/educational |
| Format | print and electronic |
| Portion | figures/tables/illustrations |
| Number of figures/tables/illustrations | 1 |
| Figures | Figure 2 |
| Author of this NPG article | no |
| Your reference number | None |
| Title of your thesis / dissertation | Establishing a fluorescence in situ hybridization approach for subcellular mRNA localization in Arabidopsis thaliana |
| Expected completion date | Dec 2015 |
| Estimated size (number of pages) | 128 |
| **Total** | 0.00 CAD |

**License Agreement for Figure 1.2**

ELSEVIER LICENSE TERMS AND CONDITIONS

Dec 21, 2015

This is an Agreement between Johanna Halbauer ("You") and Elsevier ("Elsevier"). It consists of your order details, the terms and conditions provided by Elsevier, and the payment terms and conditions.

**All payments must be made in full to CCC. For payment instructions, please see information listed at the bottom of this form.**

| | |
|---|---|
| Supplier | Elsevier Limited<br>The Boulevard,Langford Lane<br>Kidlington,Oxford,OX5 1GB,UK |
| Registered Company Number | 1982084 |
| Customer name | Johanna Halbauer |
| Customer address | 6451 Silver Springs Way NW<br>Calgary, AB t3b3g1 |
| License number | 3773720649669 |
| License date | Dec 21, 2015 |
| Licensed content publisher | Elsevier |
| Licensed content publication | Current Opinion in Cell Biology |
| Licensed content title | mRNA localisation gets more complex |
| Licensed content author | Veronique Van De Bor,Ilan Davis |
| Licensed content date | June 2004 |
| Licensed content volume number | 16 |
| Licensed content issue number | 3 |
| Number of pages | 8 |
| Start Page | 300 |
| End Page | 307 |
| Type of Use | reuse in a thesis/dissertation |
| Intended publisher of new work | other |
| Portion | figures/tables/illustrations |
| Number of figures/tables/illustrations | 1 |
| Format | both print and electronic |
| Are you the author of this Elsevier article? | No |

| | |
|---|---|
| Will you be translating? | No |
| Original figure numbers | figure 1 |
| Title of your thesis/dissertation | Establishing a fluorescence in situ hybridization approach for subcellular mRNA localization in Arabidopsis thaliana |
| Expected completion date | Dec 2015 |
| Estimated size (number of pages) | 128 |
| Elsevier VAT number | GB 494 6272 12 |
| Price | 0.00 CAD |
| VAT/Local Sales Tax | 0.00 CAD / 0.00 GBP |
| **Total** | 0.00 CAD |

**License Agreement for Figure 1.3**

ELSEVIER LICENSE TERMS AND CONDITIONS

Dec 21, 2015

This is an Agreement between Johanna Halbauer ("You") and Elsevier ("Elsevier"). It consists of your order details, the terms and conditions provided by Elsevier, and the payment terms and conditions.

**All payments must be made in full to CCC. For payment instructions, please see information listed at the bottom of this form.**

| | |
|---|---|
| Supplier | Elsevier Limited<br>The Boulevard,Langford Lane<br>Kidlington,Oxford,OX5 1GB,UK |
| Registered Company Number | 1982084 |
| Customer name | Johanna Halbauer |
| Customer address | 6451 Silver Springs Way NW<br>Calgary, AB t3b3g1 |
| License number | 3773721174703 |
| License date | Dec 21, 2015 |
| Licensed content publisher | Elsevier |
| Licensed content publication | Current Opinion in Plant Biology |
| Licensed content title | mRNA-based protein targeting to the endoplasmic reticulum and chloroplasts in plant cells |
| Licensed content author | Li Tian,Thomas W Okita |
| Licensed content date | December 2014 |
| Licensed content volume number | 22 |
| Licensed content issue number | n/a |
| Number of pages | 9 |
| Start Page | 77 |
| End Page | 85 |
| Type of Use | reuse in a thesis/dissertation |
| Intended publisher of new work | other |
| Portion | figures/tables/illustrations |
| Number of figures/tables/illustrations | 1 |
| Format | both print and electronic |

| | |
|---|---|
| Are you the author of this Elsevier article? | No |
| Will you be translating? | No |
| Original figure numbers | figure 1 |
| Title of your thesis/dissertation | Establishing a fluorescence in situ hybridization approach for subcellular mRNA localization in Arabidopsis thaliana |
| Expected completion date | Dec 2015 |
| Estimated size (number of pages) | 128 |
| Elsevier VAT number | GB 494 6272 12 |
| Price | 0.00 CAD |
| VAT/Local Sales Tax | 0.00 CAD / 0.00 GBP |
| **Total** | 0.00 CAD |